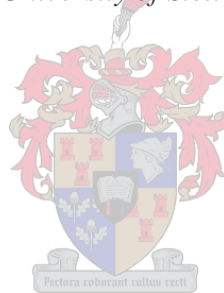


Development of a Process Chain for Digital Design and Manufacture of Patient-Specific Intervertebral Disc Implants with Matching Endplate Geometries

by
Neal de Beer

*Dissertation presented for the degree of Doctor of Engineering at the
University of Stellenbosch*



Promoter: Dr. André Francois van der Merwe
Faculty of Engineering
Department of Industrial Engineering

Co-Promoter: Prof. Cornie Scheffer
Faculty of Engineering
Department of Mechanical & Mechatronic Engineering

Co-Promoter: Prof. Dimitri Dimitrov
Faculty of Engineering
Department of Industrial Engineering

March 2011

Declaration

By submitting this thesis/dissertation electronically, I declare that the entirety of the work contained therein is my own, original work, that I am the sole author thereof (save to the extent explicitly otherwise stated), that reproduction and publication thereof by Stellenbosch University will not infringe any third party rights and that I have not previously in its entirety or in part submitted it for obtaining any qualification.

March 2011

Copyright © 2011 University of Stellenbosch

All rights reserved

Synopsis

Back pain is a common concern amongst a growing population of people across the world today, where in most cases the pain can become unbearable resulting in major lifestyle adjustments. Seventy to eighty percent of the population of the Western world experiences low-back pain at one time or another. Pain can be produced as a worn disc becomes thin, narrowing the space between the vertebrae. Pieces of the damaged disc may also break off and cause irritation to the nerves signalling back pain.

Depending on the severity of a patient's condition, and after conservative treatment options have been exhausted, a disc replacement surgery (*arthroplasty*) procedure may be prescribed to restore spacing between vertebrae and relieve the pinched nerve, while still maintaining normal biomechanical movement.

Typical complications that are however still observed in some cases of disc implants include: anterior migration of the disc, subsidence (sinking of disc) and lateral subluxation (partial dislocation of a joint).

Issues such as function, correct placement and orientation, as well as secure fixation of such a disc implant to the adjacent vertebrae are highly important in order to replicate natural biomechanical behaviour and minimise the occurrence of the complications mentioned.

As various imaging and manufacturing technologies have developed, the option for individual, patient-specific implants is becoming more of a practical reality than it has been in the past. The combination of CT images and Rapid Manufacturing for example is already being used successfully in producing custom implants for maxilla/facial and cranial reconstructive surgeries.

There exists a need to formalise a process chain for the design and manufacture of custom-made intervertebral disc implants and to address the issues involved during each step. Therefore this study has investigated the steps involved for such a process chain and the sensible flow of information as well as the use of state-of-the-art manufacturing technologies. Strong emphasis was placed on automation of some of the processes as well as the user-friendliness of software where engineers and surgeons often need to work together during this multi-disciplinary environment.

One of the main benefits for customization was also investigated, namely a reduction in the risk and potential for implant subsidence. Stiffness values from pressure tests on vertebrae were compared between customized implants and implants with flat endplate designs. Results indicated a statistically significant improvement of customized, endplate matching implants as opposed to flat implant endplates. Therefore it may be concluded that the use of customized intervertebral disc implants with patient specific endplate geometry may decrease the risk and potential for the occurrence of subsidence.

Opsomming

Rugpyn is 'n algemene bekommernis vir 'n groeiende populasie van mense in die wêreld vandag, waar in meeste gevalle die pyn ondraagbaar kan raak en groot leefstyl aanpassings vereis. Sewentig tot tagtig persent van die populasie in die Westerse wêreld ondervind lae rugpyn op een of ander stadium. Die pyn kan veroorsaak word deur 'n intervertebrale skyf wat verweer en dunner word, en veroorsaak dat die spasie tussen die vertebrae vernou. Stukkies van die beskadigde skyf mag ook afbreek en irritasie aan die senuwees veroorsaak wat verdere pyn kan veroorsaak.

Afhangende van die ernstigheid van 'n pasiënt se geval, en nadat opsies vir konservatiewe behandeling uitgeput is, kan 'n skyf vervangings-prosedure (artroskopies) voorgeskryf word om die spasie tussen die vertebrae te herstel en sodoende die geknypte senuwee te verlos. Die skyf vervanging herstel spasiëring tussen vertebrae terwyl die normale biomeganiese beweging ook behoue bly, in teenstelling met 'n fusie-prosedure wat die betrokke vertebrae aanmekaar vasheg en normale beweging belemmer. Tipiese komplikasies wat egter steeds na 'n skyf vervanging in sommige gevalle waargeneem word sluit in: anterior migrasie van die implantaat, insinking, sowel as laterale sublukasie (gedeeltelike dislokasie van 'n gewrig). Faktore soos funksie, korrekte posisionering en orientasie, sowel as vashegting van so 'n skyf implantaat tot die aanliggende vertebrale bene is besonder belangrik om natuurlike biomeganiese beweging te herstel en sodoende bogenoemde komplikasies te verminder.

Soos wat verskeie beeldings- en vervaardigingstechnologie verbeter het oor die laaste dekade, het die moontlikheid vir individuele, pasiënt-spesifieke implantate al hoe meer 'n praktiese realiteit begin word. Die kombinasie van Gerekenariseerde Tomografie (GT), tesame met Snel Vervaardiging word byvoorbeeld reeds suksesvol aangewend tydens die ontwerp en vervaardiging van pasiënt-spesifieke implantate vir maksilla- en kraniale rekonstruktiewe chirurgie. Daar bestaan egter 'n behoefte om 'n formele prosesketting vir die ontwerp en vervaardiging van pasiënt-spesifieke intervertebrale skyf implantate te ontwikkel en om belangrike faktore tydens elke stap noukeurig te beskryf.

Hierdie studie het na die verskillende stappe in die prosesketting gekyk om 'n sinvolle vloei van informasie en benutting van hoë gehalte vervaardigingstechnologie saam te snoer. Sterk klem was gelê op outomatisering van prosesse asook gebruikersvriendelikheid van sagteware waar ingenieurs en medici dikwels saam moet werk tydens hierdie kruisdissiplinêre omgewing.

Een van die hoof verwagte voordele met die gebruik van pasklaar skyf implantate, naamlik die vermindering van moontlike insinking van die implantaat in die been, is ook ondersoek. Die ondersoek het druktoetse behels en die vergelyking van ooreenstemmende styfheid tussen implantate wat die kontoer van die bene volg teenoor gewone plat eindplate. Die resultate was statisties beduidend in die guns van die pasklaar implantate wat die beenkontoere gevolg het, en bewys dus dat die risiko vir insinking verminder is.

Dedication

To my wonderful wife, Cindy

Thank you for all of your unyielding love, support and encouragement.

And

To my son, Noah

While I was still trying to figure out how the spine works...

God was busy creating yours!

*“For You created my inmost being, You knit me together in my mother’s womb. I
praise You because I am fearfully and wonderfully made;
Your works are wonderful, I know that full well.”*

Psalms 139: 13-14

Acknowledgements

I would like to express my sincere gratitude to the following people who have contributed to make this work possible:

- *Dr. André van der Merwe*, for your guidance and support throughout the duration of this project. I always appreciated the way in which you simplified a challenge and helped me to stay focused.
- *Prof. Cornie Scheffer*, for your input and assistance in many areas of this project. Thank you for your willingness to collaborate from the Department of Mechanical Engineering and by making many hardware and software resources available.
- *Prof. Dimitri Dimitrov*, for your input and guidance, especially during the initial stages of this project when things were starting to take shape.
- Several surgeons from the medical field have been of tremendous help in giving us better insight into the issues they face regarding spinal surgery. Thanks to *Dr. Jack Eksteen* from Paarl Medi-Clinic and his assistant *Byron Whitehouse* from the company Neurophysics for giving me the opportunity to witness your surgical procedures. Thanks also to *Drs. Francois Wahl, Ian Vlok, Adriaan Liebenberg, Don du Toit, Hanno Vivier, Willem Strydom, and Thys Boeyens* for providing valuable guidance to ensure that the project remains relevant to the constraints and challenges you encounter during surgery.
- *Prof. Ben Page*, head of the Department of Anatomy and Histology, for your help in acquiring the cadaver specimens for this study, as well as providing guidance regarding the relevance of this project. Thanks also to *Mrs. Marie de Beer* for your logistical support during these procedures and *Mr. Lionel du Toit* for your technical support during the preparation of the specimens.
- *Dr. Richard de Villiers*, from Van Wageningen & Partners, Stellenbosch Medi-Clinic, for your assistance in acquiring the necessary CT data for our experiments.
- *Dr. Graham Ellis*, from the Helderberg Osteoporosis Clinic, for your assistance in having the cadaver bone specimens scanned to assess their bone mineral density.
- *Mr. Johan Els*, from the Centre for Rapid Prototyping and Manufacturing at the Central University of Technology, Bloemfontein, for manufacturing the implants used during the pressure tests.
- *Mr. Jakkie Blom* and your colleagues from the Stellenbosch University Central Mechanical Services, for manufacturing some of my test equipment as well as providing a hydraulic press for my non-destructive test experiments.
- *Prof. Gerhard Venter* and *Mr. Hans Heunis*, from the Department of Mechanical Engineering, for providing hydraulic pressure testing facilities and training.
- Finally, to my student colleagues, *Lorita Christelis, Adriaan Odendaal, Celia j.v. Rensburg, Naömi Bloem* and *Alwyn van Zyl* – thank you for your diligence in your individual projects. You have all added substantial value to this project as a whole.

Table of Contents

1	Introduction.....	1
1.1	Background.....	1
1.2	Problem Statement	2
1.3	Aims, Objectives and Hypothesis	4
1.4	Roadmap of Document.....	5
2	Literature Review	7
2.1	Relevant Spinal Anatomy.....	7
2.2	Artificial Disc Technology.....	13
2.2.1	History of Development	13
2.2.2	Critical Analysis of Existing Artificial Discs	15
2.2.3	Listed studies investigating clinical outcome after TDR	21
2.2.4	Indications and contraindications	23
2.3	Customization of Implants by Layer Manufacturing in General.....	26
2.3.1	Classification for Implant Customization.....	27
2.3.2	Regulatory Issues.....	28
3	A Process Chain for Developing Patient-Specific IVD Endplates	31
3.1	Introduction.....	31
3.2	Scope and Exclusions.....	31
3.3	Diagnosis.....	33
3.4	Imaging/Scanning	33
3.5	Data Transformation	33
3.5.1	Thresholding.....	34
3.5.2	Region Growing	34
3.5.3	3D Model	34
3.6	Design and Customization	36
3.6.1	Surgical Planning.....	37
3.6.2	Automated Parametric Disc Design.....	40

3.6.3	Endplate Design	41
3.7	Biomechanical Simulation	42
3.8	Regulatory Approval	45
3.9	Rapid Manufacturing	47
3.10	Post Processing Phase, Sterilization & Surgery	48
4	Reduced Subsidence for Patient-Specific IVD Endplates.....	51
4.1	Introduction.....	51
4.2	Materials & Methods.....	52
4.2.1	Study Design	52
4.2.2	Imaging and Specimen Preparation	53
4.2.3	Implant design and manufacturing	57
4.2.4	Mechanical Testing.....	59
4.2.5	Data Analysis.....	64
4.3	Results	66
4.3.1	Non-Destructive Tests	66
4.3.2	Destructive Tests	72
5	Conclusions and Recommendations.....	79
6	References	83
	Appendix A: Medical and Anatomical Terminology.....	92
	Appendix B: Comparison of published studies concerning TDR (Galbusera, et al., 2008).....	96
	Appendix C: Load Displacement Curves and Failure Images for Destructive Tests.....	109

List of Figures

Figure 1 – Bones of the vertebral column (Gilroy, MacPherson, & Ross, 2008)	7
Figure 2 – Typical cervical vertebra (C4) (Gilroy, MacPherson, & Ross, 2008)	8
Figure 3 – Typical thoracic vertebra (T6) (Gilroy, MacPherson, & Ross, 2008).....	8
Figure 4 – Typical lumbar vertebra (L4) (Gilroy, MacPherson, & Ross, 2008).....	8
Figure 5 – Joints of the vertebral column (Gilroy, MacPherson, & Ross, 2008).....	9
Figure 6 – Sagittal section of T11-T12, left lateral view, indicating intervertebral disc (Gilroy, MacPherson, & Ross, 2008)	10
Figure 7 – Structure of intervertebral disc (Gilroy, MacPherson, & Ross, 2008)	10
Figure 8 – Posterior herniation – modified from (Gilroy, MacPherson, & Ross, 2008).....	11
Figure 9 – Posterolateral herniation – modified from (Gilroy, MacPherson, & Ross, 2008)	12
Figure 10 – Progressive disc degeneration (Adams & Roughley, 2006).....	12
Figure 11 - Subsidence failure of Fernström’s steel balls.....	14
Figure 12 – Kostuik’s total disc replacement design (Bono & Garfin, 2004).....	15
Figure 13 – An approach to the surgical management of chronic low back pain (Kishen & Diwan, 2010)	25
Figure 14 – Clinical process chain for design & manufacture of patient-specific IVD endplates.....	32
Figure 15 – Process flow following CT scanning.....	33
Figure 16 – Threshold selection of HU limits.....	34
Figure 17 – 3D model generation after thresholding and region growing.....	35
Figure 18 – Enlarged view of 3D model generated in Mimics.....	35
Figure 19 – Design phase process chain.....	37
Figure 20 – Identification of sagittal, coronal and transverse planes (Van Zyl, 2010)	37
Figure 21 – Rotation and translation of selected vertebra (Van Zyl, 2010)	38
Figure 22 – Anatomical landmarks for design of patient-specific IVD endplates (Odendaal, 2010).....	39
Figure 23 – Semi-automated identification of landmarks along intersection planes (Van Zyl, 2010)	40
Figure 24 – Link between Surgical Planning Tool and Custom Disc Generator.....	40
Figure 25 – Diagram representing mid-sagittal section of prosthesis with feature dimensions (Odendaal, 2010).....	41
Figure 26 – Customized disc prosthesis designed using the CDG (Odendaal, 2010)	41
Figure 27 – Boolean subtraction of implant and vertebrae to create bone-matching endplate geometries (Odendaal, 2010).....	42
Figure 28 – Advantages and limitations of external motion capturing technologies (Christelis, 2008)	43
Figure 29 - Advantages and limitations of internal motion capturing technologies (Christelis, 2008).....	44
Figure 30 – Basic iterative process flow for design improvements using simulation models.....	45
Figure 31 – Simulation process flow including regulatory approval	46

Figure 32 – Clinical process chain indicating relative position for regulatory approval.....	46
Figure 33 – EOSINT M270 Direct Metal Laser Sintering Machine	48
Figure 34 – Overview of study design for pressure-related subsidence testing	52
Figure 35 – CT scanning of a cadaver specimen.....	53
Figure 36 –Support structure designed to orientate bone endplates during vertical loading.....	56
Figure 37 – Fitment and orientation of datum plane	57
Figure 38 – L3 Implant design showing (a) footprint profile & centroid, and (b) final implant	58
Figure 39 – Manufactured implants prior to removal from base plate	58
Figure 40 – Non-destructive test setup.....	59
Figure 41 – Pressure transmitter pin.....	60
Figure 42 – I-Scan 5051 sensor map and specifications.....	61
Figure 43 – Typical setup for destructive testing	63
Figure 44 – Position of cameras in relation to test setup and their line of vision.....	63
Figure 45 – Percent Contact and Max Pressure Comparison.....	67
Figure 46 – Box & Whisker plot for % contact measured using contour and flat implant designs.....	70
Figure 47 – Normal probability plots of % contact for contour and flat implants	71
Figure 48 – Maximum failure loads for contour and flat implants per vertebra	73
Figure 49 – Typical load-displacement response from failure testing of vertebrae	74
Figure 50 – Stiffness values per vertebra during failure testing	75
Figure 51 – Box & Whisker plot for stiffness during destructive failure tests.....	75
Figure 52 – Normal probability plot of stiffness for different implant designs during destructive tests.....	76

List of Tables

Table 1 – Classification of lumbar disc prostheses that were reviewed (Galbusera, et al., 2008).....	18
Table 2 – List of studies analyzing the outcomes following lumbar total disc replacement (adapted from Kishen & Diwan, 2010)	21
Table 3 – List of studies analyzing the outcomes following cervical total disc replacement (adapted from Kishen & Diwan, 2010)	23
Table 4 – Metal fabrication comparison matrix suitable for medical applications (De Beer, et al., 2008).....	47
Table 5 – BMD scan results of cadaver specimens.....	55
Table 6 – Non-destructive loads per vertebral grouping	62
Table 7 – Upper and Lower Loads used for Stiffness Calculation of Failure Test Results	65
Table 8 – Summary of Non-Destructive Test Results – Contour Implants	66
Table 9 – Summary of Non-Destructive Test Results – Flat Implants	66
Table 10 – Pressure distribution maps from I-Scan sensors	68
Table 11 – Summary of Destructive Test Results – Contour Implants	73
Table 12 – Summary of Destructive Test Results – Flat Implants	73
Table 13 – Published studies concerning lumbar kinematics after TDR (Galbusera, et al., 2008).....	97
Table 14 – Published studies concerning loads, stresses and sagittal balance after TDR (Galbusera, et al., 2008).....	101
Table 15 – Published studies of biomaterials, wear and osseointegration (Galbusera, et al., 2008)	103

Glossary of Terms

Throughout the document, words included in this glossary are highlighted by using italics and are presented here alphabetically. Other specific anatomical terms of movement and terms of reference are described in Appendix A.

Term	Description
Arthrodesis	The fusion of bones across a joint space, thereby limiting or eliminating movement. It may occur spontaneously or as a result of a surgical procedure, such as fusion of the spine.
Arthroplasty	The surgical reconstruction or replacement of a malformed or degenerated joint
Cobb angle	A technique used to measure the severity of a spinal curve - in degrees - from spinal images
Discectomy	A discectomy is a surgical procedure in which the central portion of an intervertebral disc, the nucleus pulposus, which may be causing pain by stressing the spinal cord or radiating nerves, is removed
Facet arthrosis	Degenerative changes of the facet joints
Heterotrophic ossification	"Heterotrophic" essentially means "wrong place," while "ossification" refers to bone formation. Subsequently heterotrophic ossification refers to the growth of bone material in the soft tissues of the body, including muscles, tendons and fascia.
Kyphoplasty	A minimally invasive procedure to alleviate pain from vertebral compression fractures. An orthopedic balloon is placed in the affect vertebra and inflated; the resulting cavity is filled with bone cement in order to stabilise the vertebral fracture.
Morphometry	Morphometrics is a field concerned with studying variation and change in the form (size and shape) of organisms or objects
Osteolysis	Osteolysis refers to an active resorption of bone matrix by osteoclasts as part of an ongoing disease process.
Osteomyelitis	Osteomyelitis is an inflammation of bone and bone marrow (usually caused by bacterial infection). Infection is more common in the long bones of the body, but it can affect any bone in the body. Osteomyelitis can occur in children of any age, but is more common in premature infants and babies born with complications.
Osteopenic	The medical condition of having low bone density, but not low enough to be considered osteoporosis
Osteoporosis	A disease, occurring especially in women following menopause, in which the bones become extremely porous and are subject to fracture.
Pseudoarthrosis	Pseudoarthrosis (or "non-unions") is the movement of a bone at the location of a fracture resulting from inadequate healing of the fracture.
Radiculopathy	Radiculopathy refers to chronic injuries of the spinal nerve roots caused by prolonged nerve irritation or compression. Patients with radiculopathy feel burning pain, pins and needles, and numbness. Muscle weakness and atrophy may also occur if the compression persists.

Sacroiliitis	In medicine, sacroiliitis is an inflammation of the sacroiliac joint
Sciatica	A description of pain and/or numbness associated with inflammation of the sciatic nerve, usually due to compression of the spinal nerve between fifth lumbar (L5) and first sacral vertebrae(S1). It is often the result of a herniated nucleus pulposus at the L4-5 or L5-S1 levels.
Scoliosis	A congenital condition where there is abnormal lateral curvature of the spine
Spondylolisthesis	Spondylolisthesis is defined as the movement of adjacent vertebra relative to each other.

Introduction



1

1 Introduction

1.1 Background

Back pain is a common concern among a growing population of people across the world today, where in most cases, the pain can become unbearable resulting in major lifestyle adjustments. Low back pain is not specifically a disease, but rather a symptom from several possible sources and factors that combine to incite pain.

The causes for back pain can largely be grouped in three main categories (Borenstein, 2000), (Anonymous, 2010):

- Nerve root syndromes which produce symptoms from pinched nerves, often due to a herniated (or bulging) of the soft, cartilaginous cushions (intervertebral discs) between the back bones (vertebrae).
- Musculoskeletal pain syndromes where local pain, stiffness and a loss of range of motion is reported in the muscle groups involved.
- And other skeletal causes of back pain where infections occur in the bones of the spine (*osteomyelitis* or *sacroiliitis*). This pain is usually worse at night and when sitting or standing for a long time. Tumours can also be a source of skeletal pain.

The intervertebral discs, which provide structural support to the spine, act as shock absorbers, taking on stresses created by movement and any external loads. However age, repetitive strain, and (possibly) genetic factors result in deterioration of the biological and mechanical integrity of these intervertebral discs, ultimately causing disc wear and tear. This gradual deterioration of the discs between the vertebrae is referred to as degenerative disc disease (DDD).

Whether through direct or indirect ways, intervertebral disc degeneration is a leading cause of pain and disability in adults. Seventy to eighty percent of the population of the Western world experiences low-back pain at one time or another (Bertagnoli & Kumar, 2002), (Viscogliosi, Viscogliosi, & Viscogliosi, 2004). It can produce pain as a worn disc becomes thin, narrowing the space between the vertebrae. Pieces of the damaged disc may also break off and cause irritation to the nerves. As the disc loses its ability to absorb stress and provide support, other parts of the spine become overloaded, thus leading to irritation, inflammation, fatigue, muscle spasms, and back pain.

Depending on the severity of injury and history of a patient, current treatment options for low back pain range from conservative home treatment and medication, to surgery. Patients are usually encouraged for the first 30 days to try to continue with normal activities as much as possible. The use of anti-inflammatory drugs is allowed but bed rest for more than 48 hours is normally discouraged. If the pain still persists after

this initial conservative treatment, a range of other non-invasive techniques may be considered. These may include among others, chiropractic spinal manipulation, acupuncture, transcutaneous electric nerve stimulation (TENS), exercises, and spinal decompression, (Anonymous, 2010).

In other cases surgical procedures may however be prescribed where non-invasive methods are not sufficient. Minimally invasive procedures such as a microdiscectomy or laminectomy are first considered. In a microdiscectomy (microdecompression spine surgery), a small portion of the bone over the nerve root and/or disc material from under the nerve root is removed to relieve neural impingement and provide more room for the nerve to heal. Similarly, the lumbar laminectomy (open decompression) is also designed to remove a small portion of the bone, but in the region of the facet joint. The lumbar laminectomy also differs from the microdiscectomy in that the incision is longer and there is more muscle stripping in order to gain access to the lamina (Ullrich, 2009).

In more severe cases, where the intervertebral disc has degenerated significantly, disc fusion (*arthrodesis*) or a total disc replacement (*arthroplasty*) procedure may be considered. The choice in treatment is however still controversial, and two philosophies of support have emerged – namely those who “refuse to fuse” and the “I don’t believe in disc replacement” groups. For a long time, disc fusion has been considered the “gold standard” for treating DDD. In many cases, surgeons are unable to identify the exact location of the pain generator prior to surgery, and fusion is effective in eliminating the source(s) of pain by stabilizing the entire joint. However, concerns about how disc fusion affects degeneration in the adjacent discs (so-called adjacent disc disease or adjacent level degeneration (ALD)), has led a growing trend towards the use of motion preserving devices, such as intervertebral disc implants, to treat DDD (Park, Garton, Gala, Hoff, & McGillicuddy, 2004), (Cheh, et al., 2007), (Harrop, et al., 2008), (Matsumoto, et al., 2009), (Higashino, et al., 2010).

These intervertebral disc implants are however not without their own set of concerns. With a stringent list of contraindications, patient eligibility in many cases is limited (up to 95% contraindicated for lumbar TDR, (Huang & Cammisa, 2004), (Wong, 2005)) and surgeons are left with few options but to default back to a fusion procedure in such cases.

With strong arguments and clinical follow up studies for both treatment philosophies (Khan & Stirling, 2007), (Kishen & Diwan, 2010), the role of total disc *arthroplasty* (TDA) in the treatment of spinal pathology is still unclear (De Kleuver, Oner, & Jacobs, 2003), (Gamradt & Wang, 2005), (Guyer & Ohnmeiss, 2003), (Huang, Girardi, Cammisa, Tropiano, & Marnay, 2003).

1.2 Problem Statement

Typical complications that are still observed in some cases of disc implants include: Anterior migration of the disc, subsidence (sinking of the disc), lateral subluxation (partial dislocation of a joint), evidence of

polyethylene wear, and loosening with *osteolysis* (degeneration of bone tissue through disease) (Van Ooij, Oner, & Verbout, 2003). One of the most prevalent reasons for disc failure is incorrect positioning of the implant (Bertagnoli, 2005). This is made more difficult by the fact that every patient's anatomy and condition requiring surgery is unique. Manufacturers of disc implants compensate for these dissimilarities by creating different standard size implants. Surgeons then try to select the most suitable match during surgery after *discectomy*, by pushing various trial sizes into the vertebral space before placing the final implant. This trial-and-error technique relies heavily on the level of experience of the surgeon and could lead to TDR device under sizing and inaccurate positioning of the implant, which could lead to implant subsidence and fracture (Leary, Regan, Lanman, & Wagner, 2007), (Shim, Lee, Maeng, & Lee, 2005), (Van Ooij, Oner, & Verbout, 2003), (Van Ooij, Schurink, Oner, & Verbout, 2007), (Cinotti, David, & Postacchini, 1996), (Zeegers, LMLJ, Laaper, & Verhaegen, 1999).

Although long-term follow-up is necessary to fully understand the variety of complications that may occur due to subsidence with TDR, recent studies from both TDR and fusion cage literature have shown that kyphotic deformity (deformity of the natural spine curvatures), neural element compromise, great vessel compression, small bowel obstruction, pain, wear debris leading to *osteolysis*, and the need for revision surgery are some of the complications that may develop (Leary, Regan, Lanman, & Wagner, 2007), (Van Ooij, Oner, & Verbout, 2003), (Van Ooij, Schurink, Oner, & Verbout, 2007), (Wagner, et al., 2006), (Cinotti, David, & Postacchini, 1996), (Oxland, Grant, Dvorak, & Fisher, 2003).

Subsidence depends, among other things, on the stiffness and strength of the implant-endplate interface and factors that influence this interface include the bone mineral density (BMD), amount of the cartilaginous endplate removed during surgery, anteroposterior position of the implant (the posterolateral region has been shown to give greatest resistance to subsidence while central region the least (Lowe, et al., 2004)), implant shape and implant size (Hasegawa, Abe, Washio, & Hara, 2001), (Tan, Bailey, Dvorak, Fisher, & Oxland, 2005), (Gstoettner, D, Liebensteiner, & Bach, 2008), (Auerbach, Ballester, Hammond, Carine, Balderston, & Elliott, 2010), (Van der Houwen, Baron, Veldhuizen, Burgerhof, Van Ooijen, & Verkerke, 2010).

Most existing disc implants consist of endplates that are designed relatively flat in comparison to the concave bony endplate geometry. In order to accommodate the implant, the bone endplates are often surgically reduced to a flat plane and a slot is cut to receive the implant keel (fin-like protrusion to secure the implant). This action compromises the strength of the vertebral shell and reduces its ability to withstand pressure and can lead to implant subsidence or vertebral fracture (Auerbach, Ballester, Hammond, Carine, Balderston, & Elliott, 2010), (Lowe, et al., 2004). A more elegant solution will be to leave the endplates as intact as possible and rather adapt the shape of the implant to match the geometry of the bone.

One approach may be to design the implant endplates with some measure of generic concavity to match that of the bone, based on morphometric studies of different population groups. However Van der Houwen contends that data on the prevalent shapes of the vertebral surfaces are scarce, citing 10 studies that have investigated the *morphometry* of vertebral bodies and their endplates, using a variety of methods (Cadaver, CT, MRI, and X-Ray). (Van der Houwen, et al., 2010).

Therefore, considering the issues mentioned above, it is feasible to conclude that there exists a need for improving the design and manufacture of the endplates of artificial disc implants, in both form and function. And addressing this need should assist surgeons to consistently position disc implants more accurately, improve the fitment and fixation of the endplates to the vertebrae, while simultaneously decreasing the risk of implant subsidence.

As various imaging and manufacturing technologies have developed, the option for individual, patient-specific implants is becoming more of a practical reality than it has been in the past. The combination of CT images and Rapid Manufacturing for example is already being used successfully in producing custom implants for maxilla/facial and cranial reconstructive surgeries (De Beer, Dimitrov, & Van der Merwe, 2008).

However in the area of spinal implants, customization has not yet come to the forefront and with growing capabilities in both software and manufacturing technologies, these opportunities need to be investigated and exploited wherever possible.

1.3 Aims, Objectives and Hypothesis

The aim of this study will be to develop and propose a process chain that will enable the custom design and manufacture of an intervertebral disc implant. Customization will specifically be focused on matching the interface of the implant to the geometry of the vertebral endplates. Specific objectives to reach these aims are as follows:

- Develop and verify procedures for obtaining patient information and appropriate scan data.
- Develop the procedures and tools for designing the disc implant according to identified anatomical landmarks.
- Assess and measure the improvement in expected load distribution
- Measure the expected improvement in stiffness and related reduction in subsidence

Research Hypothesis

The research hypothesis for the study is defined as follows:

The use and implementation of a new, integrated methodology for digital design and manufacturing of patient-specific intervertebral disc implants with matching endplate interface geometries will significantly reduce the risk of implant subsidence during total disc replacement.

1.4 Roadmap of Document

The outline for this thesis has included the preceding introduction and a description of the problem that is being addressed. Chapter 2 provides a literature basis for this study and includes an historical review of intervertebral disc designs and the move toward motion preservation. A critical assessment of selected disc implants is included, which is followed by a review of literature that has studied the clinical outcomes of TDR and how they compare with the fusion procedure. The conditions are also highlighted for treatment selection based on indications and contraindications of the patient. Chapter 2 concludes by discussing the concepts and classification of customization in general and then specifically for implants, along with the regulatory issues that are required. Chapter 3 presents the steps involved in the process chain for the design and manufacture of a custom-fit intervertebral disc implant. A diagram representing the process chain with eight steps are shown and discussed in detail. Chapter 4 presents the proof of the hypothesis in the form of experimental research results. A mechanical test comparison between flat and custom-fit endplate geometry was performed on cadaveric bones to investigate decreased levels of subsidence due to better load distributions. Results are analysed statistically and Chapter 5 brings the report to a close with conclusions as well as a set of recommendations for further studies in this field of research.

Literature Review



2

2 Literature Review

This chapter gives a brief introduction to the anatomy of the vertebral column and intervertebral disc, which is followed by a discussion on the artificial disc implant and how it has developed over the years. A critical analysis of the most common existing disc implants is discussed after which customization of implants in general will be considered along with the regulatory issues that accompany customization.

2.1 Relevant Spinal Anatomy

Vertebral column and bones

The musculoskeletal system of the human body is made up from a very intricate combination of bones, muscles and tendons. Within this system, the vertebral column forms the skeleton of the back and the main part of the axial skeleton (Figure 1).

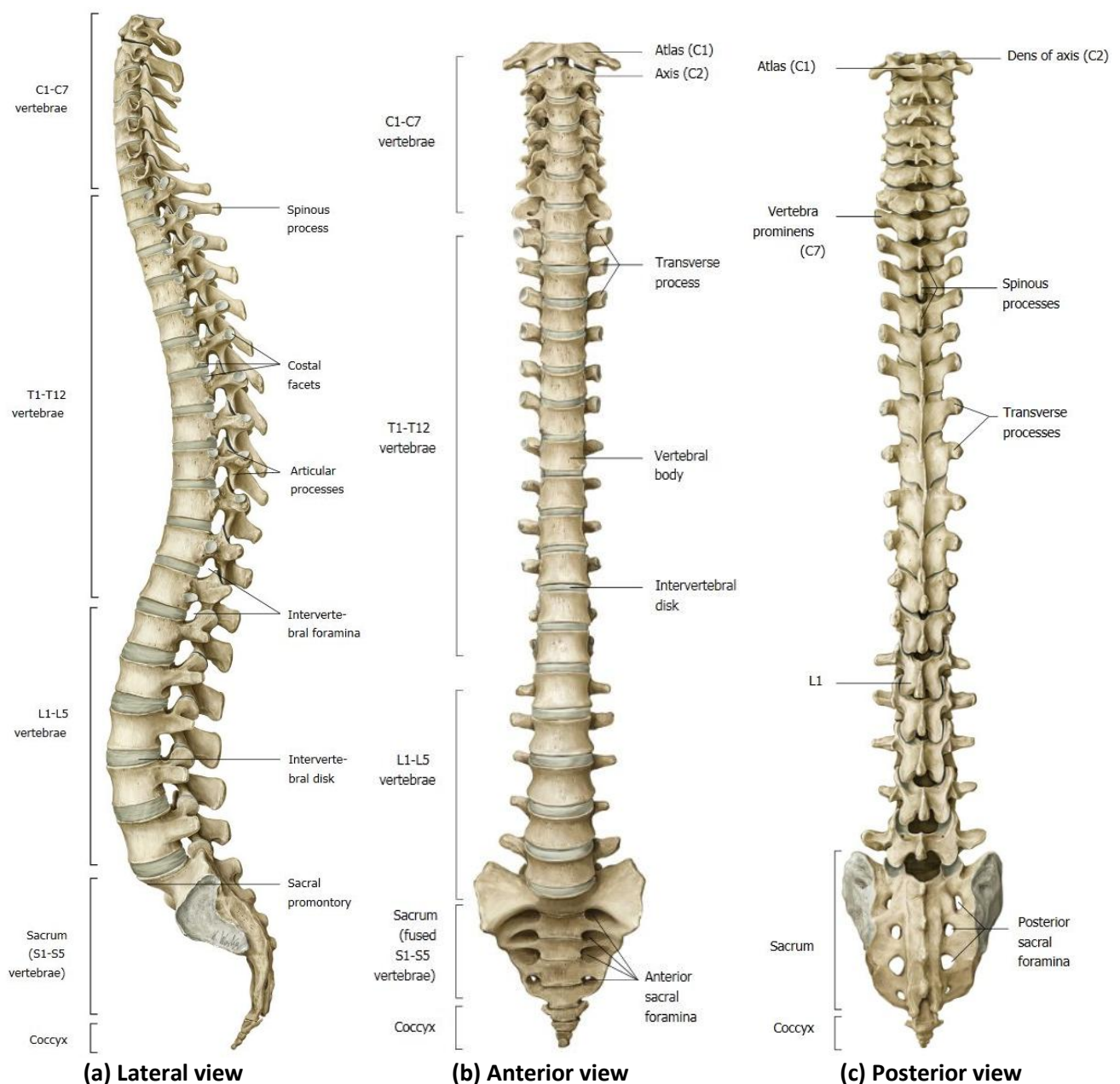


Figure 1 – Bones of the vertebral column (Gilroy, MacPherson, & Ross, 2008)

It consists of 33 bones called vertebrae, 24 of which are mobile (7 cervical, 12 thoracic, and 5 lumbar). Note in Figure 1 where these bone groups are situated. The abbreviations C, T, and L are used as prefixes followed by a number that refers to a specific vertebra at each different region of the column. The bones are numbered sequentially from the top down. For example, L5 would refer to the lowest vertebral bone in the lumbar region. The four natural curvatures of the spine are also visible in Figure 1(a). The thoracic and sacral curvatures (primary curvatures) are concave anteriorly, whereas the cervical and lumbar curvatures (secondary curvatures) are concave posteriorly. Figure 2 to Figure 4 shows superior views of the anatomy of typical vertebrae for the cervical, thoracic and lumbar regions respectively. Notice that the vertebral body increases in size to carry higher loads as one progresses down the spine towards the lumbar region.

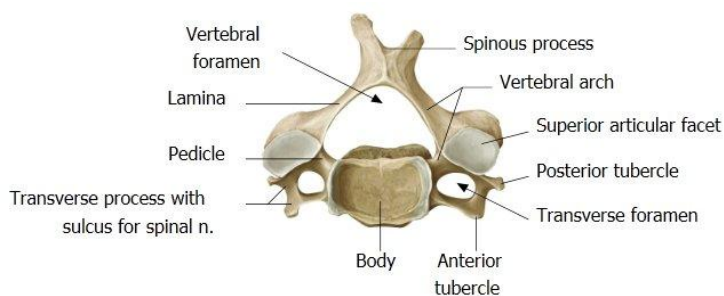


Figure 2 – Typical cervical vertebra (C4) (Gilroy, MacPherson, & Ross, 2008)

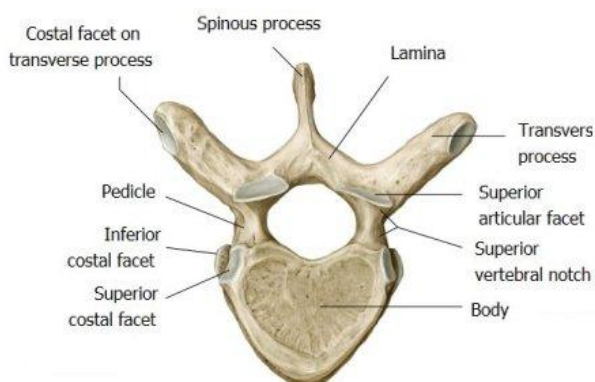


Figure 3 – Typical thoracic vertebra (T6) (Gilroy, MacPherson, & Ross, 2008)

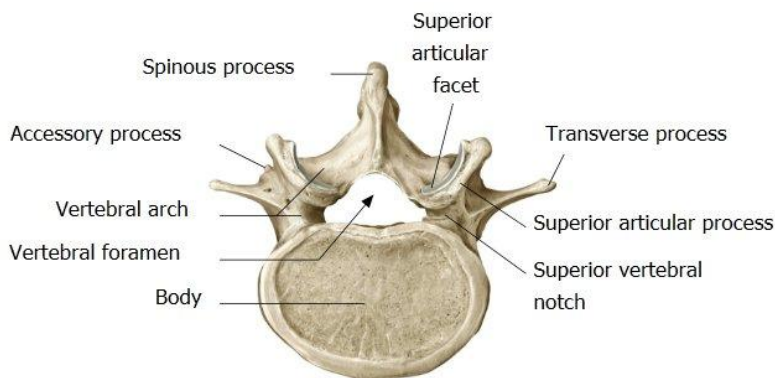


Figure 4 – Typical lumbar vertebra (L4) (Gilroy, MacPherson, & Ross, 2008)

Joints of the Vertebral Column

The vertebral column provides a partly rigid and partly flexible axis for the body and a pivot for the head. Consequently, it has important roles in: posture, support of body weight, locomotion, and protection of the spinal cord and nerve roots. The stability of the vertebral column is provided by the shape and strength of the vertebrae and by the intervertebral discs, ligaments and muscles. The movable vertebrae are connected by five main types of joints, namely the atlanto-occipital, atlantoaxial, uncovertebral, intervertebral and zygapophyseal (or facet) joints – all of which work together to give the column its range of motion. Figure 5 indicates the relative locations for each of these types of joints.

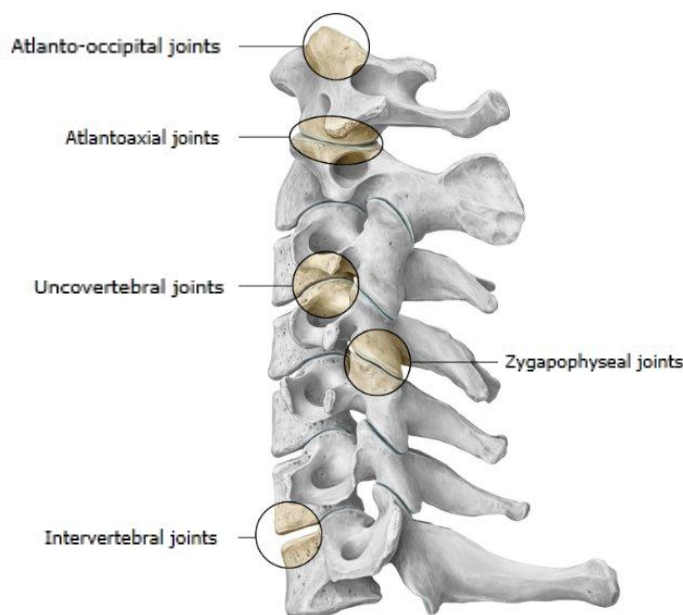


Figure 5 – Joints of the vertebral column (Gilroy, MacPherson, & Ross, 2008)

The resilient intervertebral discs form the main connection between the vertebral bodies and play an important role in movements between the vertebrae, and in absorbing shocks transmitted up or down the vertebral column. They vary in size and thickness in the different regions of the column. For example, the discs are thinnest in the thoracic region and thickest in the lumbar region. In the cervical and lumbar regions the discs are thicker anteriorly, making them wedge-shaped to accommodate the natural curvatures of the spine. Each disc is composed of an external annulus fibrosus which surrounds the internal gelatinous nucleus pulposus.

The annulus fibrosus is composed of concentric lamellae of fibrocartilage, which run obliquely from one vertebra to another. Some fibres in one lamella are at right angles to those in adjacent ones. This arrangement, while allowing some movement between adjacent vertebrae, provides a very strong bond between them.

The nucleus pulposus core of the intervertebral disc is more cartilaginous than fibrous and is normally highly elastic. It is located more posteriorly than centrally and has a high water content until old age. It acts like a shock absorber for axial forces and like a semi-fluid ball bearing during flexion, extension, rotation, and lateral flexion of the vertebral column. The nucleus pulposus is avascular and receives its nourishment by diffusion from blood vessels at the periphery of the anulus fibrosus and from the adjacent surfaces of the vertebral bodies. Figure 6 and Figure 7 provide sagittal and superior sectioned views of the intervertebral disc. Notice how the relative position of the nucleus is situated more posteriorly and the internal cancellous or trabecular bone structure is revealed.

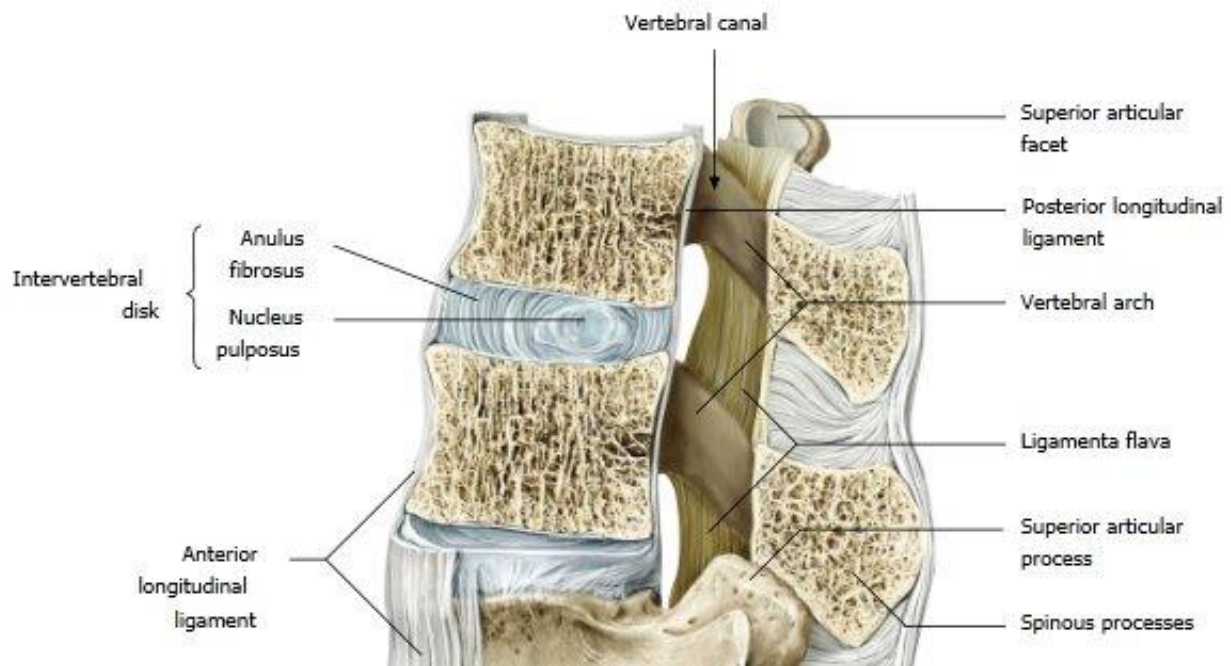


Figure 6 – Sagittal section of T11-T12, left lateral view, indicating intervertebral disc (Gilroy, MacPherson, & Ross, 2008)

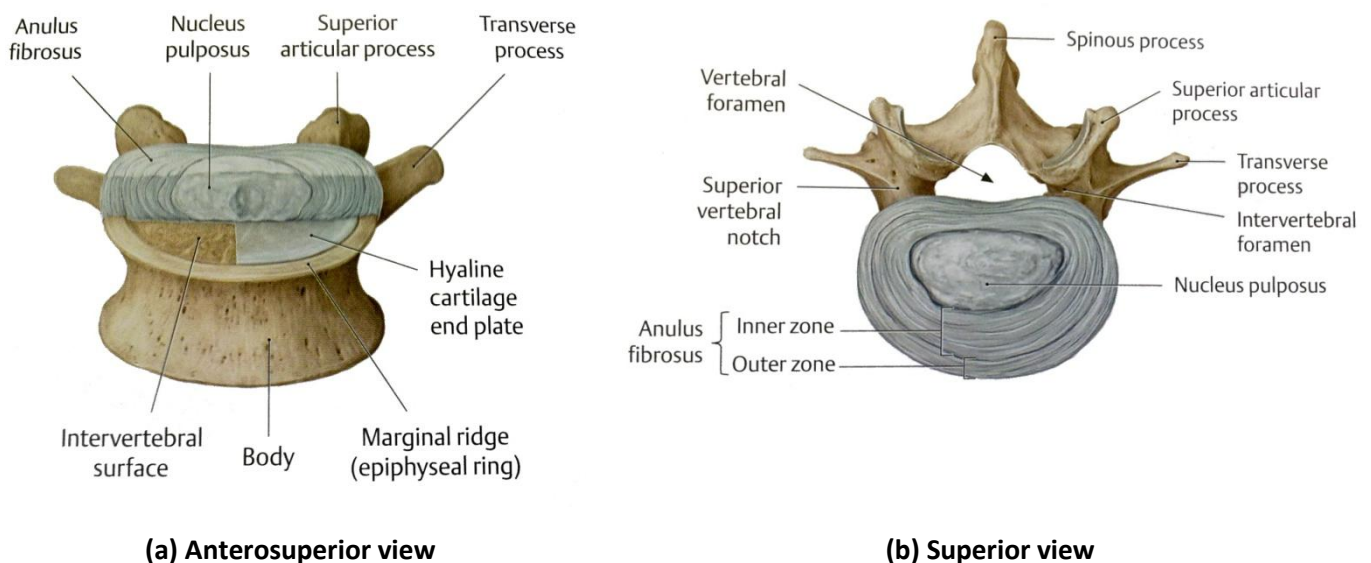


Figure 7 – Structure of intervertebral disc (Gilroy, MacPherson, & Ross, 2008)

Disc herniation in the lumbar spine

As people get older, their nuclei pulposi lose their turgor and become thinner due to dehydration and degeneration. Signs of moderate degeneration are already observed in 20% of teenagers, and with ageing, this percentage rapidly increases especially with men. Subsequently, 10% of men aged 50 years and 60% of men aged 70 years already indicate severe disc degeneration (Miller, Schmatz, & Schultz, 1988). As the stress resistance of the annulus fibrosus declines with age, the tissue of the nucleus pulposus may protrude through weak points under loading (especially during flexion of the spine). If the fibrous ring of the annulus ruptures completely (either posteriorly (Figure 8) or posterolaterally (Figure 9)), the herniated material may compress nerve roots and blood vessels of the intervertebral foramen. The herniated nucleus is highlighted by red circles in the figures below. These patients often suffer from severe local back and/or leg pain and may also experience weakening of the associated muscles that are connected to the affected spinal nerve(s). With treatment, this type of back pain usually begins to fade, but it may gradually be replaced by *sciatica* (pain resulting from irritation of the sciatic nerve). About 95% of lumbar disc protrusions occur at the L4/L5 or L5/S1 levels (Moore, 1992). The remaining protrusions occur at the L3/L4 level.

Symptom-producing disc protrusions occur in the cervical region almost as often as in the lumbar region. When the neck undergoes hyperflexion or extension (such as in the case of a head on collision), a cervical disc may rupture and result in a herniated disc. The cervical discs most commonly ruptured are those between C5/C6 and C6/C7, compressing spinal nerve roots C6 and C7 respectively. The general rule is that when a disc protrudes, it may compress the nerve roots numbered inferior to the disc, i.e. L5 nerve by L4 disc, and C7 nerve by C6 disc. Such cervical disc protrusions result in neck, shoulder, and arm or hand pain.

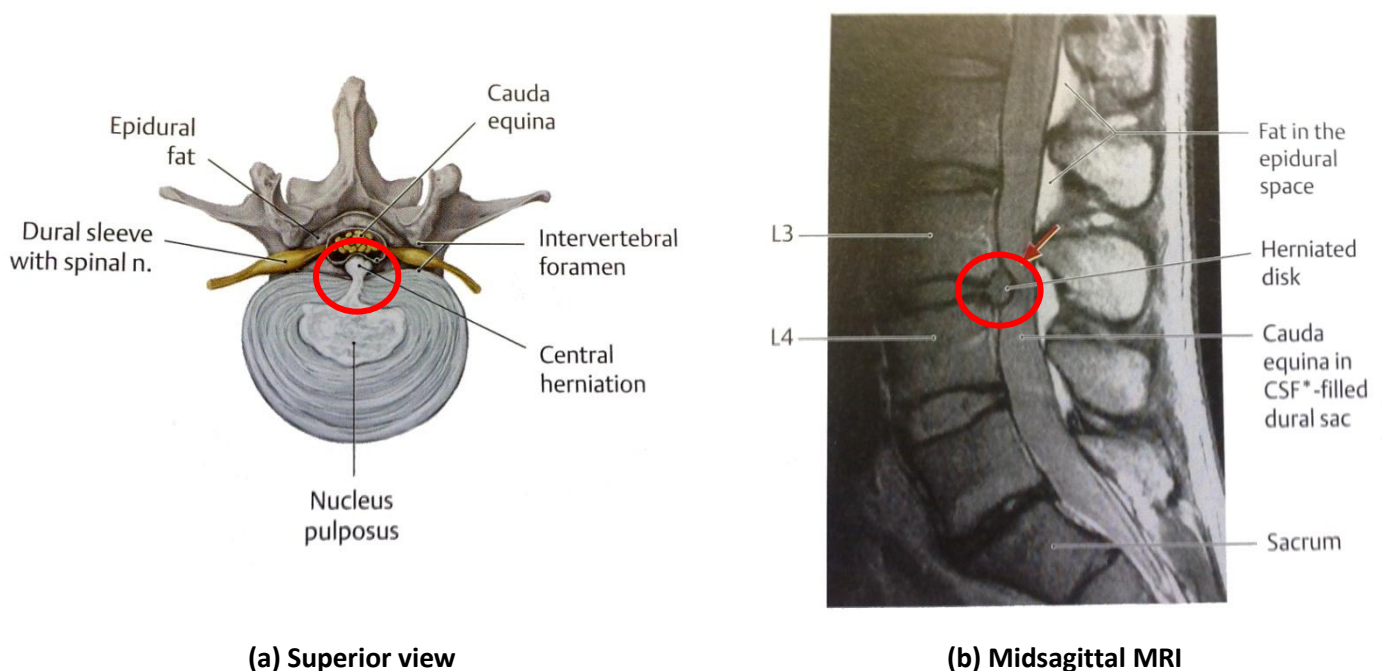
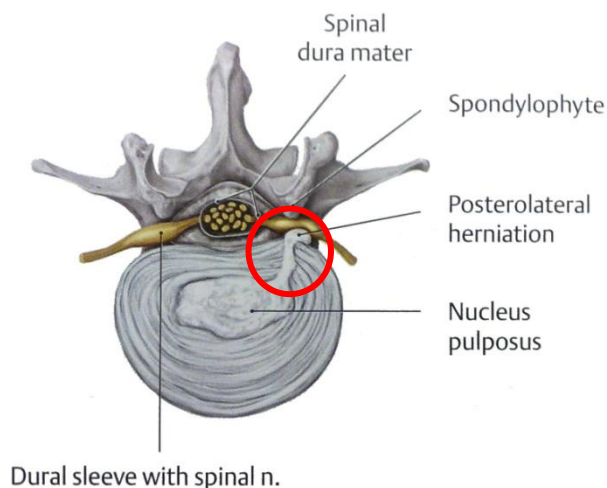
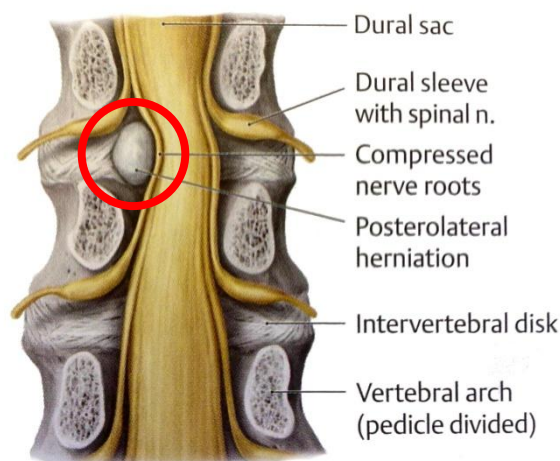


Figure 8 – Posterior herniation – modified from (Gilroy, MacPherson, & Ross, 2008)



(a) Superior view



(b) Posterior view, vertebral arches removed

Figure 9 – Posterolateral herniation – modified from (Gilroy, MacPherson, & Ross, 2008)

Disc herniation is one of several possible complications that may occur during the process commonly referred to as degenerative disc disease (DDD). A formal definition has been proposed by Adams:

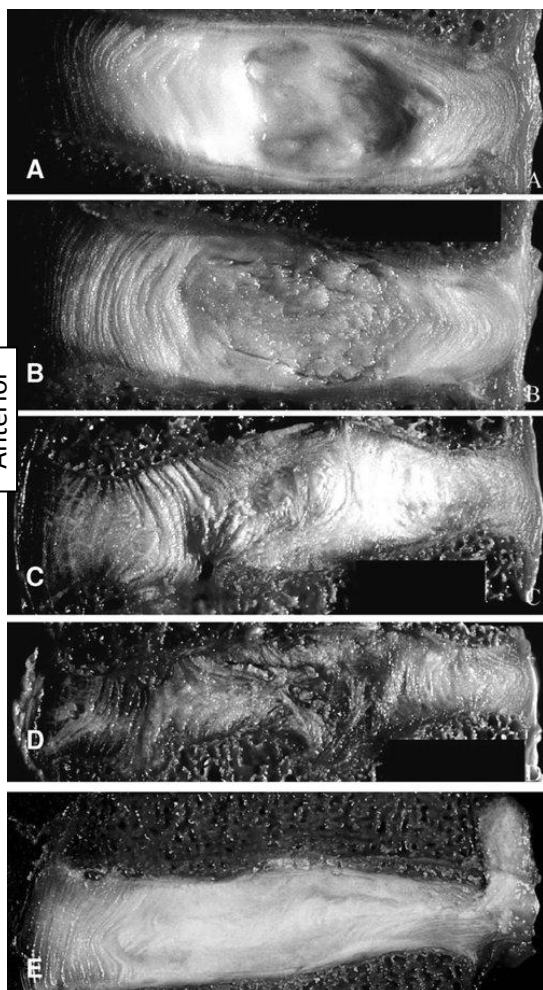


Figure 10 – Progressive disc degeneration (Adams & Roughley, 2006)

“The process of disc degeneration is an aberrant, cell-mediated response to progressive structural failure. A degenerate disc is one with structural failure combined with accelerated or advanced signs of aging. Early degenerative changes should refer to accelerated age-related changes in a structurally intact disc. Degenerative disc disease should be applied to a degenerate disc that is also painful.” (Adams & Roughley, 2006)

Figure 10 shows cadaveric lumbar intervertebral discs sectioned at the midsagittal plane (anterior on left). Discs (A-D) correspond to the 4-point scales typically used to grade “disc degeneration” from macroscopic features. (A) Young healthy disc (male, 35 yrs). (B) Mature disc (male, 47 yrs). (C) Disrupted young disc (male, 31 yrs). Note the endplate damage and inward collapse of the inner annulus. (D) Severely disrupted young disc (male, 31 yrs). Note the collapse of disc height. (E) Disc induced to prolapse in the laboratory (male, 40 yrs). Some nucleus pulposus has herniated through a radial fissure in the posterior annulus.

2.2 Artificial Disc Technology

The following section is included to describe the fundamentals and background to the development of artificial intervertebral discs. Starting off, a short history of the development of artificial disc technology is presented and includes a discussion about the current drive towards motion preservation and restoration through disc replacement (*arthroplasty*) in contrast to previous treatments of disc fusion (*arthrodesis*) which results in rigid fixation of spinal segments.

A critical analysis of existing and available artificial discs is then presented and includes an outline of essential design considerations that have been gathered from literature.

Finally this section is concluded with a brief look at indications and contraindications for TDR treatment and a step-wise philosophy for treating chronic degenerative low back and neck pain.

2.2.1 History of Development

The following historical overview has been adapted from (Bono & Garfin, 2004), and (Blumenthal S. , 2002):

Early Attempts

The first study that was published on the replacement of intervertebral discs was by David Cleveland in 1955 (Cleveland, 1955). Methylmethacrylate was injected between the vertebrae in the disc spaces of 14 patients during *discectomy*. According to Cleveland, this procedure yielded “acceptable” results.

Apart from injecting cement between the vertebrae, other concepts for disc replacement were also being explored in the 1960s and 1970s. In 1959, Paul Harmon created Vitalium spheres which, during the next two years, he implanted in 13 patients via an anterior retroperitoneal approach. He never published these results (Blumenthal S. , 2002). Following these attempts, Nachemson reported on a study which involved the injection of silicon rubber between the vertebrae into the disc space (Nachemson, 1962). From silicon rubber, to steel balls, Reitz and Joubert from South Africa reported on their results in 1964 after implanting 19 steel ball prostheses in the cervical spines of patients after *discectomy* (Reitz & Joubert, 1964). Similar to Reitz and Joubert, Fernström from Sweden, also independently implanted stainless steel spheres. However he implanted them in both the cervical as well as lumbar spine after *discectomy* (Blumenthal S. , 2002). In 1966, his results were published after implantation of more than 100 patients (Fernström, 1966). He concluded that the results obtained were better than *discectomy* on its own and similar to the results of *discectomy* and fusion. Even though this procedure gave acceptable clinical results, it was ultimately abandoned due to subsidence occurring between the steel balls and the vertebral end plates. These subsidence failures were due both to the inherent stress concentrations at the point of contact as well as the biomechanical modulus mismatch between the metal and the bone. Figure 11 shows an example of subsidence that was observed. The profiles of the subsided vertebral endplates are indicated with red lines, showing the amount by which the steel balls have been depressed.

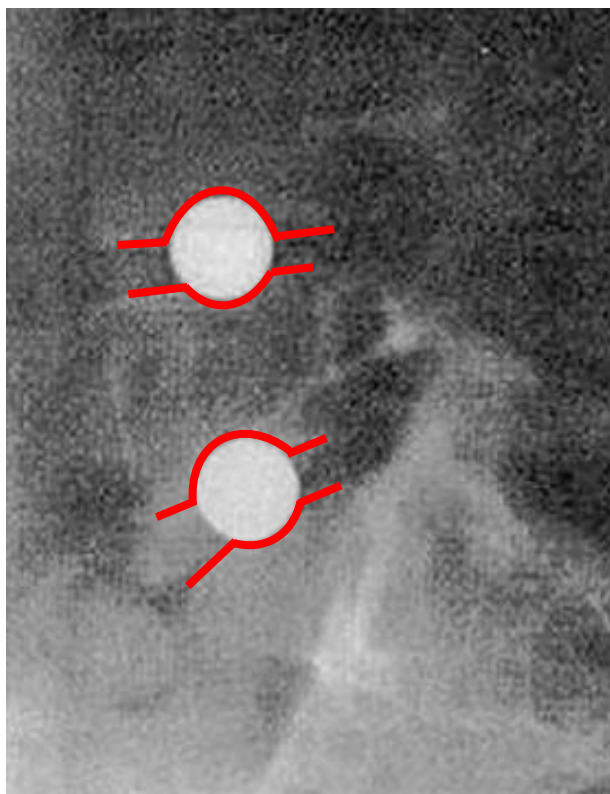


Figure 11 - Subsidence failure of Fernström's steel balls

Addressing these failure mechanisms, Fassio was the first to design a clinically implanted elastic disc replacement. The central part of his design resembled Fernström's steel ball, except that it was made out of silastic – an inherently compressible material with shock-absorbing properties. In addition to this silastic central portion, it was bordered by a horseshoe-shaped, flat, incompressible plateau, which was intended to prevent subsidence. After a 4 year follow-up on three patients that received this implant, the device had subsided and migrated into the vertebral body in all the patients (Alsema, Deutman, & Mulder, 1994).

In retrospect, the overall surface of the implant, although greater than that of Fernström's metal ball, covered only a small percentage of the end plate. Also, articulation still relied, at least partly, on shear forces between the silastic implant and bone. No further implantations were undertaken, or reported. The lessons learned from the failure of Fernström's balls and Fassio's silastic device can be summarized as follows (Bono & Garfin, 2004):

- First, the area of contact between the implant and host bone should be maximized to minimize the chance for subsidence.
- Second, a synthetic-on-synthetic, instead of synthetic-on-bone, articulating surface should be employed.
- Third, the material that is in contact with the bone should have as close a modulus of elasticity to the bone as possible.

- Another feature that was common to both implants, but was not clearly a contributing factor to failure, was a fixed axis of rotation within the posterior third of the disc space.

Other devices progressed to animal testing but were never clinically implanted. Kostuik (Kostuik, 1997) developed a total disc replacement that rotated around an articulating hinge within the posterior third of the disc space (Figure 12). A spring, interposed between the two metallic end plates anterior to the hinge, was intended to produce some shock-absorption properties. Although it performed well during cyclical in vitro testing, the device failed with animal implantation and clinical use has not been reported.

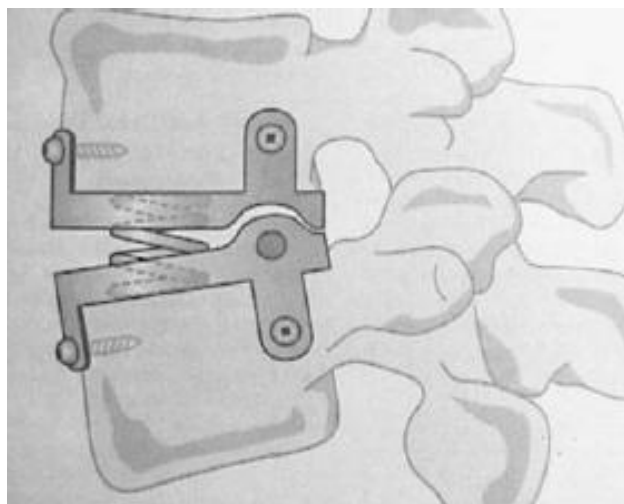


Figure 12 – Kostuik's total disc replacement design (Bono & Garfin, 2004)

Several other disc designs were introduced in the 1970s and 1980s. Many of these discs never progressed into clinical applications and were abandoned after very limited use. During the 1980s and 1990s, the most commonly used total disc replacements, the SB Charité and the ProDisc, were developed and introduced. Since then, various other disc manufacturers have followed suit by developing different iterations of an essentially typical ball-and-socket type design.

While results over the last 20 years are showing promise and improvements over early attempts, there still remain several concerns over the efficacy and longevity of these devices. The following section will therefore pose a critical review of devices that have shown the most promise, in order to achieve a summarised list of areas for possible improvement.

2.2.2 Critical Analysis of Existing Artificial Discs

There are a number of factors which must be considered in the design and implantation of an effective disc prosthesis. The device must maintain the proper intervertebral spacing, allow for motion, and provide stability. Natural discs also act as shock absorbers, and this may be an important quality to incorporate into prosthetic disc design, particularly when considered for multilevel lumbar reconstruction. Furthermore, the artificial disc must not shift significant axial load to the facets. Placement of the artificial disc must be done

in such a way as to avoid the destruction of important spinal elements such as the facets and ligaments. The importance of these structures cannot be overemphasized.

An artificial disc must exhibit tremendous endurance. The average age of a patient needing a lumbar disc replacement has been estimated to be in the region of 35 years. This means, that to avoid the need for revision surgery, the prosthesis must last at least 50 years. It has been estimated that an individual will take 2 million strides per year and perform 125,000 significant bends; therefore, over the 50-year life expectancy of the artificial disc, there would be over 106 million cycles. This estimate discounts the subtle disc motion which may occur with the 6 million breaths taken per year. A number of factors in addition to endurance must be considered when choosing the materials with which to construct an intervertebral disc prosthesis. The materials must be biocompatible and display no corrosion. They must not incite any significant inflammatory response. The fatigue strength must be high and the wear debris minimal, and should allow for scan imaging (MRI, CT, or X-Rays, etc.).

The intervertebral disc prosthesis ideally would replicate normal range of motion in all planes. At the same time it must constrain motion. A disc prosthesis must reproduce physiologic stiffness in all planes of motion plus axial compression. Furthermore, it must accurately transmit physiologic stress. For example, if the global stiffness of a device is physiologic but a significant non-physiologic mismatch is present at the bone-implant interface, there may be bone resorption, abnormal bone deposition, endplate or implant failure.

Finally, the implant must be designed and constructed such that failure of any individual component will not result in a catastrophic event. Neural, vascular, and spinal structures must be protected and spinal stability maintained in the event of an accident or unexpected loading.

A further very important aspect of the disc design is not only its efficacy during operation, but also the ease with which revision surgery can be done. McAfee states that revision anterior lumbar surgery can be exceedingly difficult, and a revision strategy for artificial disc prostheses should be developed (McAfee, Comments on the Van Ooij Article, 2005). Several other sources of literature (Van Ooij, Oner, & Verbout, 2003), (Traynelis & Haid, 2004) optimistically state that – due to the patient age (between 40-50 years old) from when typical TDR surgery is performed – artificial disc prostheses should have a lifespan of approximately 40 years. It certainly would be preferable if all joint prostheses had an average survival rate of 40 years. However, this has not been the history of total joint replacement. Total hip replacements (THRs) have been commercially available for 40 years, with an average survival rate of 15 years, and some still failing prior to that due to a variety of factors (Alsema, Deutman, & Mulder, 1994). The average total knee survivorship is 10 years (Worland, Johnson, Alemparte, Jessup, Keenan, & Norambuena, 2002). One should therefore be conservative to conclude that the same results may be expected for total disc replacement surgery, and proactive design strategies should be considered to facilitate anticipated revision surgeries.

A number of biomechanical studies about lumbar TDR have been published, but the relationship between the different designs and the resulting biomechanics of the surgically changed spine has not been clearly described (Galbusera, et al., 2008). Therefore, Galbusera conducted an extensive literature review (98 papers) of selected lumbar TDR devices and evaluated their possible relationships with the aims of TDR regarding their geometrical, mechanical and material properties. The comparison charts are shown in Appendix B along with a list of the relevant sources.

The review and basis for comparison was structured along the aims of TDR, related to the following biomechanical parameters:

- Restoration of physiological kinematics and mobility, avoiding segmental instability
- Restoration of a correct spinal alignment
- Protection of the biological structures, such as the adjacent intervertebral discs, the facet joints and the ligaments, from overloading and resulting accelerated degeneration
- Device stability and wear

The list of disc prostheses commercially available or under clinical trial that was included in the review is shown below in Table 1.

[Restoration of physiological kinematics and mobility](#)

Most papers reported that restoration of correct spinal kinematics (in terms of instantaneous axis of rotation (IAR) and range of motion (ROM)) is achieved by both semi-constrained and unconstrained disc prostheses. However, some conflicting findings have been reported, where either an increase or a decrease in ROM was reported - thus indicating that some aspects still need to be clarified. The reported difference between the geometrical centre and the IAR location of semi-constrained disc prostheses need to be verified, in particular with reference to the possible measurement error in the estimation of the IAR position.

[Spinal alignment](#)

The increase of the segmental lordosis (increase in hollowing of lower back) is a rather frequent consequence of lumbar TDR, described in many papers, with possible clinical consequences. The clinical relevance of such a significant lordosis alteration needs to be evaluated in long-term follow-up studies. Up to now, no relation between the postoperative sagittal alignment and the prosthesis design has been demonstrated. A pre-existing minor *scoliosis* should be defined as an absolute contraindication for TDR; however, exclusion criteria for lumbar TDR generally admit *scoliosis* up to 11° *Cobb angle* (McAfee, et al., 2006). Semi-constrained devices may help in the restoration of the rotational stiffness of the functional unit, as suggested by McAfee (McAfee, et al., 2006).

Name	Manufacturer	Classification	Image
Flexicore	Stryker, Kalamzoo, MI, USA	Constrained	
Maverick	Medtronic Ltd, Memphis, TN, USA	Semi-constrained	
ProDisc	Synthes Inc., West Chester, PA, USA	Semi-constrained	
Charité	Depuy Acromed Inc., Mountain View, CA, USA	Unconstrained	
Acroflex (discontinued)	Depuy Acromed Inc., Mountain View, CA, USA	Unconstrained	

Table 1 – Classification of lumbar disc prostheses that were reviewed (Galbusera, et al., 2008)

Protection of the biological structures

In general, most of the reviewed papers described an increase of the facet loads, for both semi-constrained and unconstrained artificial discs, but with some contrasting results jeopardizing a clear-cut statement. Oddly, only two papers addressed the quantification of the stresses in the adjacent levels (Dooris, Goel, Grosland, Gilbertson, & Wilder, 2001), (Goel, et al., 2005), despite the prevention of adjacent degeneration being probably the most important aim of TDR. In order to avoid spinal instability and excessive loads in the facet joints and the ligaments McAfee analysed the possibility to introduce constraints in the prosthesis design (McAfee, et al., 2006). A more constrained design should be able to share a greater portion of load,

thus decreasing the loads through the facet joints and in the ligaments, possibly allowing the restoration of a correct load sharing pattern. However, further studies, which directly determine the influence of the prosthesis design on the segmental internal stress condition, are required to demonstrate the validity of this assertion.

Device stability and wear

Generally, due to the lower stress sustained and the interface with surrounding biological structures, unconstrained designs appear to be more suitable than semi-constrained designs. However, as discussed in the previous paragraph, more constrained designs may be advantageous in terms of load sharing, protecting the surrounding biological structures from overloading. In $\frac{3}{4}$ patients, implant wear was associated with biomechanical issues such as subsidence, migration, under sizing, and adjacent fusion (van Ooij, Kurtz, Stessels, Noten, & van Rhijn, 2007). Because of the demonstrated potential for *osteolysis* (reduction in bone density) in the spine, clinical problems related to these factors may be of importance and need to be investigated with long term follow-up studies.

In summary, from this critical analysis six factors for improvement have been identified for further studies and design improvement:

1. The use of multiple components – either polyethylene on metal or metal on metal – result in material wear debris. Although reported literature has shown this to be minimal, especially in the case of metal on metal devices, the ideal would be no wear debris at all. Hence the alternative of a single component device. This alternative poses other difficulties, such that the design must allow for natural movement as well as shock absorbency. Secondly, the issue of material wearing will be replaced by a concern over material fatigue as the design constraint and determining factor for component life.
2. A closely related conclusion to the use of multiple components, is the use of multiple materials. The Maverick and other similar discs have moved to metal on metal design, thereby employing the same materials in contrast to polyethylene to metal designs like the Charité and ProDisc. An unexpected result of using metal on metal – a prominent squeaking noise – has however been experience in some cases (Eksteen, 2009). The use of a single component design (as mentioned in point one above) would place a high demand on material flexibility while at the same time require high ductility. Titanium is currently a viable option, but the author suggests the possibility of employing Rapid Manufacturing in order to produce functionally graded material components. This would typically enable designs to have specific materials at strategic design locations to impart those material qualities to the design.
3. Building from experience gained in hip and knee joint replacements, the reviewed literature and discs presented here employ ball-socket designs in much the same way. The natural intervertebral

disc however does not only impart mobility to the adjacently attached vertebrae, but also provides support and constraint in conjunction with the muscles. Further research is required to confirm the differences between unconstrained versus constrained devices, and the potential for design improvements that incorporate sufficient mobility and selective constraint is warranted.

4. A lack of shock absorbcency in existing designs has already been highlighted extensively in the preceding text. It is mentioned here again for the sake of completeness.
5. Finally, literature has indicated that positioning of endplates during implant insertion is extremely critical for a successful procedure. Lateral deviations from the centre line of as little as 3mm can lead to implant failure due to core separation from the endplates. In order to correctly position disc prostheses that employ this design type, surgeons must (with the aid of insertion instruments) essentially place the disc in such a way that the middle point of the spherical core is seated centrally to the sagittal plane. It is extremely difficult to position with exactness the middle point of a sphere, and is therefore no wonder that incorrect insertion (or so-called approach-related complications) has been reported as the main cause for implant failure. Bertagnoli (Bertagnoli, 2005) reports that 98% of complications are surgeon related – either due to
 - Wrong indication;
 - Wrong segment mobilisation and application technique; and
 - Wrong positioning of the implant.

2.2.3 Listed studies investigating clinical outcome after TDR

Among the numerous artificial intervertebral discs that have been patented, very few have undergone clinical trials (Szpalski, Gunzburg, & Mayer, 2002). Kishen and Diwan present a comparison of the outcomes of spinal fusion and disc replacement for degenerative conditions of the lumbar and cervical spine by means of a thorough literature study (Kishen & Diwan, 2010). Table 2 below list the sources of literature that was used as well as summarised clinical outcomes of two US Food and Drug Administration (FDA) approved disc implants, namely the Charité and the ProDisc. The studies are presented in order of increased follow up times, first for the Charité disc and then the ProDisc, so that one can assess whether the device's performance remains consistent over time.

Authors and Study Type	Materials & Methods	Outcome	Comments
(Blumenthal, et al., 2005) RCT (FDA investigational device exemption study)	205 Charité TDR versus 99 ALIF Mean age: 39 y F/U: 2 y	No significant difference in VAS/ODI; 57% (TDR) and 46% clinical success (FDA criteria); 73% (TDR) and 53% satisfaction; 70% (TDR) and 50% would have procedure again (P< 0.05);	Industry sponsored; Stand alone ALIF; Noninferiority study; 11 TDR (5.4%) and 9 (9.1%) fusion patients underwent additional surgery at index level
(Guyer, et al., 2009) RCT	90 Charité TDR versus 43 ALIF Mean age: 39 y F/U: 5 y	No significant difference in VAS/ODI/SF-36 (PCS); 58% (TDR) and 51% clinical success (FDA criteria); 78% (TDR) and 72% of patients satisfied	Industry sponsored; 43% lost to follow-up
(David, 2007) Retrospective	108 one-level Charité TDR patients Mean age: 36 y F/U: 10 y	82% good-excellent outcome; 89% return to work with 77% return to previous hard labour; Mean flex-ext ROM = 10.1°; 8 patients (7.4%) underwent revision surgery (posterior fusion at index level) and 3 patients (2.8%) underwent adjacent level surgery (2 disc herniation and 1 spinal canal stenosis)	106 patients (98%) available for follow-up
(Lemaire, Carrier, Sariali, Skalli, & Lavaste, 2005) Retrospective	107 Charité prosthesis (1-3 levels) Mean age: 39 y F/U: 10 y	90% good-excellent outcome; 91% returned to work; Mean flex-ext ROM = 10.3°; 12 (11.2%) post surgery complications: Minor posttraumatic subsidence (2), periprosthetic ossification (3), adjacent level degeneration (2) and requiring secondary fusion (5)	100 patients (93.5%) available for follow-up
(Zigler, et al., 2007) RCT (FDA investigational device exemption study)	161 ProDisc TDR versus 75 APF (1-2 Level) Mean Age: 40 y F/U: 2 y	No significant difference in ODI, pain, SF-36 scores; 53% (TDR) and 41% success (FDA criteria); 81% (TDR) and 69% would have same procedure again	Industry sponsored 6 Failures in TDR group: prosthesis migration (1), core migration (3), improper insertion of core (1), persistent pain requiring fusion (1)
(Berg, Tullberg, Branth, Olerud, & Tropp, 2009) RCT	80 TDR versus 72 fusion Age: 20-55 y F/U: 2 y	No significant difference in ODI, 84% (TDR) and 86% (fusion) improved; Minor difference in back and leg pain in favour of TDR	Three different prostheses used and two fusion procedures (PLF, PLIF); Small numbers in each group
(Tropiano, Huang, Girardi, Cammisa, & Marnay, 2005) Retrospective	64 ProDisc patients (1-3 level) Mean age: 46 y F/U: 7 to 11 y	75% good-excellent results; significant improvements in back and leg pain and disability	55 patients (86%) available for follow-up

Abbreviations: ALIF, anterior lumbar interbody fusion; APF, anterior-posterior fusion; FDA, Food and Drug Administration; ODI, Oswestry disability index; PCS, physical component scores; PLF, posterolateral fusion; PLIF, posterior lumbar interbody fusion; RCT, randomized controlled trial; TDR, total disc replacement; VAS, visual analogue scale; SF-36, short form (36) health survey.

Table 2 – List of studies analyzing the outcomes following lumbar total disc replacement (adapted from Kishen & Diwan, 2010)

The short-term outcomes of lumbar TDR seem to be better or at least equivalent to results following lumbar fusion. There was no significant difference in the Visual Analogue Scale (VAS) or Oswestry Disability Index (ODI) scores, thus indicating similar pain relief and improvements from disability respectively. FDA clinical success criteria at 2 years, is defined as the absence of device failure, major complications, or neurologic deterioration and greater than 25% improvement in ODI score. During the FDA investigational device exemption studies for the Charité (Blumenthal, et al., 2005) and the ProDisc (Zigler, et al., 2007), the TDR devices achieved 57% and 53% clinical success respectively, while fusion patients achieved 46% and 41% respectively. Similar clinical successes were reported for the Charité after five year follow up. After a 10 year follow up, between 80-90% of patients reported their outcome as good to excellent (Charité) and 75% reported good to excellent results in the case of the ProDisc after seven- to 11-year follow ups.

Kishen and Diwan also reviewed literature of studies investigating the 1-2 year outcomes of disc replacement between cervical vertebrae. The implant devices included were the Bryan and the Prestige ST discs (Medtronic Ltd, TN, USA), the ProDisc-C (Synthes Inc., PA, USA), the Mobi-C (LDR Spine, Texas, USA), and the PCM disc (NuVasive, CA, USA). Table 3 lists these studies along with their summarised results.

Authors and Study Type	Materials & Methods	Outcome	Comments
(Anderson, Sasso, Rouleau, Carlson, & Goffin, 2004) Prospective; BRYAN disc prosthesis	97 one-level and 39 two-level TDR F/U: 1 and 2 y	75 one-levels completed 2 y f/u 45 excellent, 7 good, 13 fair, and 8 poor; 30 two-levels completed 1 y f/u 21 excellent, 3 good, 5 fair, and 1 poor Significant improvement in SF-36 scores for one- and two-levels	Early results from European trial
(Sasso, Smucker, Hacker, & Heller, 2007) RCT; BRYAN disc prosthesis	56 TDR versus 59 ACDF Mean age: 42-46 y F/U: 2 y	TDR showed significant improvement in NDI, neck pain, and physical component score of SF-36 compared with ACDF; Arm pain relief and SF-36 (MCS) were similar	Subset of FDA trial; 61% follow-up at 2 y; 4 ACDF plus 3 TDR were reoperated; ACDF: plate plus fibular allograft
(Heidecke, Burkert, Brucke, & Rainov, 2008) Prospective; BRYAN disc prosthesis	59 prosthesis in 54 patients (5 two-level) Mean age: 46 y F/U: 2 y	43 excellent and 11 good neurological outcome (Odom criteria) 12% had motion < 3 degrees 29% had <i>heterotrophic ossification</i>	Mild postoperative kyphosis in first week after surgery
(Heller, et al., 2009) RCT; BRYAN disc prosthesis	242 TDR versus 221 ACDF One level Mean age: 44 y F/U: 2 y	NDI, neck pain score, and overall success were significantly better following TDR; Arm pain score, SF-36, neurologic success, and return to work status were not statistically different. Return to work was 2-week earlier in TDR group.	ACDF: plate plus allograft; 230 TDR and 194 ACDF available for 2 y f/u; 94% successful fusion; No spontaneous fusion in TDR group; 117 patients refused participation after randomization
(Mummaneni, Burkus, Haid, Traynelis, & Zdeblick, 2007) RCT (FDA-IDE) Prestige ST disc prosthesis	276 TDR versus 265 ACDF (single level) Mean age: 43 y F/U: 2 y	No significant difference in NDI, SF-36, neck and arm pain between groups Overall success and neurologic success were significantly higher in TDR group and a lower rate of adjacent level surgery	ACDF: ring allograft plus plate; 25% fusion, lost to F/U; Revision surgery: 0 (TDR) and 5 (fusion); Adjacent level surgery: 3 (TDR group) and 11 procedures in 9 patients (fusion group); Hardware removal: 5 (TDR) and 9 (fusion)

(Nabhan, et al., 2007) RCT ProDisc-C disc prosthesis	25 TDR versus 24 ACDF (one-level) Mean age: 44 y F/U: 1 y	No significant difference in neck and arm pain between the two groups	Small numbers with short follow-up
(Murrey, et al., 2009) RCT, FDA ProDisc-C disc prosthesis	102 TDR versus 106 ACDF (one-level) Mean age: 43 y F/U: 2 y	No difference between groups in neurologic success, NDI scores, VAS scores, satisfaction, adverse events, SF36, and overall success	10% in each group had prior surgery; 90% fusion following ACDF; Higher rate of revisions following ACDF
(Beurain, et al., 2009) Prospective Mobi-C disc prosthesis	85 prosthesis in 76 patients 67 one-level and 9 two-level Mean age: 43 y F/U: up to 2 y	Significant improvement in NDI and arm and neck pain VAS; Improved return to work after surgery with reduced narcotic use; 72% success rate and 91% would have the surgery again	12% had previous surgery 6/76 hybrid construct 11% had <3 degrees motion 9.1% adjacent level degeneration
(Park, Roh, Cho, Ra, Rhim, & Noh, 2008) Retrospective Mobi-C disc prosthesis	21 TDR versus 32 ACDF (one-level) Mean age: 46 y F/U: 1 year	No difference in NDI, VAS, and satisfaction rate	Small numbers with short follow-up
(Pimenta, McAfee, Cappuccino, Cunningham, Diaz, & Coutinho, 2007) Prospective PCM disc prosthesis	71 single level versus 69 multilevel TDR (229 levels in 140 patients) Mean age: 46 y F/U: 2 mo (26 mo)	Significantly better NDI and VAS scores in the multilevel group; Success rate (Odom criteria) was 90.5% versus 93.9%	Reoperation rates and adverse events were similar between groups

Abbreviations: ACDF, anterior cervical *discectomy* and fusion; FDA, Food and Drug Administration; IDE, investigational device exemption; NDI, neck disability index; RCT, randomized controlled trial; TDR, total disc replacement; SF-36, short form (36) health survey.

Table 3 – List of studies analyzing the outcomes following cervical total disc replacement (adapted from Kishen & Diwan, 2010)

Anterior cervical *discectomy* and fusion (ACDF) is generally associated with favourable clinical outcomes with respect to relief from neck and arm pain. Overall success is defined as greater than 15-point improvement in NDI scores, unchanged or improved neurologic status, absence of implant- or procedure related adverse events, and the absence of subsequent surgery or intervention. No significant difference was found between the NDI, VAS and SF-36 (short form (36) health survey) scores of ACDF versus TDR, except in the case of the Bryan disc, where TDR outperformed ACDF (Sasso, Smucker, Hacker, & Heller, 2007), (Heller, et al., 2009). The short-term results of TDR are therefore equivalent or compare favourably with ACDF. In addition, the drawbacks of ACDF, such as like ALD and bone graft donor site morbidity, can potentially be done away with by TDR, but longer-term follow-up is necessary to make definitive treatment recommendations.

2.2.4 Indications and contraindications

Even with the promising results and potential improvements that TDR suggests, surgeons and patients need to be aware of eligible candidates for this procedure. At present, literature indicates that contraindications are far more than the indications for such treatment.

The general indications according to Blumenthal (Blumenthal S. , 2002) for total disc replacement are similar to those established in the fusion literature, including back and leg pain unresponsive to appropriate attempts at nonoperative treatment. Nonoperative treatment includes but certainly is not limited to medication, various forms of physical therapy, activity modification and pain management. Disc replacement is not used to treat significant spinal deformity or primary *radiculopathy*. It should be avoided in patients with *osteoporosis* or instability, and certainly anything greater than a Grade I *spondylolisthesis* is a contraindication. Patients with significant canal stenosis or neural compressive disease, or pain related to significant scarring from previous surgery should not be treated by disc replacement.

Although facet joint ankylosis is an absolute contraindication, the extent of facet joint involvement needs to be considered in treating anterior column disease. As with any elective spine surgery, avoidance of disc replacement in patients with significant psychosocial issues is advised. Huang, has highlighted the most severe contraindications, and are listed here below (Huang, Girardi, Cammisia, Tropiano, & Marnay, 2003):

- *Facet arthrosis*
- Central spinal stenosis
- Lateral recess spinal stenosis
- Spondylolysis
- *Spondylolisthesis*
- Herniated Nucleus Pulposus with *radiculopathy*
- *Scoliosis*
- *Osteoporosis*
- *Pseudoarthrosis*
- Deficient posterior elements

There are apparently at least 30 more contraindications according to Wong (Wong, 2005), but these have been excluded from being listed here as the most severe are already indicated above and are also acknowledged by Wong.

Figure 13 below shows a proposed stepwise approach for the management of chronic degenerative low back and neck pain (excluding *spondylolisthesis* and stenosis). The abbreviations refer as follows; ALIF (anterior lumbar interbody fusion), OA (osteoarthritis), PLF (posterolateral fusion), PLIF (posterior lumbar interbody fusion), TDR (total disc replacement), TLIF (transforaminal lumbar interbody fusion).

Following a diagnostic work-up, patients undergo an intensive rehabilitation course consisting of structured physiotherapy that incorporates cognitive training and a psychological assessment. Facet injections are performed as a diagnostic and therapeutic measure, being fully aware of its limitations. If there has been no improvement at the 3-month mark, patients are reassessed by the surgical team with input from physiotherapists. If there is no radiologic correlation and the patient continues to suffer from severe pain, pain medication is initiated. If it becomes apparent that the cause of the symptoms is surgically treatable, the patient is offered surgery based on a shared decision-making process.

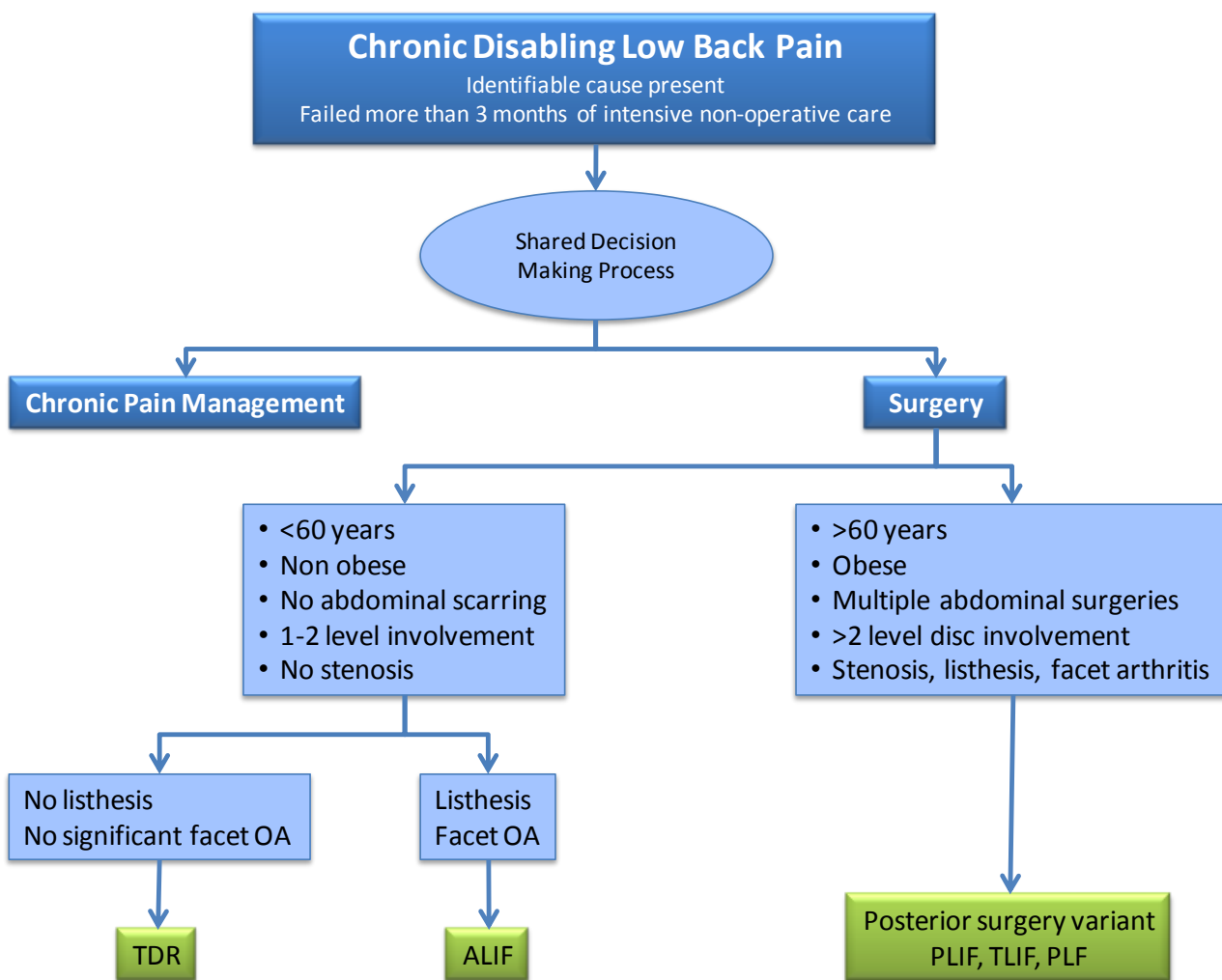


Figure 13 – An approach to the surgical management of chronic low back pain (Kishen & Diwan, 2010)

Based on the patient’s age and physical condition, further criteria determine a suitable choice of surgery. If the patient is older than 60 years, obese, has a history of previous abdominal surgeries, requires treatment to more than two levels or shows evidence of stenosis, listhesis or facet arthritis, then posterior lumbar interbody fusion (PLIF), transforaminal lumbar interbody fusion (TLIF), or posterolateral fusion (PLF) surgery is indicated. Alternatively, patients who are younger than 60 years, not obese, with no scar tissue from previous abdominal surgery, requiring treatment to one or two disc levels and show now signs of stenosis, qualify for either total disc replacement (TDR) or anterior lumbar interbody fusion (ALIF) surgery. If no listhesis and no significant facet osteoarthritis is present, TDR is indicated. Otherwise ALIF is prescribed.

A similar stepwise approach is followed when treating cervical degenerative conditions.

2.3 Customization of Implants by Layer Manufacturing in General

Over the last decade there has been a growing interest among physicians in the technology of medical models (generic term used to describe replicas of patient anatomy produced by means of Layer Manufacturing technologies) for the purpose of facilitating diagnosis, pre-operative planning and communication between colleagues and patients. An ability to create tangible models from medical imaging data (e.g. Computed Tomography (CT) and Magnetic Resonance Imaging (MRI)) has proven to be highly advantageous, especially within the field of craniofacial surgery where planning and performing an operation is extremely difficult due to the complex and variable anatomy. Historically, the uses for medical models by surgeons wanting to pre-plan surgery have fallen into the following five categories (Wohlers, 2010):

- Visualization of the patient's anatomy before treatment or surgery.
- Surgery or treatment simulation (actual cutting or measuring on the model) before intervention.
- Creation of custom implants, templates, or guides prior to surgery.
- Enhanced communication with others involved in patient treatment and their related staff.
- Improved communication and consent by the patient and patient's family concerning the upcoming procedure.

Many successful case studies have been achieved in these areas, with prominent examples from work by the Phidias Network and others (Anonymous, 2004). The RP4Baghdad project initialized in June 2005, has through its contributions also documented an extensive case study base of medical models produced (Anonymous, 2008a). What is however evident from these case studies, is the fact that the majority relate to applications in the cranio/maxillo-facial areas, and that medical models were produced for either surgical planning and communication or for the purposes of producing an implant through indirect methods (Wurm, Tomancok, Holl, & Trenkler, 2004), (Staffa, Nataloni, Compagnone, & Servadei, 2007), (Pereira, Ventura, Gaspar, Fontes, & Mateus, 2007), (Poukens, Haex, & Riediger, 2003). Further studies have been done to include applications in other areas of the body, including the hip, knee and femur (Harrysson, Cansizoglu, Marcellin-Little, Cormier, & West, 2008), (Harrysson, Hosni, & Nayfeh, 2007) and also in the foot (Schindel, Lampert, & Gross, 2005). With the advent and growth of the ability to produce end-use metal components using Layer Manufacturing (LM), direct methods for implant manufacturing have gradually emerged. These improvements in materials and manufacturing methods have been well supported by a growth in necessary software to convert, simulate and prepare imaging data for medical modelling. In addition, they have enhanced the process of implant manufacturing by facilitating the design stage to enable customized implant geometry to match the relevant anatomy interfaces. This powerful combination – to develop customized CAD (Computer Aided Design) models and subsequently produce complex geometry in final use materials by means of Layer Manufacturing – has enabled wide and far

reaching potentials for future implant manufacturing. Of specific note, is a project that has emerged within the European community and is co-funded by the Sixth Framework Programme for R&D of the EU. The project which is entitled Custom Implantable Medical Devices (or CustomIMD), focuses on applications in the area of creating a craniofacial bone plate, a lumbar intervertebral disc, and dental restorations within 48 hours and project a 20% reduction in healthcare costs (Anonymous, 2008b).

Before medical implants are approved, they are however required to comply with a stringent set of regulations. With the continuous growth and demand for new medical devices, the need for corresponding regulations has also increased, (Anonymous, 2003a), (Anonymous, 2003b), (Anonymous, 2006a), (Anonymous, 2006b), (Anonymous, 2007). And while current regulations are making provision for new medical devices, there is still some work to be done to accommodate the growth in, especially the use of customized medical implants in South Africa, (Du Toit, 2007), (Anonymous, 1973), (Anonymous, 1991).

2.3.1 Classification for Implant Customization

The Food and Drug Administration (FDA) of the United States of America has recognized three classes of medical devices based on the level of control necessary to assure the safety and effectiveness of the device. The classifications are assigned by the risk the medical device presents to the patient and the level of regulatory control the FDA determines is needed to legally market the device. As the classification level increases, the risk to the patient and FDA regulatory control increases. Class I devices have the least amount of regulatory control and present minimal potential for harm to the user. Class I devices are typically simple in design, manufacture and have a history of safe use. Examples of Class I devices include tongue depressors, arm slings, and hand-held surgical instruments.

Class II medical devices are devices where general controls are not sufficient, and existing methods/standards/guidance documents must be used to provide assurances of safety and effectiveness. In addition to compliance with general controls, Class II devices are required to comply with special controls. Special controls include for example, special labelling requirements, mandatory performance standards and post market surveillance. Examples of Class II devices include physiologic monitors, x-ray systems, gas analysers, pumps, and surgical drapes.

Class III medical devices have the most stringent regulatory controls. They usually support or sustain human life, are of substantial importance in preventing impairment of human health, or present a potential unreasonable risk of illness or injury to the patient. General or specific controls are not sufficient to regulate Class III devices, and a Pre-Market Approval (PMA) submission to the FDA is typically required to allow marketing of a Class III medical device. Examples of Class III devices that require a PMA are: replacement heart valves, silicone gel-filled breast implants, and implanted cerebella stimulators.

The classification of medical devices in the European Union (EU) is outlined in Annex IX of its Medical Devices Directive 93/42/EEC (Anonymous, 2003a). The European classification depends on rules that involve the medical device's duration of body contact, its invasive character, its use of an energy source, its effect on the central circulation or nervous system, its diagnostic impact or its incorporation of a medicinal product. Similar to the FDA classification, the EU basically define four classes (Class I, IIa, IIb, and III), ranging from low risk to high risk. Medical implants will fall into Class III for both FDA as well as EU classification.

Within the context of medical devices, the Active Implantable Medical Devices Directive (90/385/EEC) defines a custom-made device as “any active implantable medical device specifically made in accordance with a medical specialist's written prescription which gives, under his responsibility, specific design characteristics and is intended to be used only for an individual named patient” (Anonymous, 2003b). This definition is also supported by the Medicines and Healthcare products Regulatory Agency (MHRA) that regulates medical devices in the UK under European legislation (Anonymous, 2006a) and the FDA according to its Code of Federal Regulations, Title 21, Volume 8 (Anonymous, 2006b).

Conventional procedures for implant design have in the past been limited to a process of selecting standard size replacement parts from a range provided by manufacturers based on morphometric data. This works satisfactorily for some types of procedures, but there are always patients outside the standard range, between sizes, or with special requirements caused by disease or genetics. Therefore as technology increases to provide more options to surgeons, a growing need for producing custom-made implants is progressively being reached. The author suggests that implant customization may largely be divided into two main groups, namely custom-size and custom-fit implants. Custom-size refers to the custom manufacture of “in-between-size” implants that have been manufactured from the same original implant design, but scaled appropriately per patient. Custom-fit implants on the other hand denote a redesign and manufacture of part geometry to match a patient's specific anatomy. The term “custom-made” then refers to the process or action of producing either a custom-size or custom-fit medical implant.

The degree to which implant customization takes place is largely dictated by the area of application. Cranio/maxillo-facial implants for example, by virtue of their complex geometry require tailored designs to fit at the implant location, and implies a need for custom-fitting. A hip replacement on the other hand, may require less customization to the implant design while its function remains the same for different patients. Therefore, custom-sizing may be appropriate to cater for a wide variability in patients' anatomy.

2.3.2 Regulatory Issues

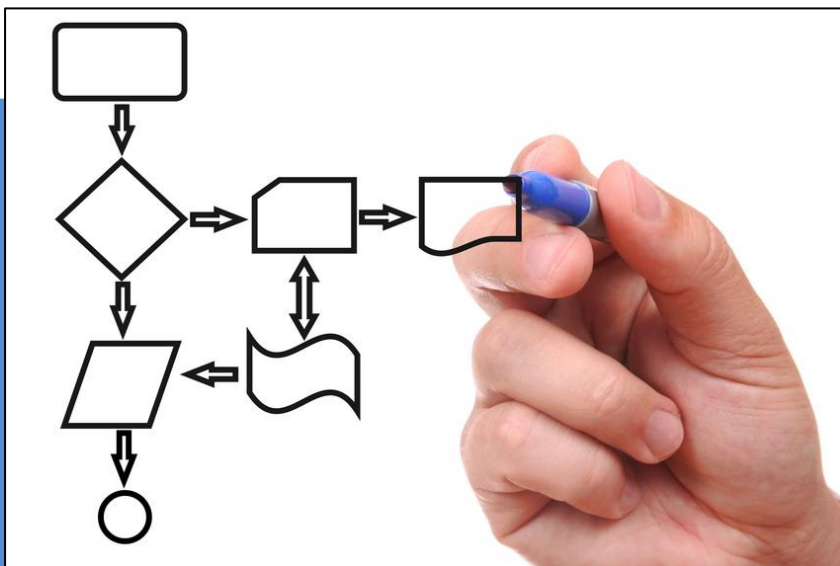
Although implants can now be manufactured so that their geometry matches that of anatomical features, the importance of implant function and efficacy is a consideration that cannot be overlooked. Customization may in fact, pose opportunities to improve functional restoration in addition to geometric

fit. Within this context, international quality standards, protocols and medical regulations are in place to ensure safety for patients regarding any undue practices. In cases where custom sizing is involved, conventional procedures demand a set of rigorous testing and clinical trials to be conducted before an implant design may be commercialized. In cases where one-off custom fit implants for individual patients are produced and inherently differ from previously tested existing designs, a situation arises where extended rigorous testing and clinical trials becomes impractical. A question therefore arises how to balance the design and manufacture of custom-fit implants while at the same time performing adequate testing prior to implantation.

The medical device market is unfortunately not very well regulated in South Africa. Medical equipment – other than electro medical devices – including disposable or single use devices, are not regulated. The Hazardous Substances Act, 1973 (Act 15 of 1973) from the Department of Health, is being used to regulate electro medical devices which fall within a so-called Group III classification (note that Group III classification here differs from Class III previously mentioned). If any product does not appear on the current Schedule of Listed Electronic Products (Anonymous, 1991), such products are under no legal requirement from the South African Department of Health in terms of importing, manufacturing or distribution (Du Toit, 2007), (Anonymous, 1973). Currently, medical implants do not appear on this schedule, and are therefore at this stage exempt. The Department of Health is in the process of drafting the necessary policy documents and has indicated that these may become available in the near future. In the absence of local regulations, international regulations should therefore be considered and adhered to.

In order to simplify the process of approval for product developers, international efforts towards collaboration in regulating medical devices are making progress. In 1992 an international forum, the Global Harmonization Task Force (GHTF), was formed embarking on a number of regulatory initiatives designed to move the participating countries closer to achieving the goal of mutual recognition of regulatory processes. As regulations are continuously being updated to reflect new developments in this industry, custom made devices are becoming more recognized and incorporated in these documents. In its most recent update, the European Commission has published an important amendment to the Medical Devices Directive (Anonymous, 2007). This amendment Directive 2007/47/EC came into effect on 21 March 2010. It introduced more than 150 changes that range from simple text corrections, to introduction of new requirements. Directive 2007/47/EC is the fifth document that introduced amendments to the original text of the Medical Devices Directive 93/42/EEC (Anonymous, 2003a).

In review of current regulations, provision is therefore made for the design and manufacture of custom-made implants. Further requirements for custom-made devices are set out in Annex I of the Medical Devices Directive 93/42/EEC (Anonymous, 2003a), of which the details fall beyond the scope of this report.



A Process Chain for Developing Patient-Specific IVD Endplates

3 A Process Chain for Developing Patient-Specific IVD Endplates

3.1 Introduction

The ability to design and produce a custom-made intervertebral disc implant prior to surgery for a patient is indeed an ambitious undertaking. However, with growing capabilities in software and manufacturing technologies, this idealistic concept is becoming a real possibility. This study has set out to develop and propose the process chain required for designing and manufacturing a custom-made intervertebral disc implant with patient-specific endplate geometry. The use of standard diagnostic procedures can be combined with state-of-the-art data manipulation and CAD software to design an implant that matches a patient's requirements. In addition, the improvements to Rapid Manufacturing technologies in quality (surface finish, accuracy and strength) and material selection (various biocompatible materials, such as titanium and cobalt-chrome) has seen a growing interest from industry in different areas of application – especially in the aerospace, automotive, medical and consumer products markets. Therefore, although there are several significant challenges ahead (technical and regulatory) the prospect for customisation in the spine is indeed an exciting one with far reaching potential benefits to the patient specifically and to health care in general. The implication being that a successful application of the principles of customization in the spine will see the same principles being applied to implants for other areas of the body as well.

3.2 Scope and Exclusions

The scope of this study included the full outline and definition of all the steps involved in the process chain for custom-made disc design and manufacture. The scope however excluded verification of some steps in the process chain that are still part of ongoing research. No clinical studies on any patients were performed and only initial results from biomechanical studies are presented. A detailed cost analysis has been initiated as a parallel study but is still ongoing and has not been included in the results of this study. One of the potential benefits of customized endplate designs, namely decreased subsidence was investigated as a sub-study within this project and the results are presented in Chapter 4.

The process chain presented here is for the design and manufacture of a generic disc implant with ball-and-socket type design. It was used as a demonstrator for the process chain and an emphasis was placed on endplate customisation.

The proposed clinical process chain is shown here below in Figure 14 and each step will be explained in further detail.

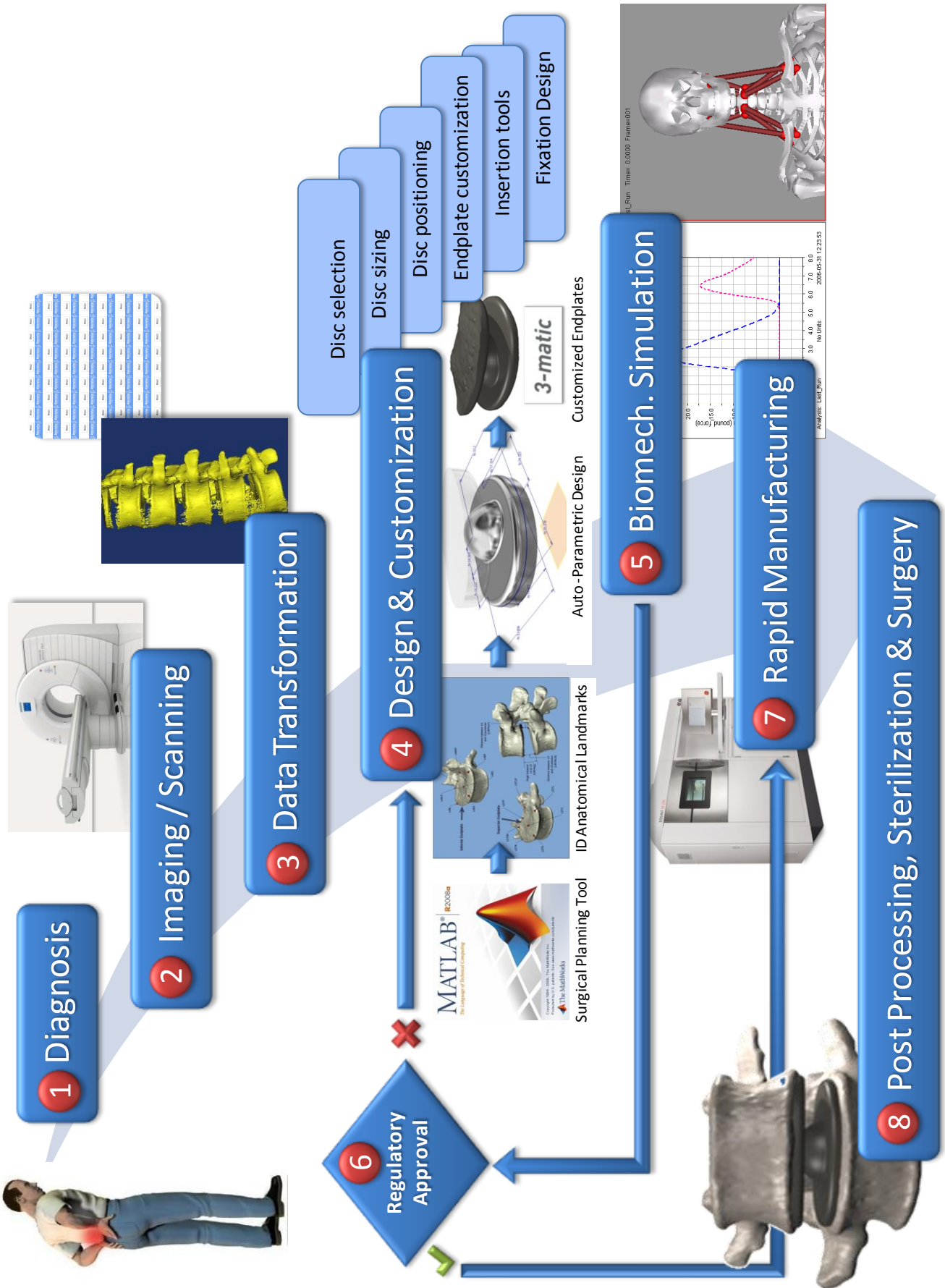


Figure 14 – Clinical process chain for design & manufacture of patient-specific IVD endplates

3.3 Diagnosis 1

The first step in the process chain is to ascertain the condition of the patient and try to identify the source and location of the pain and other symptoms that may be experienced. The basic diagnosis procedure and indications for surgery has already been outlined in Section 2.2.4 and will not be repeated here. From this point on, it will be assumed that the patient has already undergone three to six months of conservative treatment and after no significant improvement and further patient screening tests a joint decision has been made to proceed with Total Disc Replacement surgery.

3.4 Imaging/Scanning 2

In most cases, at this point at least one MRI scan will have been taken of the patient during the diagnosis stage. Not all cases however, will have had a CT scan taken of the patient. CT scans are more suitable for obtaining anatomical images of bones than MRI, while MRI is more suited for soft tissue imaging. Since information about the bone geometry is required for the implant design, it is necessary to have a CT scan taken of the patient if this has not already been done. The quality of the CT scan is critical since it will form the basis from which all design geometry is constructed. Therefore, CT scans should be acquired at a high spatial resolution with thin, contiguous image slices (<2.0mm, 0.75 – 1.25mm is ideal) and as small a field of view (FOV) as possible while still including the patient's external contour. No gantry tilt should be applied (i.e. gantry tilt = 0°), and the patient must remain completely still through the entire scan. If patient motion occurs the scan must be restarted.

The industry standard for CT data storage is the dicom format. Therefore the patient's scan data will be stored on CD or DVD for further processing during the surgical planning and implant design phases. Figure 15 schematically shows this process flow that follows CT scanning and will subsequently be described.



Figure 15 – Process flow following CT scanning

3.5 Data Transformation 3

The third step after acquiring CT scans is to convert the two-dimensional images into a 3D model by means of a segmentation process. For this purpose, the software *Mimics* (Materialise, Belgium) is used. After importing the CT data, the following steps are performed:

3.5.1 Thresholding

Thresholding is the process of defining the selection of upper and lower Hounsfield unit values (HU, named after the Nobel Prize winner, Godfrey Hounsfield) that relate to the density of the scanned anatomy. In the case of bone, the lower threshold is 226 HU and upper threshold is set at its maximum (Figure 16). Once defined, these limits are used to create a mask which filters and highlights all areas on each of the slices of the CT scan that fall within these upper and lower boundaries. The highlighted areas are referred to as regions of interest (ROI).

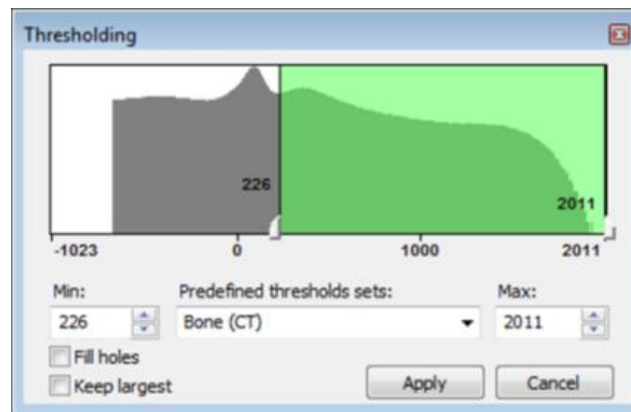


Figure 16 – Threshold selection of HU limits

3.5.2 Region Growing

After thresholding, the identified ROI that correspond to the filter criteria can be assembled into a 3D model. In most cases however, a region growing function is first applied to filter out any soft tissue-related particles that were included from the thresholding activity. A new mask is created during this step by selecting a point on the CT scan ROI. An algorithm proceeds to “grow” this pixel from the selected point to include all other pixels that are connected to it on that slice as well as any adjacent slices. So this function is helpful when bones or other anatomy need to be separated from one another, each time creating a new mask.

3.5.3 3D Model

After region growing, the collection of 2D slice images for a particular mask can be stacked together to create a 3D rendition of the data. Figure 17 shows a partial screen shot from the Mimics software after thresholding, region growing and an initial 3D model has been created. The window is divided into views each framed a different colour that show the sagittal (bottom left: green), coronal (top left: orange) and transverse (top right: red) sections at a particular CT slice layer. The cross hair in each view serves as a reference point for the positions displayed in the other view planes. Looking at the transverse plane for example, the cross hair is pointing just left (slice is viewed from inferior direction) of the spinal cord within the vertebral foramen. The two lines that make up the cross hair are coloured green and orange according to the sagittal and coronal planes respectively that it refers to. In each view, the coloured geometry

represents the filtered selection of each mask. Latent, separate traces of green are still slightly visible in the images and relate to the first mask created during the thresholding process. The yellow areas are related to the second mask that was created during the region growing activity. The fourth view is a 3D rendering compiled from this yellow mask and Figure 18 shows an enlarged view of this 3D model. At this point there are still some 3D particles at the anterior of the model which are not bone and needs to be removed manually. Further editing tools in the software are used to accomplish this. In other cases (not indicated here) when patients' bones show signs of *osteoporosis* or *osteopenia* (where bone density is lower than normal), more severe examples of such overlap and tissue joining is observed. The identification and separation of bone from soft tissues then becomes more challenging and time consuming.

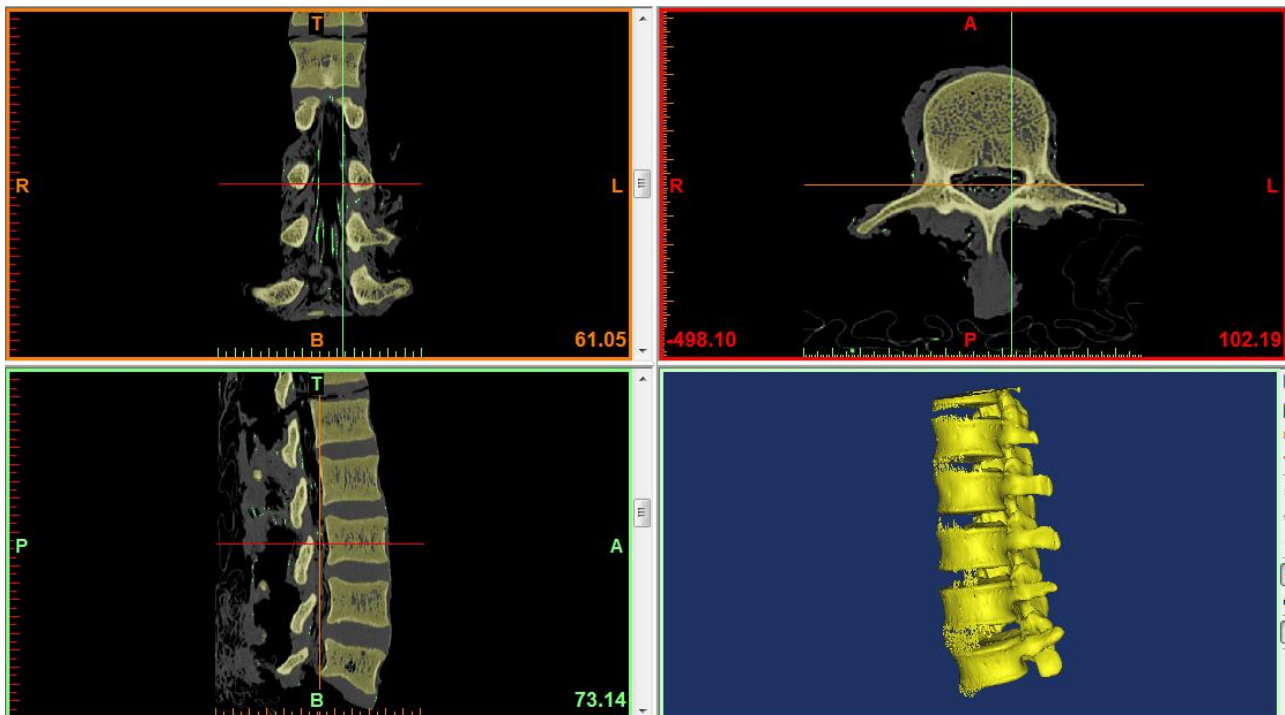


Figure 17 – 3D model generation after thresholding and region growing



Figure 18 – Enlarged view of 3D model generated in Mimics

Further surface enhancement tools such as smoothing and wrap functions are also available to improve the final 3D model. Once an acceptable 3D model has been generated from the CT scan data, it is necessary to convert and save the data as an STL (Standard Triangular Language) file, which is the common standard used by Layer Manufacturing technologies. From this point, the model is ready for the next steps, which is the design and surgical planning phase.

3.6 Design and Customization

One of several challenges to product developers in the biomedical field is the fact that knowledge and experience across the disciplines of medicine and engineering are required. An easy discrepancy is formed between the technological capabilities that engineering can offer and a proper understanding of where the real needs in medicine are. Surgeons are often not aware of the benefits that a particular technology can offer, while on the other hand, engineers often do not have a full appreciation for the clinical difficulties that surgeons encounter. So in order to develop meaningful products for the medical field, this communication gap needs to be acknowledged and well managed with joint involvement as far as possible. Therefore during the design of a customized intervertebral disc implant, the involvement of a surgical team is crucial to ensure that the design will conform to the needs of the patient. One of the ways in which this can be facilitated is through the application of a user-friendly software expert system that would become a surgical planning tool which incorporates some CAD design functionality, while at the same time including important medical aids and constraints that are familiar to surgeons. Although several software packages exist which have the capability of manipulating biomedical bone geometry with CAD operations, (notably for example 3-Matic (Materialise, Belgium)), these software solutions are invariably quite expensive and usually require CAD design experience. Observing a need therefore, to have user-friendly software with which surgeons can communicate their design changes for customization effectively to downstream manufacturers, an attempt was initiated to develop such a software design and surgical planning tool. This was done with some measured success as part of an undergraduate study project (Van Zyl, 2010). The software tool was created within the MATLAB (MathWorks, Massachusetts) software environment, and boasts a graphical user interface and ability to manipulate STL files.

Using this surgical planning software tool as a starting point for the design phase, its process chain follows as shown in Figure 19 below. After digitally correcting for spinal misalignment and intervertebral spacing, selected anatomical landmarks become the drivers for a semi-automated parametric design of the disc implant. Once the final CAD design is complete, it is imported back into position between the vertebrae upon which the geometries of the endplates are digitally adjusted to match that of the bone endplates. Finally, an STL file is generated for further steps in manufacturing if the design has been approved.

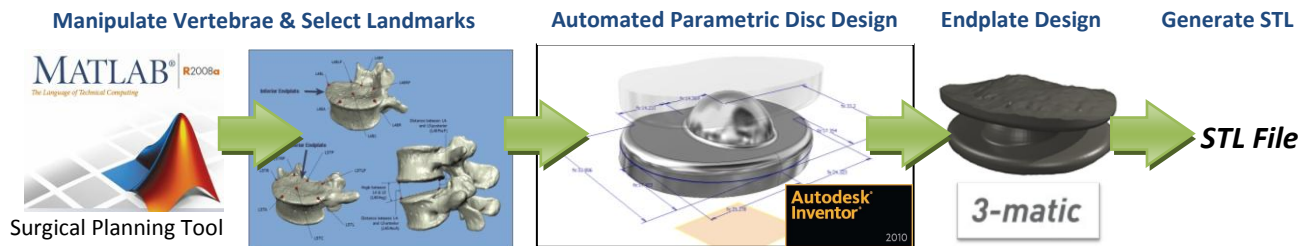


Figure 19 – Design phase process chain

3.6.1 Surgical Planning

At this point, the surgical team will assess the 3D model developed in the previous stage, for possible spinal misalignment and vertebral spacing at the pathologic joint where surgery will take place. The surgical team will have the opportunity to manipulate the individual vertebra (rotate or translate) and correct any misalignment within the digital 3D model. In order to achieve this, the following steps are taken:

Define Coordinate System

The first step in the design phase will be to import the STL files created from Mimics into the Surgical Planning Tool and redefine a coordinate system.

A function created by Doron Harlev is used to import the STL files directly into MATLAB and convert them into a suitable format for MATLAB's patch function to display the vertebrae correctly (Van Zyl, 2010).

After importing the vertebrae, they are displayed and the software automatically identifies a proposed origin point for the coordinate system (most anterior point on superior endplate of L4 vertebra). If necessary, the surgeon has the option to move this origin point. Next, the Cartesian planes are defined, starting with the sagittal plane, by calculating the average of all x-, y-, and z-coordinates of the vertices that define the model geometry. The normal vector of this point is chosen as the positive x-axis, and the sagittal plane is derived. Then coronal and transverse planes are derived with the final result as shown in Figure 20.

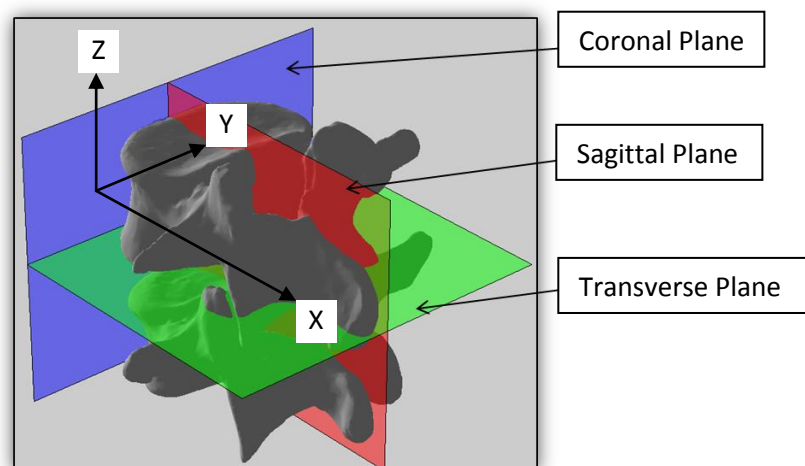


Figure 20 – Identification of sagittal, coronal and transverse planes (Van Zyl, 2010)

Reposition Vertebrae

Based on the surgical team's previous assessment of the spinal alignment and vertebral positions relative to one another (intervertebral spacing and angles), the surgeon has the option to manipulate either of these to correct any misalignment. Rotation is performed by choosing the relevant vertebra, and axis around which rotation must take place. The positive axes are shown on Figure 20 above as the following: X-axis (posteriorly along midline); Y-axis (laterally to the right); Z-axis (superiorly from origin). Incremental amounts are specified, and the vertebra is rotated by using the keyboard left or right arrow keys. Similarly, translation is achieved by selecting the vertebra and using the arrow keys to move it by the specified incremental amounts. Examples of exaggerated manipulation are shown below in Figure 21.

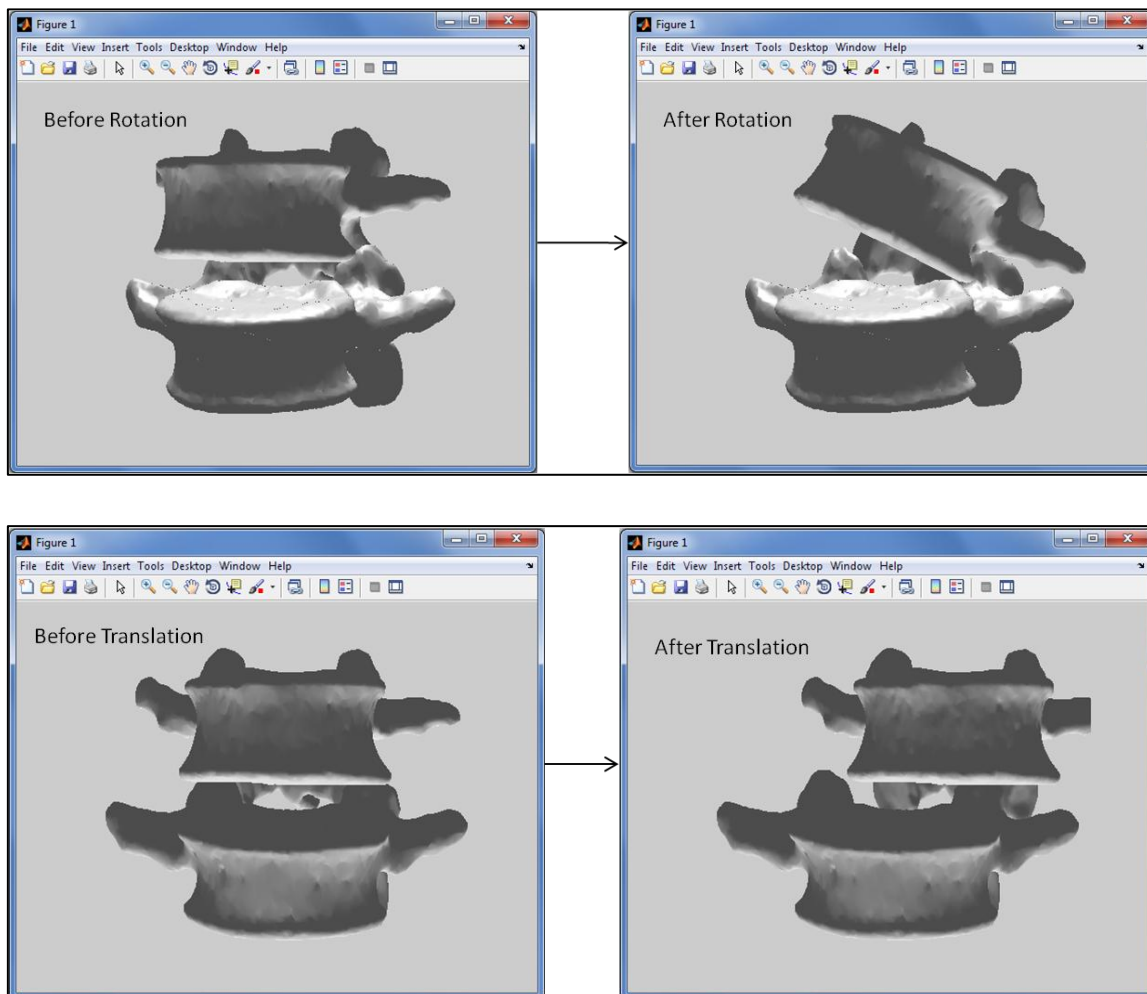


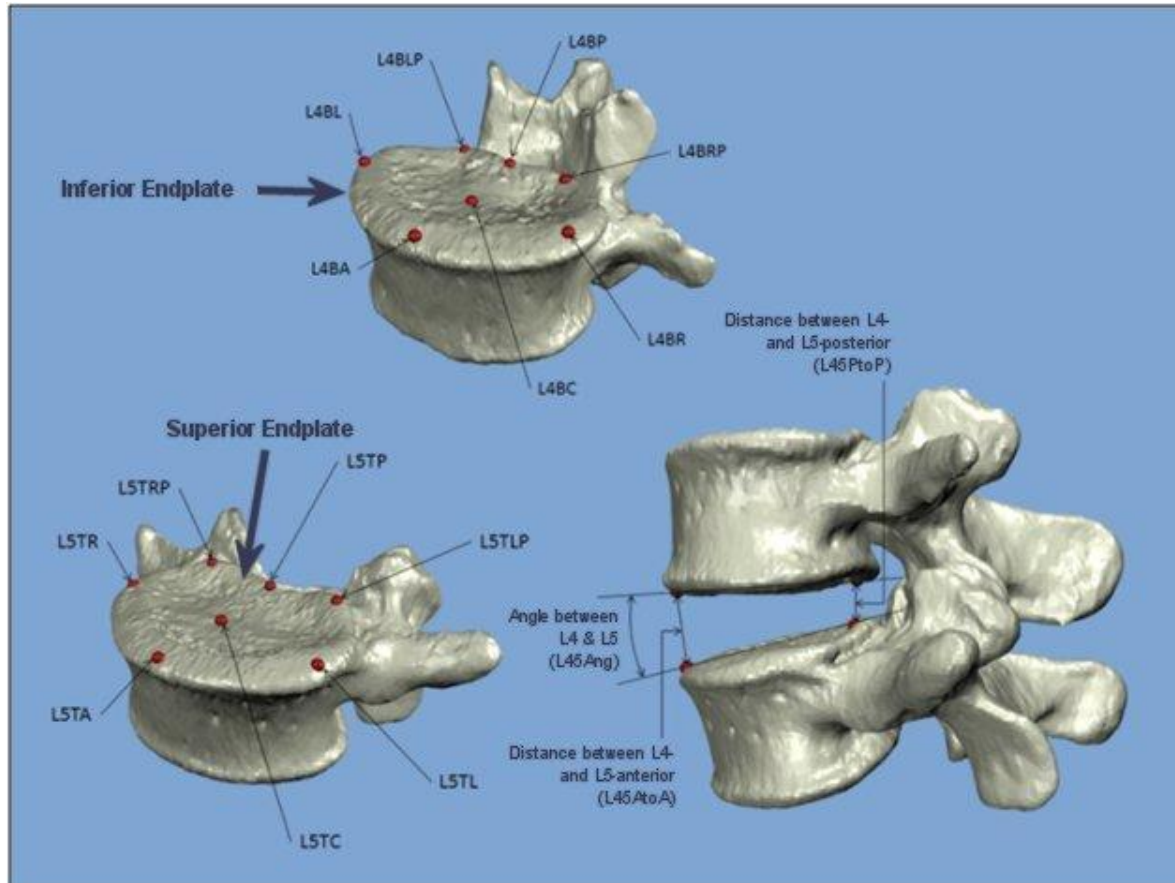
Figure 21 – Rotation and translation of selected vertebra (Van Zyl, 2010)

Select Anatomical Landmarks

Once the surgeon is satisfied with the correct alignment and spacing of the vertebrae with respect to one another, the model is ready for initiating the design process of the intervertebral disc. The steps have been semi-automated and only require the surgeon to select seven anatomical landmarks on the surface of each vertebral endplate. Six of these points are then used to define a spline curve which forms the footprint

profile for the endplate of the intervertebral disc prosthesis. The seventh landmark on each vertebra defines the centre point of the spherical ball-and-socket joint connection.

Figure 22 shows the approximate positions for each anatomical landmark as well as angles and distances that are calculated from these landmarks.



Description	L4 Vertebra	L5 Vertebra
Anterior point	L4BA	L5TA
Posterior point	L4BP	L5TP
Left point	L4BL	L5TL
Left-posterior point	L4BLP	L5TLP
Right point	L4BR	L5TR
Right-posterior point	L4BRP	L5TRP
Central point	L4BC	L5TC

Figure 22 – Anatomical landmarks for design of patient-specific IVD endplates (Odendaal, 2010)

The process of selecting landmarks is made easier by the fact that the Surgical Planning Tool has been designed to pre-select a series of landmarks from which the surgeon can choose. Using MATLAB’s built-in data cursor application, orthogonal planes are used to identify landmarks on the vertebra by highlighting the closest point where the plane and the vertebra geometry intersects. Figure 23 shows this process indicating the landmark intersection points along the snap planes. The surgeon can select a new landmark along this intersection line, or can adjust the planes to create a new set of intersection points.

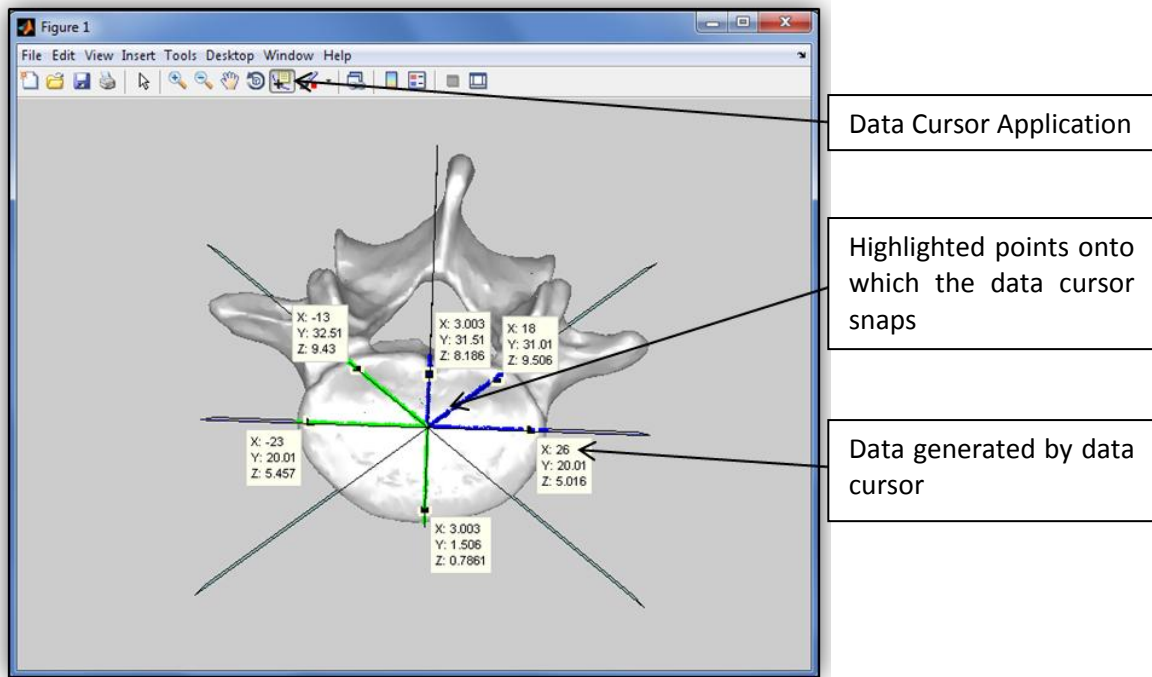


Figure 23 – Semi-automated identification of landmarks along intersection planes (Van Zyl, 2010)

3.6.2 Automated Parametric Disc Design

Once the fourteen landmarks have been identified, their coordinates are exported to a semi-automated parametric disc design tool that was developed by Odendaal, referred to as a Custom Disc Generator (CDG) (Odendaal, 2010). The CDG is a 3D parametric CAD model that has been designed using Autodesk Inventor Professional 2009 (Autodesk, California). Each feature in the CAD model has been carefully designed with linked constraints and relationships. Their dimensions are driven by a set of calculations derived from the coordinates of the anatomical landmarks that were selected using the Surgical Planning Tool. The CDG sources its input data for the feature dimensions from an MS Excel file (Microsoft Corporation, Washington), which then forms the link between the Surgical Planning Tool and the CDG (Figure 24).



Figure 24 – Link between Surgical Planning Tool and Custom Disc Generator

Features that are calculated from the selected landmarks include the following:

- Angle between L4 and L5 vertebral contact surfaces (defined as α)
- Position of the centre point of the ball-and-socket joint mechanism
- Radius of the spherical ball
- Gap between the superior and inferior endplates of the prosthesis
- Allowable size of feature rounds

As an example to demonstrate how some of the CAD features are calculated in the CDG, consider a sagittal section along the midline of the prosthesis, represented by the simple 2D geometry shown in Figure 25.

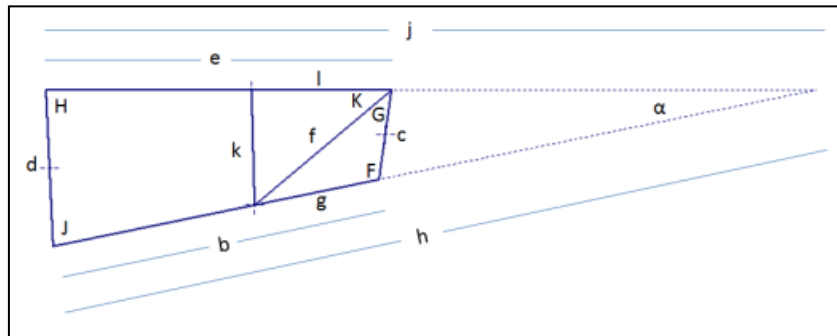


Figure 25 – Diagram representing mid-sagittal section of prosthesis with feature dimensions (Odendaal, 2010)

The feature dimensions are calculated using the identified landmarks (Figure 22) as follows:

- $e = L4BP(y)$
- $b = L5TP(y)$
- $c = L45PtoP$
- $d = L45AtoA$
- $l = L4BP(y) - L4BC(y)$
- $g = L5TP(y) - L5TC(y)$
- $\alpha = L45Ang$

The remaining dimensions can be derived by trigonometry and result in the generated design shown below.

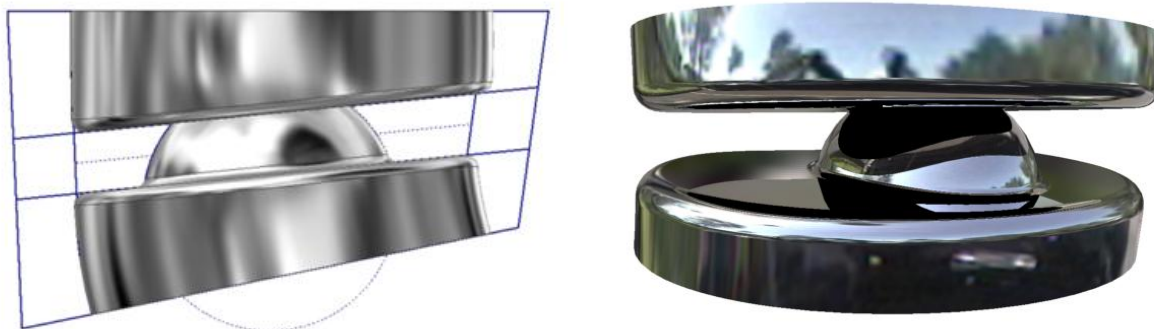


Figure 26 – Customized disc prosthesis designed using the CDG (Odendaal, 2010)

3.6.3 Endplate Design

Once the basic geometry for the intervertebral disc implant has been defined, the final step in the design process is to modify the implant endplates to match the geometry of the bone endplate surfaces. This is done by performing a simple Boolean subtraction between the implant and the vertebrae. STL files of the implant along with the bones are exported from the CDG to 3-Matic software (Materialise, Belgium) where the subtraction is performed. The subtraction step is then followed by an undercut removal function, to ensure that the implant can be inserted without obstructions caused by undercuts. Figure 27 shows the resulting steps of (a) the implant, with (b) overlapping geometries and (c) the final implant model.

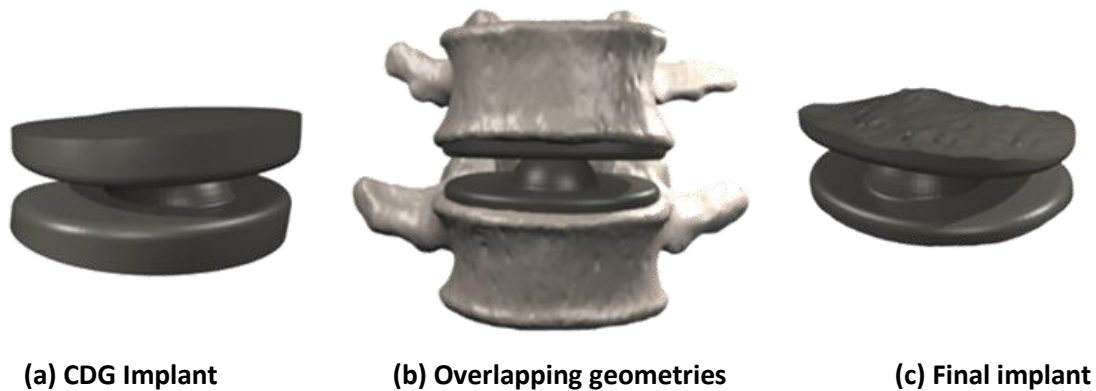


Figure 27 – Boolean subtraction of implant and vertebrae to create bone-matching endplate geometries (Odendaal, 2010)

At present, this design process makes use of several software platforms, namely the Surgical Planning Tool (Matlab), MS Excel, Autodesk Inventor (CAD software), and 3-Matic. Ideally the operations that each performs could be consolidated into a single software tool. This is envisaged as an improvement to the existing Surgical Planning and Design Tool and is part of an ongoing research study.

3.7 Biomechanical Simulation 5

In the context of intervertebral disc replacement and customized implants, biomechanical simulation studies are of great importance in helping to analyze and describe the internal dynamics of the spine. An understanding of the intervertebral movements of the spine is useful in the assessment of typical spinal disorders (such as instability) and the prediction of treatment outcomes. In the context of total disc replacement, the dynamic vertebral behavior, muscle forces as well as reaction forces before and after implantation can be digitally simulated. By doing so, a comparison can be gained between different implant designs or different placement strategies. In setting up and validating such a simulation model however, it needs to be “trained” how the bone kinematics and muscle responses need to behave and conform to natural biomechanics. These inputs are usually measured or captured from real human beings and transferred into the biomechanical simulation model. The measurement of the intervertebral movements of the spine is however notoriously difficult. This is mainly because the spine is quite inaccessible, and the nature and sequence of its movements is very complex. Radiographic, electromagnetic and electro-optical techniques have been used in the measurement of spinal motion with some success. However, radiographic techniques have the inherent health risk of repeated X-ray exposure.

A recent postgraduate study evaluated different in vivo motion capturing methods that may describe cervical kinematics and that will serve as input for simulation models (Christelis, 2008). Available technologies range from simple clinical methods, such as palpation or goniometry, to expensive technologies like optical or ultrasonic systems consisting of specialized equipment. An important distinction was made between two types of motion capturing technologies, namely external motion capturing and

internal imaging technologies. The available external motion capturing technologies pose many advantages in terms of cost, safety, simplicity, portability and producing accurate three dimensional positions and orientation. However, as Figure 28 shows, these technologies still have several limitations or drawbacks (indicated by the “thumb down” tags).

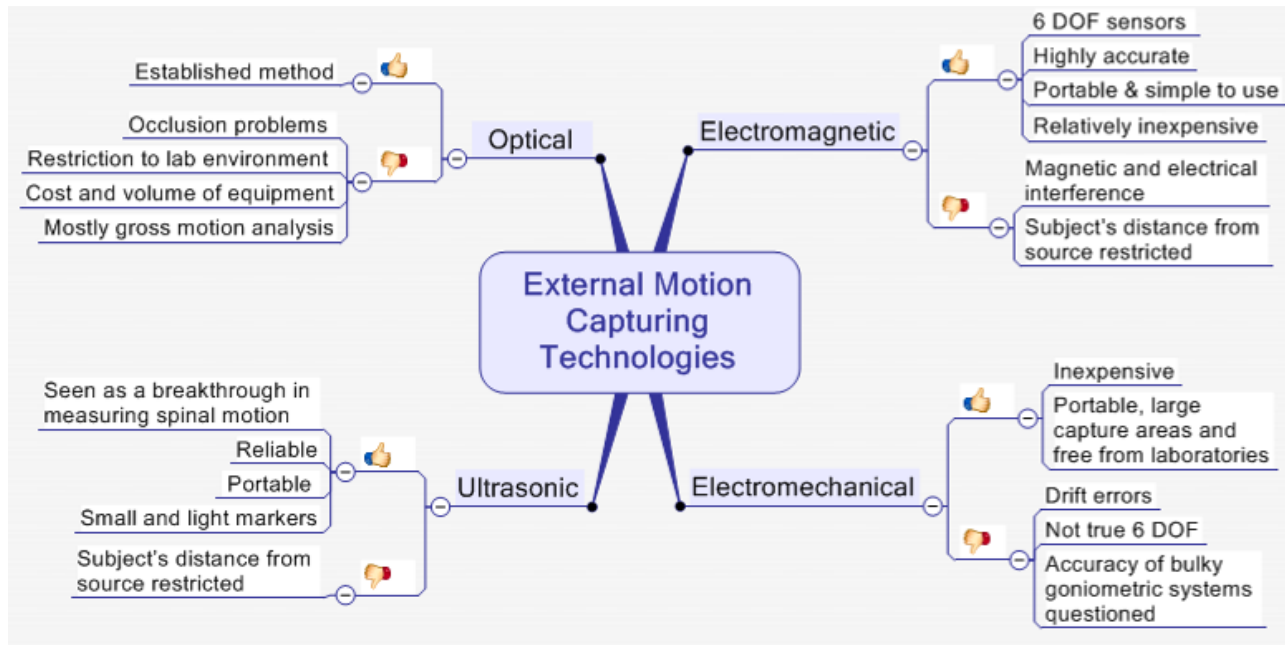


Figure 28 – Advantages and limitations of external motion capturing technologies (Christelis, 2008)

A common drawback of external motion capturing systems is that these systems often lacked the ability to accurately capture motion at the intervertebral level. Quantitative assessment of the spinal kinematics at an individual vertebral level can yield important and necessary information and is crucial for the purposes of obtaining kinematic data for simulation studies and research on the intervertebral disc. Although many external marker systems provide valuable information about total movement of the spine or posture, they fail to produce information about motion at each vertebral level. The most challenging and common limitation to all external motion capturing devices is that external markers, transmitters or sensors are subject to movement of the skin and underlying tissue between the vertebrae and the markers. Therefore its credibility to reflect the true vertebral motion at each level is questioned.

By contrast, internal imaging technologies all have the potential to provide valuable information of motion at intervertebral level. Their main drawback however is that most rely on X-Ray technology and as such, pose dangers of high radiation dosage to the patient. These and other disadvantages (indicated by the “thumb down” tags) are shown in Figure 29. Although MRI showed excellent potential in being used for 3D kinematics, it also has the downside of being expensive and high in maintenance.

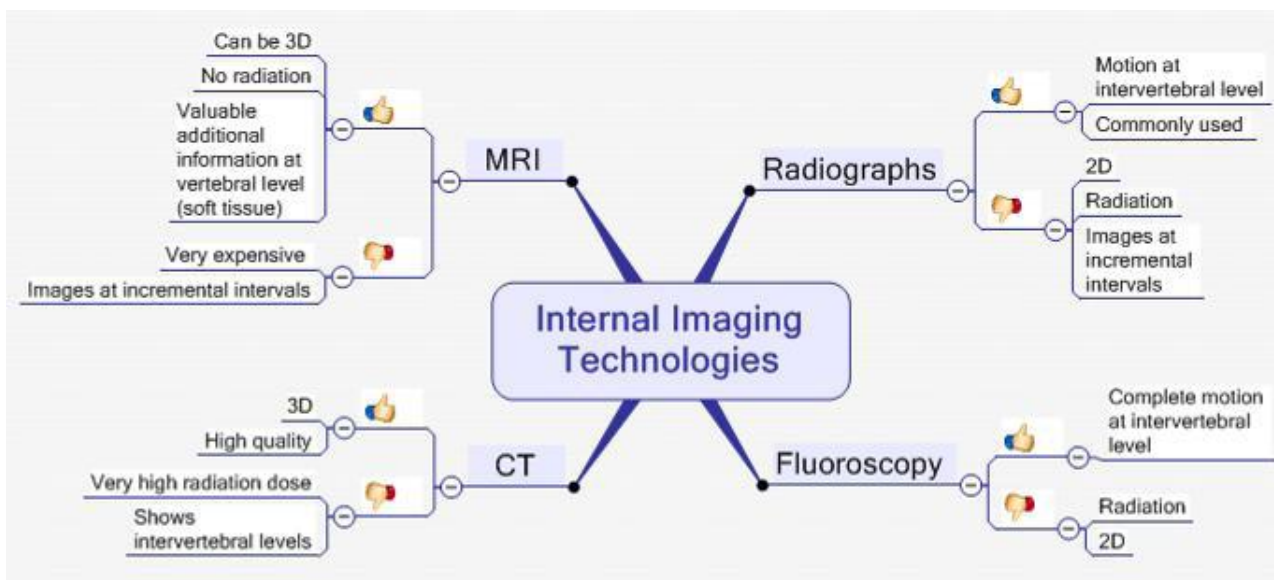


Figure 29 - Advantages and limitations of internal motion capturing technologies (Christelis, 2008)

In conclusion then, external motion capturing systems have great value and pose many advantages, but the reduced accuracy due to skin and soft tissue is a limitation which will not easily be overcome. Internal motion capturing systems can give detailed 3D kinematic information, but at the expense of high cost and high radiation to the patient.

Therefore a study was conducted to evaluate a fundamental question of whether surface markers can represent the motion of the vertebrae. This was done by observing the motion of surface markers and vertebrae on the same medium and instance. 21 asymptomatic subjects received low dosage x-rays in five different positions, while small radio opaque markers were placed on the neck representing each vertebral level. The data from the surface markers was obtained and processed. Results included vertebral kinematics for simulation purposes as well as the relationship between surface markers and vertebrae.

The results from this study showed that it is possible to formulate a correlation between external marker positions and internal vertebral motion. The scanned movement data can then be used as input to defining a simulation model for the patient. Figure 30 shows a depiction of the basic process flow during an iterative process of design improvements to the customized intervertebral disc implant using simulation. Information is collected about the patient with regards to bone geometry (through CT scanning) and other anthropometric data such as age, height, weight etc. Making use of movement capturing technologies, patient kinematics can be collected by allowing the patient to perform a set of predefined movements, such as sitting, walking or lifting objects. It is important to assess the patient’s full range of motion through these exercises. Given the patient’s information, simulation model of the patient’s condition is derived through the use of inverse kinematics. A second generic simulation model can be scaled to match the patient’s basic anatomy, age and weight. This generic “healthy” simulation model is then compared with the model of the patient in terms of ranges of motion for the same set of exercises. Based on an initial

comparison, an assessment is then made in terms of what corrective action is needed to rectify spinal alignment and vertebral positions and in doing so, recommendations and boundary conditions are derived for the design and placement of an intervertebral disc implant. The implant is designed using the Surgical Planning Tool and Custom Disc Generator described in the previous section and once designed, the patient's simulation model is updated to include the implant. A new comparison between the implanted patient model and the generic "healthy" model is then made as before. This iterative process is repeated until a satisfactory resemblance between the models is achieved.

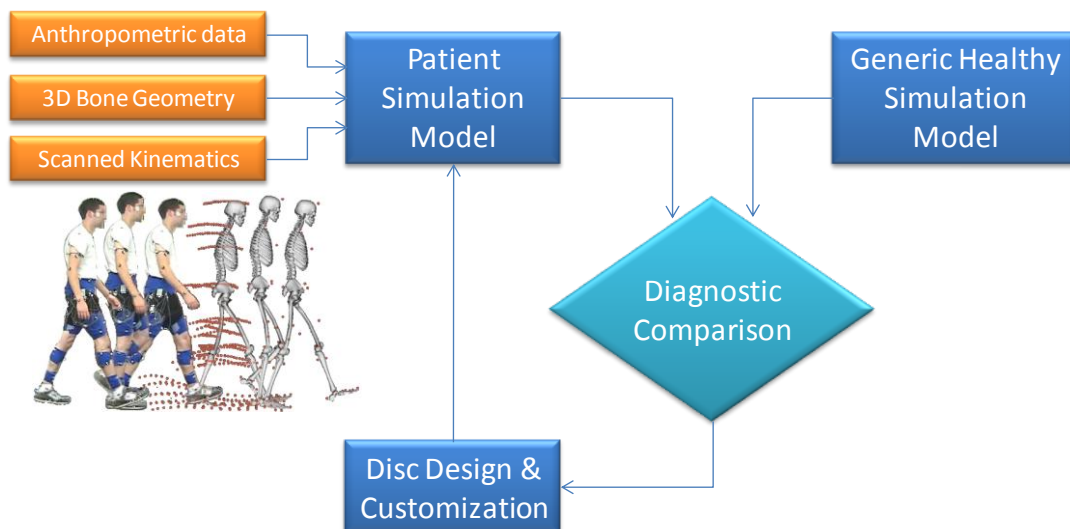


Figure 30 – Basic iterative process flow for design improvements using simulation models

3.8 Regulatory Approval 6

Regulatory issues have already been broadly discussed in Section 2.3.2 and will not be elaborated much again, except to describe how it should fit within the process chain for customization. An inherent difficulty by definition for customized products, lie in the fact that each design is essentially unique and needs to adhere to the same set of performance and safety standards. At present it is not feasible for a customized implant design to undergo the same FDA or CE certification procedures that other standard size implants have to go through. The process takes years to complete and involves extensive clinical trials before approval is granted.

Currently however, allowance is made for customized implants in general by having both the patient and surgical team sign consent before implantation proceeds. Examples of such implants occur commonly for operations in the cranio- maxillo/facial regions, where patient anatomy already require unique geometry solutions. This situation is however not ideal as a long term solution. Along with manufacturing technologies such as Layer Manufacturing which can use a variety of biocompatible materials such as titanium, cobalt chrome and PEEK (Polyether ether ketone), performance of software and simulation technology has also increased dramatically. As simulation models increase in their ability to more closely resemble the natural kinematic and dynamic behavior of the human body, it seems apparent that such

techniques should become standard practice during the testing and approval of a spinal implant. A specific set of outcome demands must be established which an implant design needs to adhere to before approval can be granted. Once established, these passing criteria can be built into the simulation model process flow as shown in Figure 31. Therefore it is proposed that regulatory approval for customized intervertebral disc design can take place during an iterative design stage of its process chain. Its position in the larger process chain is shown here again in orange (Figure 32).

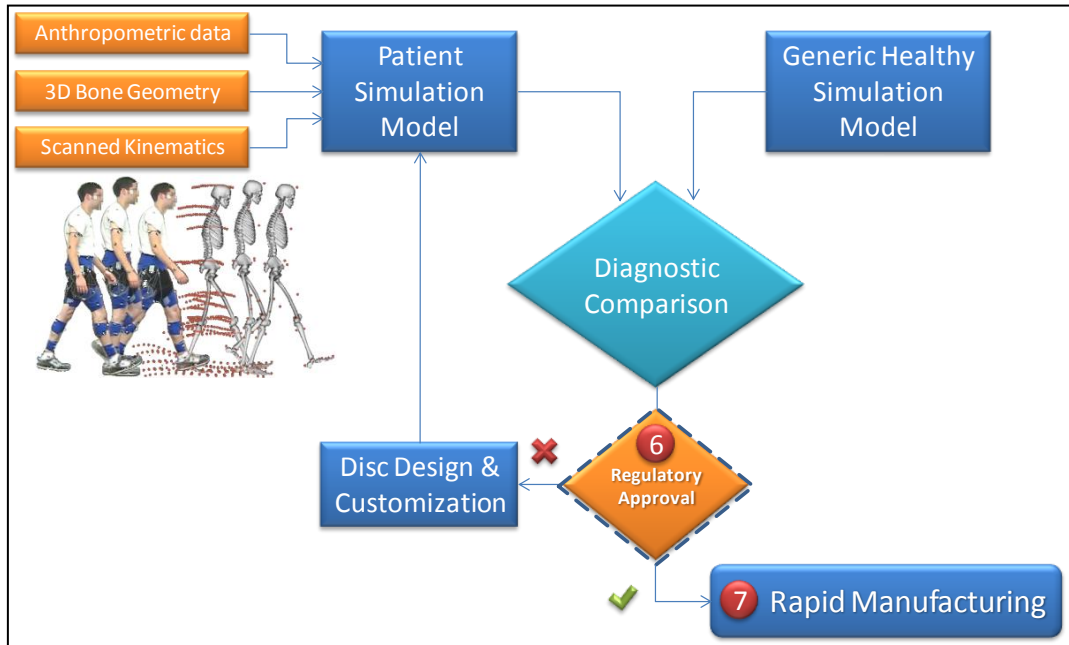


Figure 31 – Simulation process flow including regulatory approval

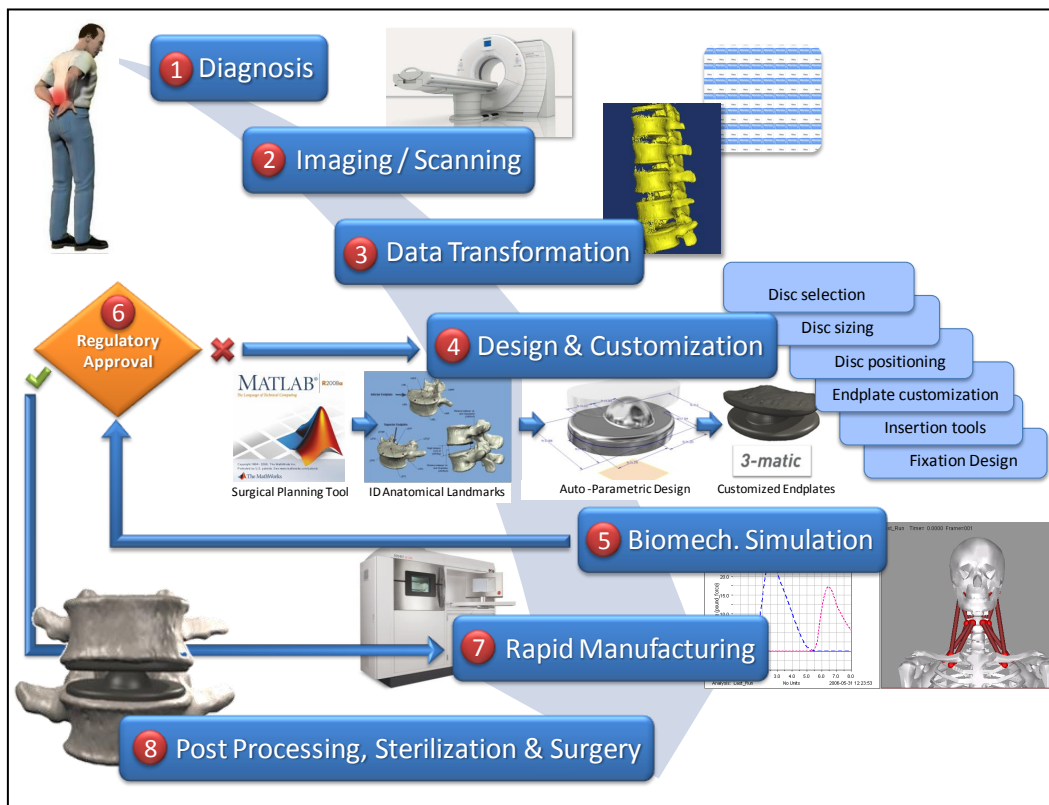


Figure 32 – Clinical process chain indicating relative position for regulatory approval

3.9 Rapid Manufacturing 7

Over the last decade several LM technologies have emerged that are showing notable promise in their ability to directly manufacture customized implants in final, end-use materials. Direct metal fabrication processes can be grouped into three categories (Wohlers, 2010). The first group describes systems that use a laser to heat powder to form metal parts. All of the systems in this group produce parts in a powder bed, such as for example, Direct Metal Laser Sintering and LaserCUSING. The second group includes systems that use a powder deposition head to deposit the metal powder, such as Direct Metal Deposition. The third group consists of systems that use special approaches to produce metal parts and do not fit into the first two groups, e.g. Direct Metal Printing (from ProMetal).

LM System developers are investing a lot of effort to improve the quality of metal parts produced on these systems in order to meet customer requirements and deliver components by means of Rapid Manufacturing (RM). Specific emphasis has been placed on the ability to deliver 100% dense, high strength parts with superior surface finish for engineering applications. Apart from the need for high strength parts, medical implants however do not always share the same emphasis on part quality requirements. The essential material issues in the medical field relate mostly to biocompatibility. In many cases poor surface finish and porosity is a desirable feature for implants to allow bone ingrowth. In other cases where articulating surfaces (such as knee or hip joints) are involved, surface roughness must be very low. Also, accuracy in medical terms is usually quantified in millimetres with only selected situations (e.g. some dental applications) requiring more narrow tolerances. What is more of interest, is an ability to create very detailed features. In medical models for example, fine features such as arteries, nerves and small bones are critical to include for accurate and proper representation during pre-surgical planning. A selection of metal fabrication LM technologies is shown here in Table 4 with a comparison of characteristics and key areas for medical application. Therefore, based on an assessment of the identified needs of the implant design, a selection of a suitable RM technology can be made. In the case of this project, due to its availability, DMLS was the RM technology chosen and parts were produced on the EOSINT M270 machine (Figure 33), using Ti_6Al_4V powder as suitable material.

System		Characteristics		Key Application Areas			
Key Process	Company	Materials	Detail ability [mm]	Cranio/maxillofacial	Dental	Orthopedics (Hip, knee, shoulder)	Other
Direct Metal Laser Sintering (DMLS)	EOS GmbH	Metal powder blends	0.6	√	√	√	√
Electron Beam Melting (EBM)	Arcam	Powder metals	0.25	√	√	√	√
LaserCUSING	Concept Laser	Powder metals: SS, Tool steels, Ti, Al	0.4	√	√	√	√
Selective Laser Melting (SLM)	F&S/ MCP	Non-proprietary; SLM processes any metal powder (10 to 75 micron particles)	< 0.2	√	√	√	√

Table 4 – Metal fabrication comparison matrix suitable for medical applications (De Beer, et al., 2008)



Figure 33 – EOSINT M270 Direct Metal Laser Sintering Machine

3.10 Post Processing Phase, Sterilization & Surgery 8

The steps involved during post processing vary depending on the elected RM technique that was chosen, but generally involve removal from the machine after cooling, some form of surface treatment, assembly of components, and sterilization.

Base Plate Removal

In the case for DMLS using the EOSINT M270 machine, the parts were created on a base plate which needed to be removed from the parts by means of wire cutting.

Surface Treatments

The parts were then individually bead blast to ensure an even surface finish and to remove traces of fine burring on the edges of the parts and where they had been separated from the base plate.

Further surface treatment (which was not followed in this case, but prescribed in future), may involve polishing of the articulating spherical surfaces where the two halves of the implant are in contact. This is necessary to reduce friction and minimize wear debris.

Assembly

In cases such as this project, where the implant consists of more than one component, these will need to be assembled together and ensure proper function. Other design scenarios (which were not investigated here) may also include a modular approach where the majority of the implant size is manufactured separately and only the endplate geometries are manufactured using RM. These would then need to be assembled and attached.

Sterilization

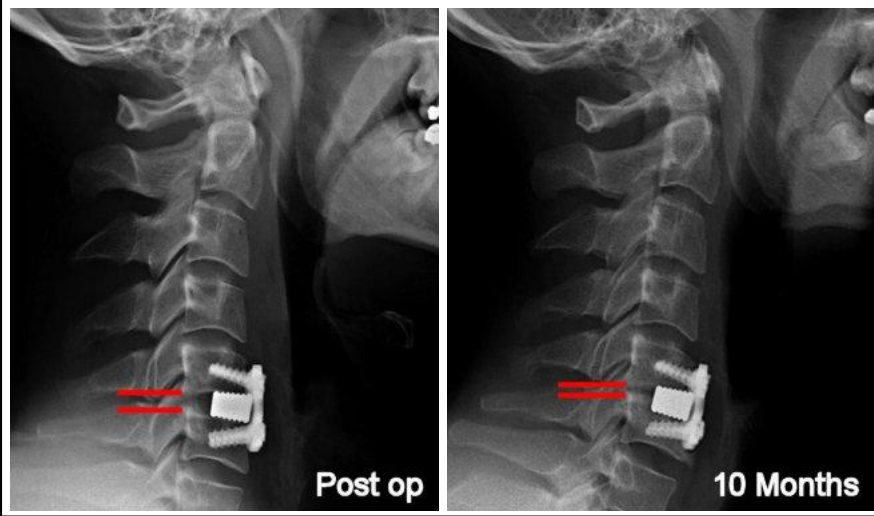
Sterilization is a qualifying requirement for any implant for the human body, or object that is used in the theatre room that a surgeon may come in contact with.

This process can be accomplished by either heat or gas sterilization, or by using sterilant chemicals (Voigt, Patel, & Howes, 2009). Common sterilization methods include using a steam autoclave (high temperature method), ethylene oxide gas sterilizer (low temperature chemical method), and cold sterilization (Presept – a hypochlorite based surface disinfectant). Either method would be suitable and can be used to sterilize the manufactured intervertebral disc implant.

Delivery & Surgery

The final stage of the process chain involves packaging, delivery and surgery. Once again, packaging needs to be sterile in order not to contaminate the sterilized implant. In addition, packaging of the product should include a fully traceable patient-implant identification system. Since implants will be produced to be patient specific, assurance of matching the correct implant to the correct patient is essential. Identification should be put on both the packaging as well as on the implant components.

Finally, the intervertebral disc prosthesis is implanted at the location of joint pathology. The normal TDR procedure is followed, i.e. a *discectomy* and endplate preparation. Most conventional disc implant designs incorporate a fin-like protrusion (the keel) perpendicular to each endplate which helps with implant to bone fixture. This design feature may still be possible with patient-specific endplates (although not incorporated in this process chain example). However the focus of this study sought to investigate and develop a process chain for customizing the endplate geometries to match the bone interface. The use of a keel or other alternative securing technique, along with the necessary surgery insertion tools becomes a design optimization project, and falls outside the scope of this study.



Reduced Subsidence for Patient-Specific IVD Endplates

4

4 Reduced Subsidence for Patient-Specific IVD Endplates

4.1 Introduction

As mentioned previously, there is evidence to suggest that implant sizing and shape is a critical component for success during TDR (Auerbach, Ballester, Hammond, Carine, Balderston, & Elliott, 2010), (Gstoettner, D, Liebensteiner, & Bach, 2008), (Tan, Bailey, Dvorak, Fisher, & Oxland, 2005), (Lowe, et al., 2004), (Steffen, Tsantrizos, & Aebi, 2000). Failure to achieve adequate support as a result of lumbar TDR device undersizing could lead to implant subsidence and/or vertebral fracture.

Subsidence depends, in part, on the stiffness and strength of the implant-end plate interface, and factors that influence this interface include bone mineral density, amount of cartilaginous end plate removal during surgery, anteroposterior position of the implant on the vertebral end plate (i.e., variable regional bone strength), implant shape, and implant size.

Within the context of the proposed process chain discussed in Chapter 3, a sub-study was undertaken to investigate one of the main expected benefits of implant customization, namely reduced subsidence due to increased biomechanical stiffness. Hence the purpose of this study was to examine and compare the compressive behaviour of the vertebral endplates when subjected to different contacting interface geometries. The following hypotheses were investigated:

1. The use of contour implants during non-destructive tests will result in a significantly higher contact area between the prosthesis and the vertebra when compared to using flat implants.
2. The use of contour implants during destructive tests will result in a significant increase in measured stiffness of the implant-vertebral construct, when compared to using flat implants

Roadmap of Chapter 4

Under Materials and Methods, this chapter begins by describing the steps taken to construct the study, the tools and technologies used, the way in which data was acquired and the way in which the results will be analysed. After the study methods and statistical analysis techniques have been described, the results are presented in two main sections; namely non-destructive and destructive test results relating to the experiments performed. Observations made during the experiments are also presented systematically. The results are then analysed statistically and discussed in light of the two hypotheses mentioned above. The relevance of such results within the context of a process chain for the design and manufacture of patient-specific intervertebral disc implants with matching endplate interface geometries is also presented.

4.2 Materials & Methods

4.2.1 Study Design

The study was designated into three main stages, namely preparation, experimental testing and results analysis. The diagram of Figure 34 below, gives an overview of the various steps involved during the study. The preparation phase involved the sourcing and preparation of cadaver bone specimens as well as the design and manufacture of the modified implants for pressure testing.

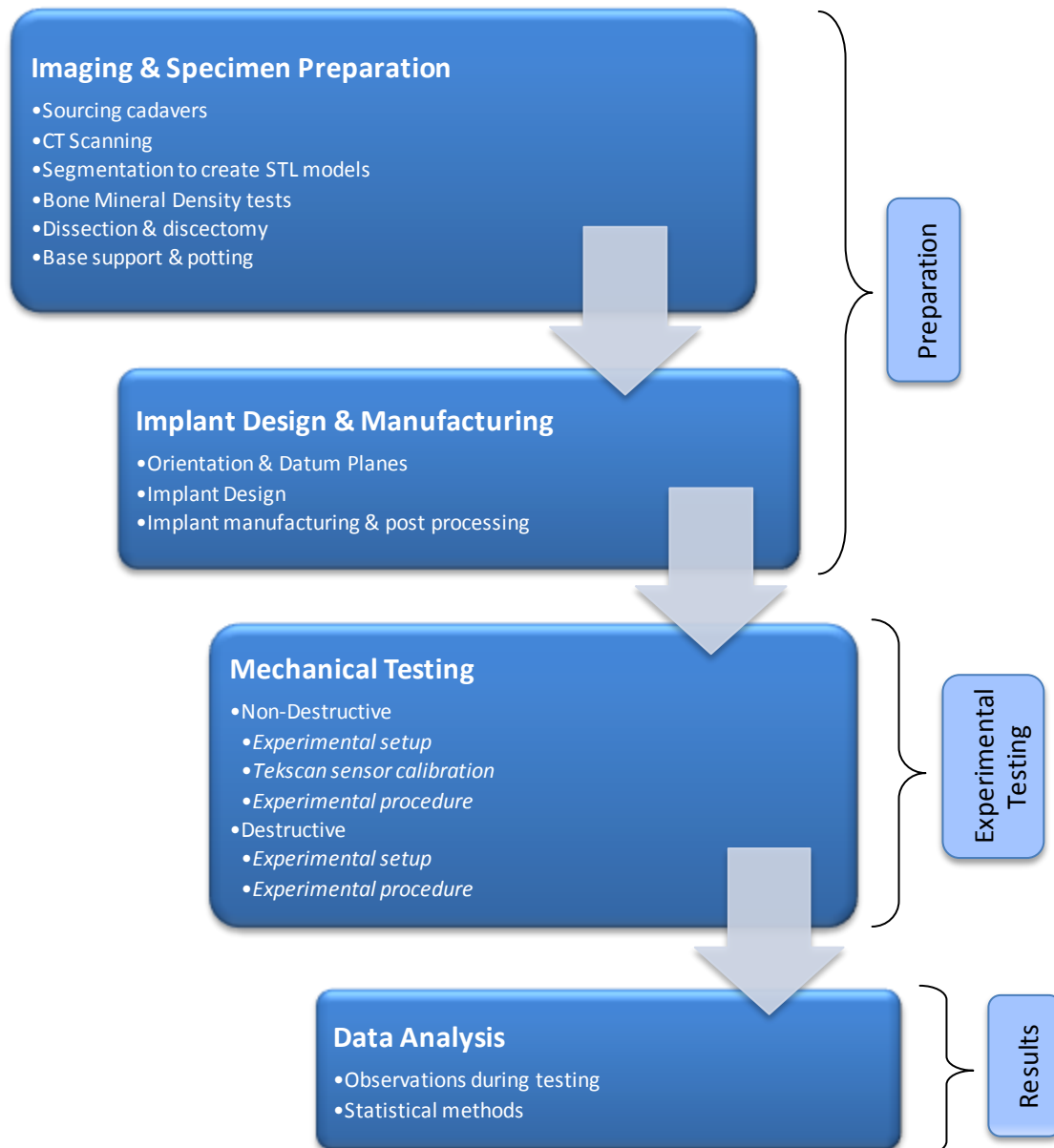


Figure 34 – Overview of study design for pressure-related subsidence testing

The experimental testing was performed in two stages, namely a non-destructive test followed by a failure mechanical test. In both cases, the effect of customizing the contact geometry between implant and vertebral endplates were investigated. Finally, observations were noted during testing and the results data was analysed according to recognised statistical methods.

4.2.2 Imaging and Specimen Preparation

Sourcing of Cadavers

Four spines from male, 2-year-old cadavers (ages 45-65 years, average 52 years), which had a total of $n=88$ vertebrae (C3 to L5) were acquired under approved institutional protocol from the Division of Anatomy and Histology, Dept. of Biomedical Sciences, at the University of Stellenbosch. Three out of the four cadaver specimens did not qualify to be included in the study as one was osteoporotic, one was *osteopenic*, and the third showed the presence of *kyphoplasty*. Therefore one cadaver (nr. K34/08), with a bone mineral density of 1.081 g/cm^2 remained for the study ($n=22$). From the remaining spine, two vertebral bones were used in a separate sub-study (Odendaal, 2010) to assess the accuracy of the manufactured implants using Layer Manufacturing technology, and therefore 20 vertebral bones remained for mechanical pressure testing.

Computed Tomography Scanning

Detailed geometry information of the vertebrae for customizing implant designs was acquired by means of computed tomography (CT) scanning. The scans were performed at the Radiology department of Stellenbosch Medi-Clinic (Van Wageningen & Partners). Figure 35 shows an example of a scan that was performed using their calibrated Siemens Somatom Emotion 16-slice CT scanner.



Figure 35 – CT scanning of a cadaver specimen

The CT scan data was collected in the standard dicom file format and used during several design steps as discussed in the proceedings sections.

Segmentation to create STL models

The dicom files were segmented using Mimics software (Materialise, Belgium) according to the steps described earlier in Section 3.2. under the heading Data Conversion (2D Dicom to 3D STL). Subsequently, from the 2D CT scan data, 3D STL files of the vertebrae were generated.

Bone Mineral Density Tests

Bone density scans were performed on each spine to evaluate whether specimens qualified with normal bone mineral density (BMD). The scans were done at the Helderberg Osteoporosis Clinic (Somerset West) using a calibrated Hologic Discovery A scanner. The scanner is calibrated on a daily basis by calculating the mean BMD from 25 scans of a spine phantom (containing a human-like spine segment made from calcium hydroxyapatite and enclosed in a block of water-simulant epoxy) and must be within acceptable range. The scans provide accurate and precise measurements of small changes in BMD measured in grams per centimetre squared (g/cm^2). Presently BMD measurements offer the physician the most reliable means of recording the rate of bone loss or gain and estimating a patient's risk of fracture. For each density scan, so-called Z-scores and T-scores were derived and compared against a reference database. The Z-score is a measure of the difference in BMD between the scanned specimen and that of healthy people of the *same age*, sex and ethnicity. The T-score compares the measured BMD to that of a *young adult population* of the same sex and ethnicity. The reference database represents the average results as a function of age, sex and ethnicity for a matched population. Reference curves specify average BMD, and standard deviation as a function of age. Each curve applies to a specific scan type, analysis type, bone region, patient gender, and ethnic group.

In preparation for the BMD scans, vertebral segments (L1-L5) from each cadaver were dissected from the rest of the spine and were submerged in containers filled with uncooked rice. The rice acted as a substitute for missing soft tissue while conveniently facilitating correct alignment and orientation of the dissected segments. A summary of the scan results is shown in Table 5 below. The first column denotes the identification number of the cadaver, which is made up from of parts separated by a forward slash character. The first being a unique number allocated and the second two digit number indicating the year in which the cadaver was embalmed. All cadavers were embalmed in the year 2008. Second column shows a graphical image of the BMD scan. Vertebrae L1-L4 were used to calculate the BMD and are shown enclosed by rectangles as the software automatically identified the individual vertebrae. Note the presence of *kyphoplasty* in cadaver K42/08 (indicated by a red oval). The third, fourth and fifth columns indicate the derived BMD, T-score and Z-score respectively. The sixth column shows the resulting patient classification which is depicted graphically in the last column. The white mark on the graph indicates the scoring position for a particular scan, plotted against BMD and T-scores on the y-axes and according to age on the x-axis. The red, yellow and green colours define levels of risk and boundaries for classification. Osteoporotic (red, T-score < -2.5); *Osteopenic* (yellow, -2.5 < T-score < -1); Normal (green, T-score > -1).

World Health Organization criteria for BMD interpretation classify patients as Normal (T-score at or above -1.0), *Osteopenic* (T-score between -1.0 and -2.5), or *Osteoporotic* (T-score at or below -2.5)

Nr	Scan Image	BMD (g/cm ²)	T-Score	Z-Score	Result	Graph
K27/08		0.638	-4.1	-3.9	Osteoporotic	
K42/08		1.365	2.9	4.7	Kyphoplasty noted	
K90/08		0.948	-1.3	-0.9	Osteopenic	
K34/08		1.081	-0.1	0.2	Normal	

Table 5 – BMD scan results of cadaver specimens

Dissection & Discectomy

After imaging, the vertebra specimens were dissected to separate them from one another and all surrounding soft tissue was removed. Posterior elements, which contribute toward vertebral compression mechanics, were kept intact. Both the inferior end plate (the end plate that would make contact with the test implant) and superior endplate was prepared by sharp dissection of the disc with a scalpel, followed by removal of the remaining disc until the hyaline cartilaginous end plate was exposed. A blunt scalpel was then used to remove the remaining cartilaginous end plate while taking care not to damage or remove any bone from the end plate. This preparation technique was performed according to the method prescribed by a spine surgeon with extensive experience in disc replacement surgery.

Base Support & Potting

Each vertebral specimen was then potted by placing the superior body centrally within a plastic container and filling it with a liquid epoxy resin (Prime 20 LV Epoxy Resin, with Prime 20 ULV slow hardener, AMT Composites, Cape Town). In order to ensure that each vertebral endplate was orientated horizontally, perpendicular with respect to the vertically applied pressure, a support structure was 3D printed using the Z-Printer 310 system (Z-Corporation, Burlington, MA), using ZP150 powder material (not infiltrated). The support structure was designed using 3-Matic software (Materialise, Belgium) in such a way that one end matched the geometry of the superior vertebral endplate (Figure 36) and would therefore accommodate the bone and orientate it correctly while the resin hardened around it to secure properly.

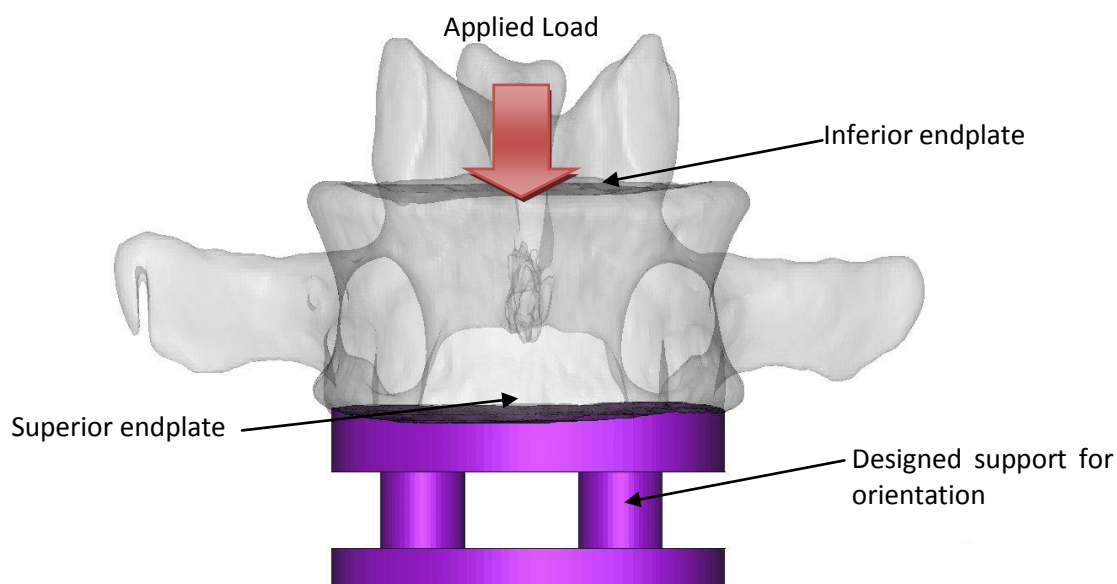


Figure 36 –Support structure designed to orientate bone endplates during vertical loading

4.2.3 Implant design and manufacturing

Modified implants for pressure testing were designed with a main focus on endplate geometry – i.e. size, footprint profile and surface geometry. Implants designed to match the vertebral endplate geometry will be referred to as **contour implants**, while implants with only a flat contact surface will be referred to as **flat implants**.

Orientation and Datum Planes

Each implant was designed using 3-Matic software (Materialise, Belgium). In order to ensure correct orientation and perpendicular force transmission of the implant during mechanical testing, it was necessary to define horizontal datum planes on each of the inferior vertebral endplates. This was achieved by highlighting the surface of the inferior endplate by inspection, and creating a plane using the “Fit Plane” function of 3-Matic. The orientation and position of the datum plane is calculated by least squares approximation of all the points (vertices of the triangulated STL file) that were included in the highlighted selection. Figure 37 below shows a representation of the procedure, indicating a highlighted selection of the inferior vertebral endplate along with the derived datum plane.

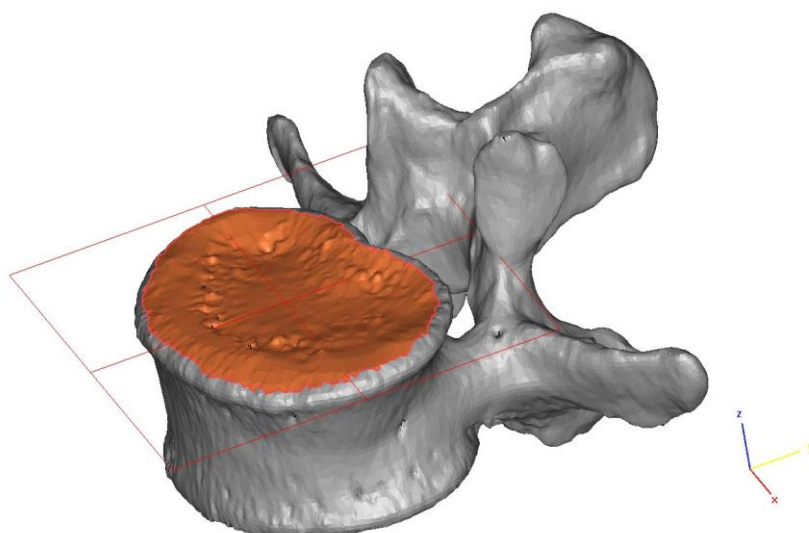


Figure 37 – Fitment and orientation of datum plane

Implant Design

The implant was designed to be a simple prismatic extrusion of a footprint profile that resembles the shape of the transverse vertebral endplate geometry. The profile for each implant was derived by tracing a spline curve on a transverse sketch plane (parallel to the datum plane created in the previous step) and extruding the profile to a 12mm height. The centroid of the two-dimensional profile was calculated and a 10mm hemispherical cut was designed on the superior surface of the implant to accommodate the pressure transmitting pin. Ten implants were then each translated inferiorly until overlapping of bone and the implant model occurred. A Boolean subtraction operation was performed, followed by an undercut removal function to ensure that the implant can be positioned without obstructions caused by undercuts.

Figure 38 shows in (a) the footprint profile (blue spline) on a sketch plane with centroid position and (b) the final implant for L3 (vertebra is shown semi-transparent to reveal contour of the orientation support part). No Boolean subtraction of undercut removal operation was performed on the remaining 10 implants. These were designed with no matching endplate geometry, and merely had flat endplate surfaces.

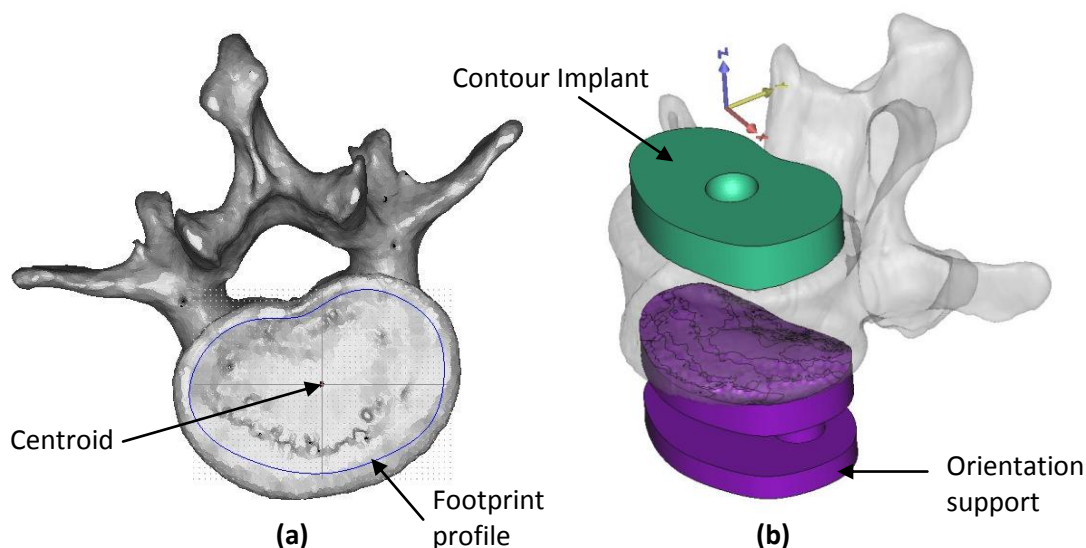


Figure 38 – L3 Implant design showing (a) footprint profile & centroid, and (b) final implant

Implant Manufacturing and Post Processing

Implants were manufactured using Direct Metal Laser Sintering (DMLS) technology. The EOSINT M250 Xtended (EOS GmbH, Germany) was used in combination with the DirectMetal 20 material. The parts were manufactured at the Centre for Rapid Prototyping and Manufacturing (CRPM) at the Central University of Technology (Bloemfontein, South Africa). The manufacturing parameters were set according to the machine's standard DirectTool exposure setting at a layer thickness of 0.02 mm. Post processing involved the removal of a base plate that parts were created on by means of wire cutting, followed by a mild bead blasting process to ensure a smooth and uniform surface finish. Figure 39 shows the implants that were manufactured at the stage just prior to the removal of the base plate.



Figure 39 – Manufactured implants prior to removal from base plate

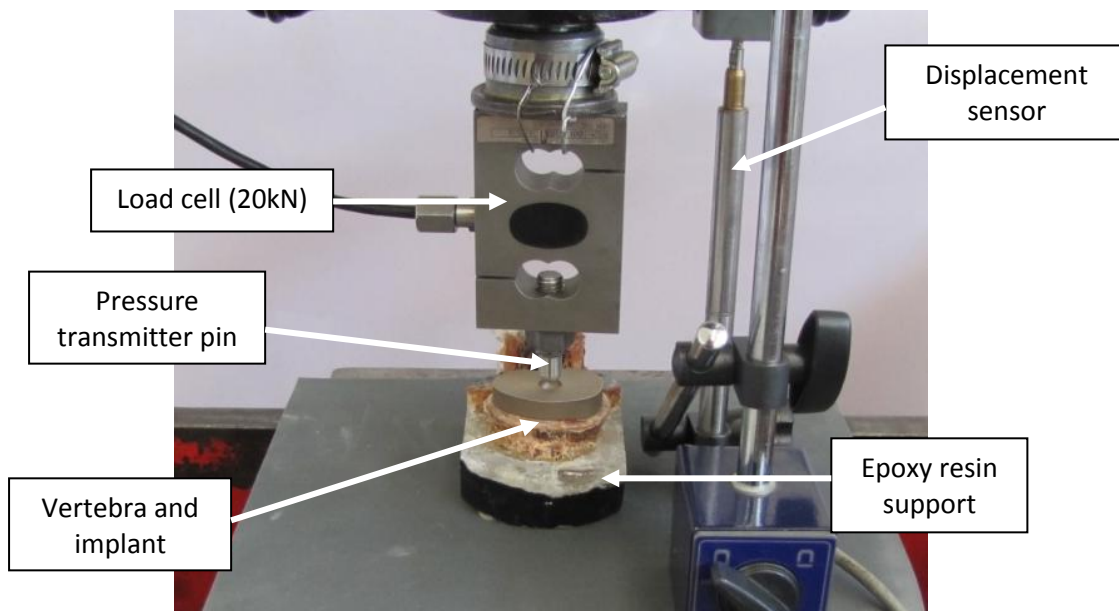
4.2.4 Mechanical Testing

First, non-destructive tests were performed at low loads in order to investigate the distribution of force based on the percentage of surface contact between the implant and the vertebral endplate. Secondly, failure testing was performed to determine failure loads, displacement and calculated stiffness.

Non-Destructive Testing

Experimental Setup

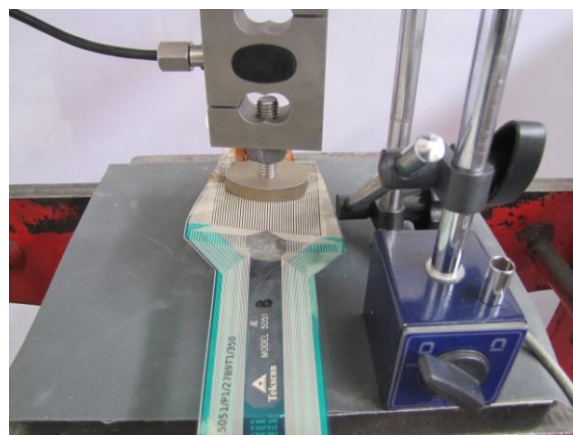
Non-destructive tests were performed using a Schulz hydraulic hand press with a pump stroke of 0.4mm. Therefore adequate control could be achieved as pressure was applied slowly and evenly by hand. Figure 40 shows the setup that was used for the non-destructive tests. A calibrated 20kN load cell was used along with a displacement sensor. Both were linked to an 800MHz Spider data logger (not shown in figure) to gather the measured values of each, using the Catman Easy software (HBM, Darmstadt). An I-Scan sensor (Tekscan Inc., Massachusetts) was used to record the contact load distribution between the implant and the bone endplates.



(a) Setup overview



(b) Close-up showing implant seating



(c) I-Scan pressure sensor position

Figure 40 – Non-destructive test setup

Figure 41 shows the detail of the pressure pin that was used to transmit the load onto the centroid of the implant and distribute over the endplate surface. On the one end a spherical ball nose was created to match the spherical hole of the implants. Due to the irregular freeform shape of the vertebrae and the inherent difficulties in applying pure vertical load onto the endplates, the pressure pin was designed with a spherical nose so that natural alignment could take place during the load tests and thereby reduce the transfer of moments. Flat ends were created near the spherical end to facilitate manual tightening against the implant before applying full loads. In this way, preloads could be applied with accurate control. The other end of the rod was blunt and solid and contained M12 thread all along up to the spherical ball nose. A lock nut was used to fasten the pressure pin securely to the load cell.



Figure 41 – Pressure transmitter pin

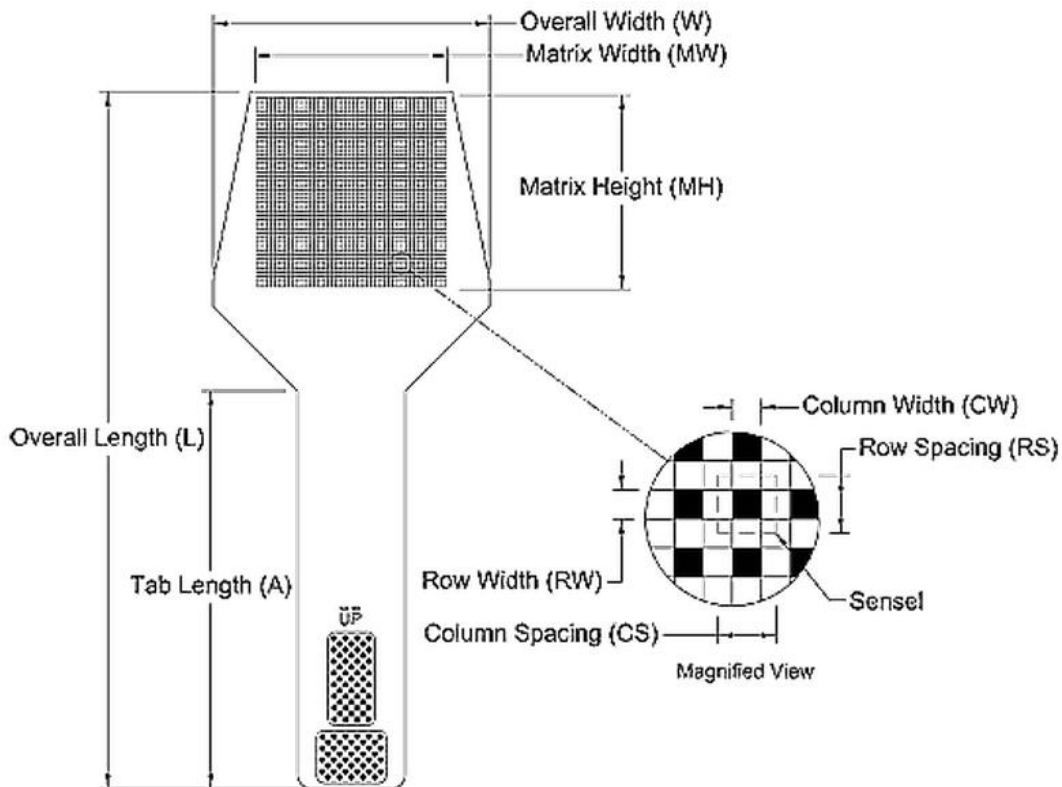
I-Scan Sensor Preparation

I-Scan is a resistive-based technology where a normal force applied to an active sensor causes changes in the resistance of each sensing element (sensel) in inverse proportion to the force applied. Figure 42 shows the sensor (model 5051) that was selected for this study based on its dimensions and pressure range.

Equilibration: Since the process for creating sensors results in some variation, each sensor is somewhat unique. In particular, the distribution of pressure-sensitive ink throughout a sensor is not precisely uniform. In addition, as a sensor is used, certain areas may become less responsive than others. The I-Scan system provides a method, called equilibration, by which this source of error can be minimized. Equilibration is accomplished by applying a highly uniform pressure across the individual sensing elements. Each element within the sensor should produce a uniform output. When this is not the case, the software determines a unique scale factor for that sensel to compensate for the slight variation.

In preparing the I-Scan sensor for the pressure tests, its sensitivity was set to its default setting and an equilibration process was performed using the PB100B equilibration device (Tekscan Inc., Massachusetts) at 10 intermittent uniform pressures from 50 kPa to 250 kPa, allowing the I-Scan software to make the necessary adjustments.

Calibration: The I-Scan system enables one to perform two different types of calibration – linear and 2-point power law, either before or after a recording has been taken. In this case, all sensors were calibrated before test recordings were taken. When performing a linear calibration, a known load is applied to the sensor. The I-Scan software then performs a linear interpolation between zero and the known calibration loads (refer to Table 6 and the discussion below). A linear calibration is the most simple to perform, and is suitable for tests in which the load range is limited. When performing a 2-point power law calibration, two different known loads are applied to the sensor. The software then performs a power law interpolation based on zero load and the two known calibration loads, using the equation $y = ax^b$. A 2-point power law calibration is preferable if measurement loads vary considerably during testing. As a rule of thumb, the applied calibration loads should be approximately 20% and 80% of the expected maximum test load. Both techniques for calibration were considered, however the 2-point power law calibration was preferred giving more accurate results over the range of loads applied during testing.



L [mm]	W [mm]	A [mm]	MW [mm]	MH [mm]	CW [mm]	CS [mm]	Col Qty	RW [mm]	RS [mm]	Row Qty	Nr of Sensels	Sensel Density [sensels/cm ²]	Pressure Range [kPa]
252.5	81.3	166.2	55.9	55.9	0.76	1.27	44	0.76	1.27	44	1936	62.0	2413

Figure 42 – I-Scan 5051 sensor map and specifications

Experimental Procedure

An initial preload of 50N was applied, after which the force was increased slowly at an even rate until the predetermined non-destructive load was reached. This load was not the same for all vertebrae, since the endplate surface area decreases from L3 to C3 and as a precaution, the loads were also decreased. The vertebrae were allocated into five groups of four with the maximum loads applied as follows:

Group	Vertebrae	Maximum non-destructive load
1	L3, L2, L1, T12	400 N
2	T11, T10, T9, T8	350 N
3	T7, T6, T5, T4	300 N
4	T3, T2, T1, C7	250 N
5	C6, C5, C4, C3	200 N

Table 6 – Non-destructive loads per vertebral grouping

The selection of these loads were based on previous literature with similar experimental procedures (Auerbach, Ballester, Hammond, Carine, Balderston, & Elliott, 2010), (Hasegawa, Abe, Washio, & Hara, 2001), (Tan, Bailey, Dvorak, Fisher, & Oxland, 2005). Data was recorded simultaneously from the I-Scan sensor as well as from the load cell and displacement sensor. The maximum non-destructive loads were held for 10 seconds before being released.

Destructive Testing

Experimental Setup

After completing non-destructive testing, failure testing was performed once on each vertebral specimen. Figure 43 shows the setup for a typical failure test. Testing was performed using an MTS hydraulic pressure tester (MTS, Minnesota, USA). A calibrated 20kN load cell was used to measure the applied load. Two displacement sensors were used in order to measure any displacement that may occur in the resin holding the vertebrae. The first was placed on the resin material, as close as possible to the vertebral body. The second reference sensor was placed on the moving pressure cylinder. Two cameras were used to record the failure tests. One was placed in front of the pressure tester at the same horizontal level as the test specimen, while the other was placed slightly higher looking down diagonally. Figure 44 shows the positions of the cameras as well as their lines of vision marked by red dash lines. A metric ruler was also placed behind the specimen to serve as a visual frame of reference for the recordings.

Experimental Procedure

Samples were placed on the pressure tester and a preload of 100N was applied and held for 20 seconds. After preload, camera recording commenced, displacement sensors were zeroed and a slow ramp was applied at 0.1mm/s using the MTS Model 407 Controller. Destructive tests were therefore displacement controlled as opposed to force-controlled. Similar to the non-destructive tests, data from the displacement

sensors and load cell was recorded using an 800MHz Spider data logger in combination with Catman Easy software (HBM, Darmstadt). The test was stopped when fracture had occurred or the load-displacement curve dropped. A slow ramp down was performed until the cylinder reached its original position.

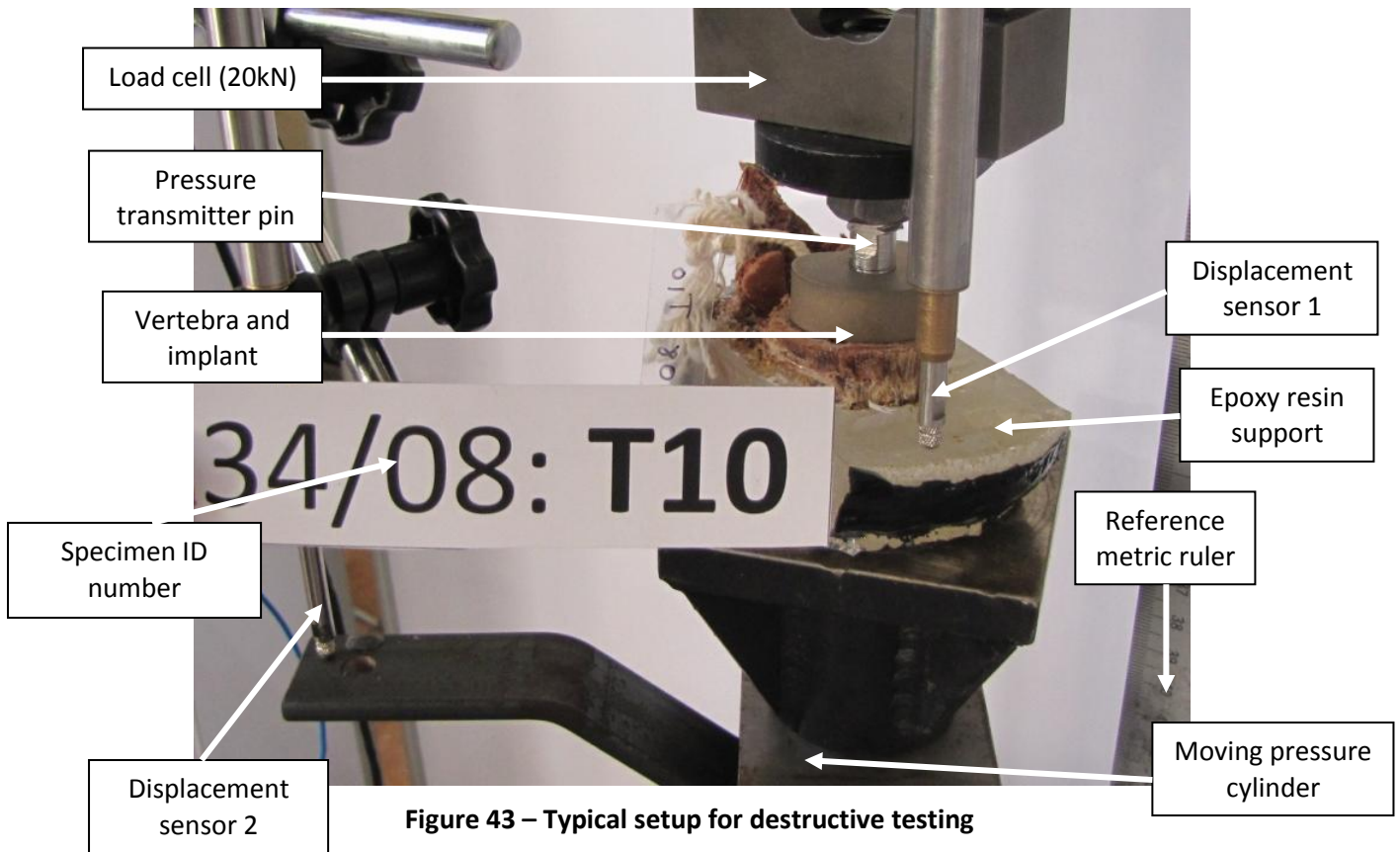


Figure 43 – Typical setup for destructive testing

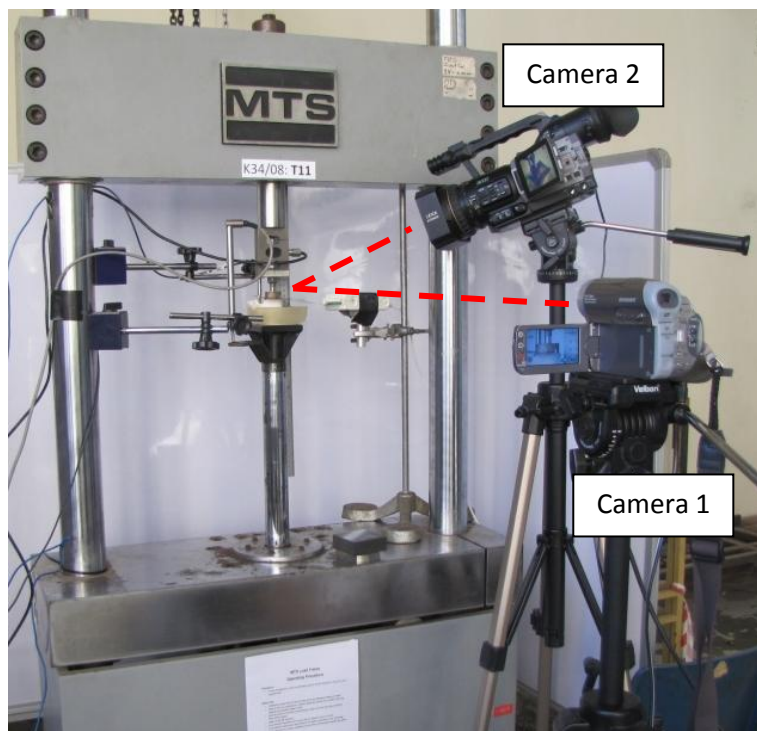


Figure 44 – Position of cameras in relation to test setup and their line of vision

4.2.5 Data Analysis

Observations during Testing

General observations were noted throughout the different stages of non-destructive and failure testing and will be discussed later when results are reviewed. The results obtained from each compression mechanical test were analyzed as follows:

Non-destructive tests:

1. The I-Scan recordings were reviewed and a percent contact was calculated as the measured contact area divided by the area of the vertebra endplate at maximum load. The area of the vertebral endplate is an important measurement and in practice, usually quite difficult to measure physically due to its irregular geometry. A technique for measuring this area has been cited in literature and usually involves approximating it by the area of an ellipse superimposed on a transverse view of the vertebral CT scan image. The minor and major diameters of the ellipse are then based on the endplate's maximum anteroposterior and lateral dimensions. (Auerbach, Ballester, Hammond, Carine, Balderston, & Elliott, 2010), (Steffen, Tsantrizos, & Aebi, 2000), and (Labrom, Tan, Reilly, Tredwell, Fisher, & Oxland, 2005). Even though the approximation of endplates as ellipses has been shown to overestimate the actual endplate area by less than 10% (Steffen, Tsantrizos, & Aebi, 2000), a more accurate measurement was sought during this study. The vertebral endplate areas were therefore calculated from the highlighted areas of the relevant 3D surface geometry in the CAD models that were derived from their CT scan data as previously shown in Figure 37. Typically, as expected, these areas would slightly exceed the encompassed areas of the footprint profile of the implant indicated in Figure 38(a).
2. The pressure distribution mapping that was recorded digitally from the I-Scan sensors were graphically superimposed over images of the vertebrae to give a visual indication of the load distribution in relation to the footprint area of the implant.

Destructive tests:

1. Load-displacement curves were derived from the test data and failure was defined as the maximum load in the load-displacement response. In those instances where the load-displacement response exhibited an early drop or a break in the curve, these were not recorded as maximum loads as long as the load continued to rise over a subsequent 0.5 mm displacement.
2. The stiffness was calculated using linear regression of the elastic portion of the load-displacement graph. For this purpose, the spine vertebrae were grouped according to their anatomical definitions and stiffness was calculated between the loads shown in Table 7 below:

Grouping	Vertebrae	Stiffness Calculated between	
		Lower Load Limit [N]	Upper Load Limit [N]
Cervical	C3-C7	1000	4000
Upper-Thoracic	T1-T6	1000	4000*
Lower-Thoracic	T7-T12	1000	5000
Lumbar	L1-L3	2000	8000

* With the exception of T2 where an upper limit of 3500N was used because failure occurred at 4000N

Table 7 – Upper and Lower Loads used for Stiffness Calculation of Failure Test Results

Statistical Methods

As mentioned before, the effect of customized matching endplate geometry during load testing was investigated and the following statements were hypothesised:

1. The use of contour implants during non-destructive tests will result in a significantly higher contact area between the prosthesis and the vertebra when compared to using flat implants.
2. The use of contour implants during destructive tests will result in a significant increase in measured stiffness of the implant-vertebral construct, when compared to using flat implants

The test results were examined statistically using basic methods of analysis as follows:

Analysis of non-destructive results:

- Hypothesis testing was performed on the percentage surface contact that was measured for each vertebra and implant combination to test if there is a statistically significant difference between those loaded with contour implants versus flat implants.

Analysis of destructive test results:

- Hypothesis testing was performed on the stiffness results of the failure tests in order to determine if there is a statistically significant difference between using the contour implant versus the flat implant. A higher stiffness effectively implies that a higher load can be withstood before the same amount of displacement (or in this case subsidence) occurs.

4.3 Results

4.3.1 Non-Destructive Tests

A summary of the main results from the non-destructive tests for contour implants and flat implants are shown in Table 8 and Table 9 respectively. The bone endplate areas, which were measured digitally on the STL files of the vertebrae, reduce as expected along the progression of the spine. The smallest area relates to the smallest bone, C3. The percentage contact (6th column) is an important result. The average contact for contour implants was 45.27%, while flat implants only made an average of 10.49% contact. This is depicted graphically in Figure 45.

Vertebra	Max Load [N]	I-Scan Contact Area [mm ²]	Bone Endplate Area [mm ²]	% Contact
L3	402.0	485	1577.86	30.74%
L1	402.0	442	1489.64	29.67%
T11	354.6	411	1179.28	34.85%
T9	352.8	327	948.90	34.46%
T7	306.6	306	812.46	37.66%
T5	302.4	256	653.77	39.16%
T3	252.0	311	544.04	57.16%
T1	252.0	231	532.87	43.35%
C6	202.8	302	400.56	75.39%
C4	202.8	248	353.01	70.25%
Averages	303.0	331.90	849.24	45.27%

Table 8 – Summary of Non-Destructive Test Results – Contour Implants

Vertebra	Max Load [N]	I-Scan Contact Area [mm ²]	Bone Endplate Area [mm ²]	% Contact
L2	400.8	69	1488.63	4.64%
T12	403.2	116	1313.70	8.83%
T10	352.8	116	1067.45	10.87%
T8	352.8	97	875.68	11.08%
T6	303.6	92	735.36	12.51%
T4	303.0	68	593.79	11.45%
T2	252.0	37	535.03	6.92%
C7	253.8	55	407.16	13.51%
C5	202.8	47	344.01	13.66%
C3	203.4	40	350.38	11.42%
Averages	302.8	73.70	771.12	10.49%

Table 9 – Summary of Non-Destructive Test Results – Flat Implants

The solid bars indicate the percentage contact for contour implants, and it is significant to note that this level of contact increases from the lumbar to the cervical bones. This is due to the fact that the endplates of the vertebrae become increasingly concave from lumbar to cervical, allowing for a more distinct and comprehensive fit between bone and implant. Despite the increase in concavity of the endplates, the percentage contact that the flat implants made (light blue bars), remained relatively constant at above or below 10%. Thus the vertebral level did not play a significant role in the performance of the flat implants with regards to percent contact.

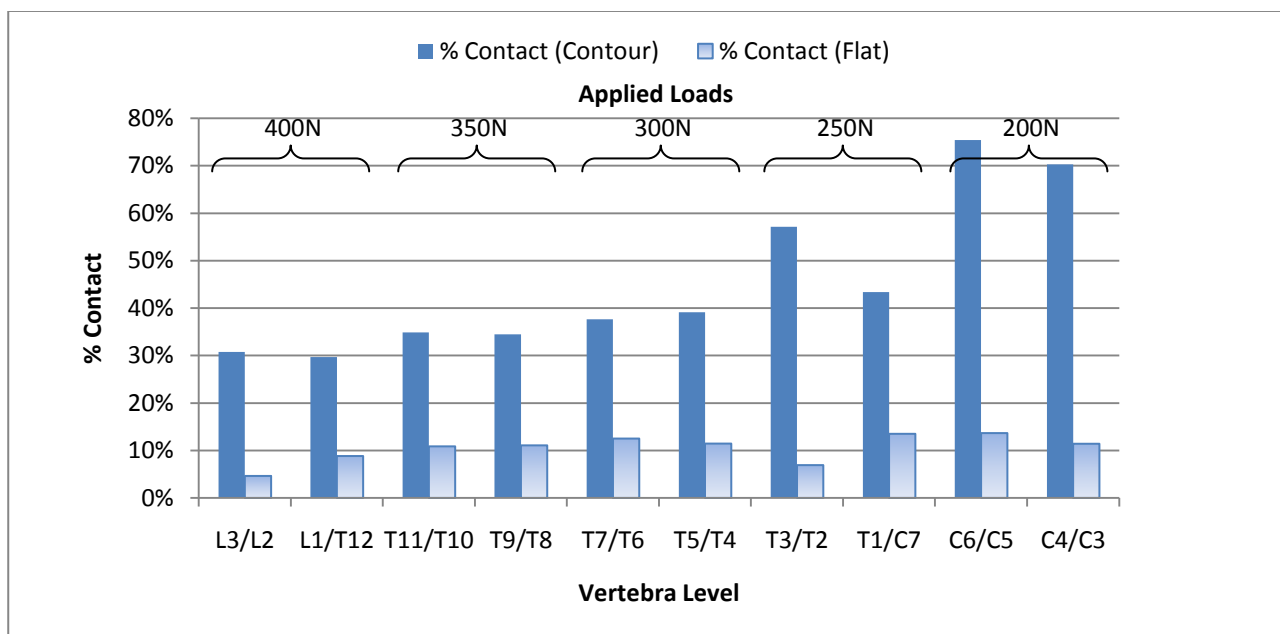


Figure 45 – Percent Contact and Max Pressure Comparison

The way in which the loads were distributed was measured using an I-Scan pressure sensor (Tekscan, Massachusetts, USA) and is shown in Table 10. The scan result images were scaled uniformly and superimposed over images of the vertebrae. The profiles of the implants are represented by a blue line which provides a border for the pressure distributions. A clear distinction is visible between the contact percentages of the different implants, with the contour ones showing a marked improvement over their flat counterparts. What is also evident in the case of the flat implants, is that all the loads were transmitted onto the peripheral sides of the endplates where the high rims of the concave bone geometry made first contact and created stress concentrations. This was especially true in the case of the upper thoracic and cervical vertebrae where the concavity is quite pronounced.

Group 1: Vertebrae loaded at 400N			
L3 (Contour)	L2 (Flat)	L1 (Contour)	T12 (Flat)

Group 2: Vertebrae loaded at 350N			
T11 (Contour)	T10 (Flat)	T9 (Contour)	T8 (Flat)

Group 3: Vertebrae loaded at 300N			
T7 (Contour)	T6 (Flat)	T5 (Contour)	T4 (Flat)

Group 4: Vertebrae loaded at 250N			
T3 (Contour)	T2 (Flat)	T1 (Contour)	C7 (Flat)

Group 5: Vertebrae loaded at 200N			
C6 (Contour)	C5 (Flat)	C4 (Contour)	C3 (Flat)

Table 10 – Pressure distribution maps from I-Scan sensors

Even though the contour implants exhibit a wider load distribution than their flat counterparts, it was surprising to see that the average percentage contact of 45.27% was not indeed higher. Though care was taken to remove most of the cartilage from the vertebral endplates, there may have been some discrepancy between the final bone geometry and its CT scan from which the implant endplate designs were derived. This is an important consideration to take into account when regarding surgical procedures for future implant insertion. Current surgical techniques for removing the natural disc before replacing it with an implant are usually done with limited visibility of the endplates and rely heavily on the experience of the surgeon to remove all cartilage by feel instead of sight. If custom-fit implants are employed in future, surgical techniques will need to ensure that no significant cartilage remains on the endplates and may possibly involve the use of endoscope equipment to inspect and confirm proper site preparation.

One may also consider whether any inaccuracies in manufacturing of the implant may have caused an improper fit to the bone and result in decreased percent contact. However, Odendaal claims that accuracy within 0.37mm can be achieved over the contact geometry with 95% confidence level (Odendaal, 2010).

On the other hand, the low percentage contact observed for contour implants may be attributed to inherent limitations of the I-Scan measuring equipment. The sensor used was a polyester film of 0.1mm thickness, and although thin, did not have the flex capability to fill every dip and groove of the irregular vertebral endplate geometry as pressure was being applied. So although the sensor has a high scan resolution of 62 sensels/cm² (as shown in the specifications of Figure 42), and the results obtained give a good indication of general surface contact, it may be possible that the percent contact may indeed be higher for contour implants than was recorded. This limitation did however not impair the measurements taken for the flat implants, since the sensor remained flush against the flat implant and contacts occurred against ridges and high points of the vertebral endplates.

In future, a theoretical approach may be considered to calculate expected percent contact by using photogrammetry technology to measure the bone surface and the implant surface. In this way, by overlapping the two data sets, a best fit approximation can be made of what the expected contact or error distribution may be. However in this study, due to the physical nature of the pressure tests performed, a more pragmatic and tangible approach was pursued. Although the measured results of percent contact for contour implants were lower than expected, and taking into consideration the limitations of the measuring equipment discussed above, the contour implants still exhibited improved contact and better load distribution than the flat implants – the results of which are statistically significant as will be shown in the next section.

Percentage Contact Hypothesis Testing

A hypothesis test was done to investigate if there is a statistically significant difference in the percent coverage of the two types of implant designs. For this purpose, the parameters of interest were μ_1 and μ_2 , the average percent coverage of the contour and flat implant designs respectively, and the test investigated if $\mu_1 - \mu_2 = 0$, or $\mu_1 = \mu_2$.

Null hypothesis: $H_0: \mu_1 = \mu_2$;

Alternative hypothesis: $H_1: \mu_1 \neq \mu_2$

The hypothesis test in this case involved the difference in means of two distributions with unknown variances. Figure 46 shows a Box & Whisker plot for the two different implant designs, indicating both their location and spread. By inspection, this depiction reaffirms the preceding observations from Figure 45 and Table 10 that there is a discernable difference in the calculated means. What is more clearly shown in Figure 46 is also the difference between sample variations. With a lower standard deviation equal to 2.89%, one may conclude that flat implants consistently achieved low percentage contact with the bone endplates.



Figure 46 – Box & Whisker plot for % contact measured using contour and flat implant designs

The sample sizes were relatively small, and therefore the populations were assumed to be normally distributed, and the hypothesis test and confidence intervals were based on the t distribution

(Montgomery & Runger, 2007). Figure 47 below shows a normal probability plot for the two variables. The assumption of normality appears quite reasonable, but since the slopes of the two straight lines are very different, and as already observed from Figure 46, it is unlikely that the population variances are the same.

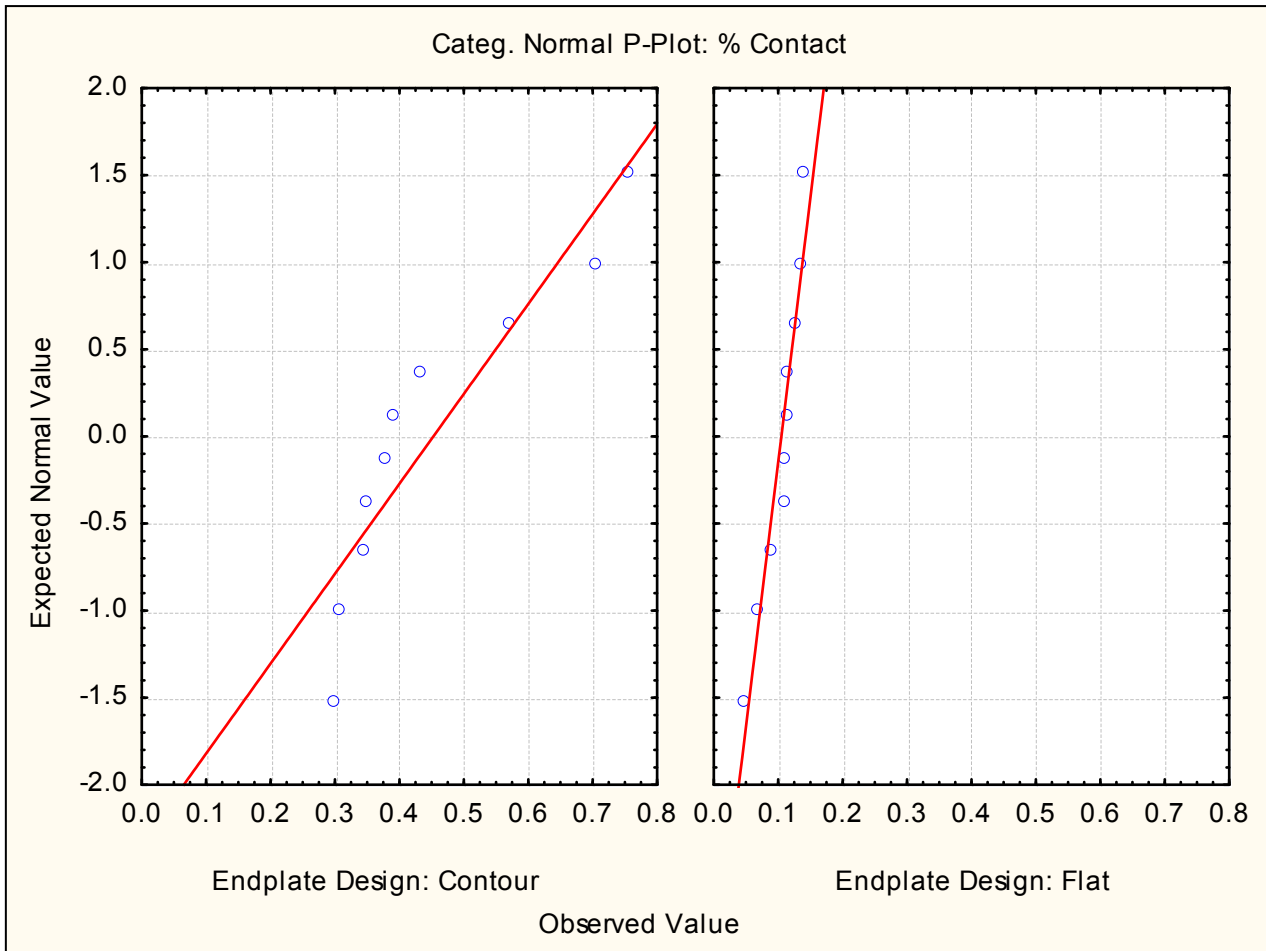


Figure 47 – Normal probability plots of % contact for contour and flat implants

In cases where the variances of the populations are unequal, there is not an exact *t*-statistic available for testing $H_0: \mu_1 = \mu_2$. However, an approximate result can be applied (Montgomery & Runger, 2007).

Let X_1 and X_2 be random variables that refer to the percentage contact achieved using the contour and flat implant designs respectively. If $H_0: \mu_1 - \mu_2 = \Delta_0$ is true, the statistic

$$T_0^* = \frac{\bar{X}_1 - \bar{X}_2 - \Delta_0}{\sqrt{\frac{s_1^2}{n_1} + \frac{s_2^2}{n_2}}} \tag{1}$$

is distributed approximately as *t* with degrees of freedom given by

$$v = \frac{\left(\frac{s_1^2}{n_1} + \frac{s_2^2}{n_2}\right)^2}{\frac{(s_1^2/n_1)^2}{n_1 - 1} + \frac{(s_2^2/n_2)^2}{n_2 - 1}} \tag{2}$$

If v is not an integer, round down to the nearest integer.

\bar{X}_1 and \bar{X}_2 are the sample means of the two random variables, and Δ_0 is some chosen value. In this case $\Delta_0 = 0$. The variables s_1 and s_2 refer to the standard deviations while n_1 and n_2 refer to the sample sizes.

The rejection criteria for the null hypothesis are as follows:

$$\text{Reject } H_0 \text{ in favour of } H_1 \text{ if: } t_{\alpha/2,v} < t_0^* < -t_{\alpha/2,v}$$

Therefore, making use of the values in the 6th column of Table 8 and Table 9, $s_1 = 16.51\%$ and $s_2 = 2.89\%$, while $n_1 = n_2 = 10$.

$$v = \frac{\left[\frac{(16.51)^2}{10} + \frac{(2.89)^2}{10} \right]^2}{\frac{[(16.51)^2/10]^2}{9} + \frac{[(2.89)^2/10]^2}{9}} = 9.55 \cong 9$$

Therefore, using $\alpha = 0.05$, we would reject $H_0: \mu_1 = \mu_2$ if $t_0^* > t_{0.025,9} = 2.262$ or if $t_0^* < -t_{0.025,9} = -2.262$.

$$t_0^* = \frac{45.27 - 10.49 - 0}{\sqrt{\frac{(16.51)^2}{10} + \frac{(2.89)^2}{10}}} = 6.56$$

In conclusion then, since $t_0^* = 6.56 > t_{0.025,9} = 2.262$, the null hypothesis is rejected, and there is a statistically significant difference in the percentage contact made by the contour implants in comparison to that of flat implants. The p-value for this two-tailed hypothesis test is smaller than 0.001.

4.3.2 Destructive Tests

A summary of the destructive failure test results for contour implants and flat implants are shown in Table 11 and Table 12 respectively. The maximum failure loads (2nd column) that were recorded is also displayed graphically in Figure 48. In all cases (although in some only marginally), the contour implants achieved a higher failure load than their flat counterparts. As expected, the lumbar and low-thoracic vertebrae withstood the highest loads. This observation is verified by the red trend line of Figure 48, which shows a decline and then a slight incline again for the cervical vertebrae. This slight increase in cervical loads is attributed to their higher percentage cortical bone content. The stiffness values of Table 11 and Table 12 were calculated using linear regression of the elastic portion of the load-displacement graphs. For this purpose, the spine vertebrae were grouped according to their anatomical definitions and stiffness was calculated between the loads shown in Table 7.

Vertebra	Max Failure Load [kN]	Stiffness [kN/mm]
L3	12.2136	13.367
L1	11.0748	8.719
T11	10.914	9.348
T9	8.2404	9.660
T7	6.7356	8.476
T5	5.4792	7.581
T3	5.3436	7.416
T1	7.0104	7.759
C6	6.7596	10.440
C4	7.0644	8.182
Average	8.084	9.095

Table 11 – Summary of Destructive Test Results – Contour Implants

Vertebra	Max Failure Load [kN]	Stiffness [kN/mm]
L2	10.6224	5.271
T12	10.7172	7.136
T10	9.2208	5.656
T8	6.6756	5.656
T6	5.5092	4.888
T4	5.3148	2.348
T2	4.1484	1.720
C7	5.214	2.139
C5	5.3688	1.634
C3	6.4656	1.849
Average	6.926	3.830

Table 12 – Summary of Destructive Test Results – Flat Implants

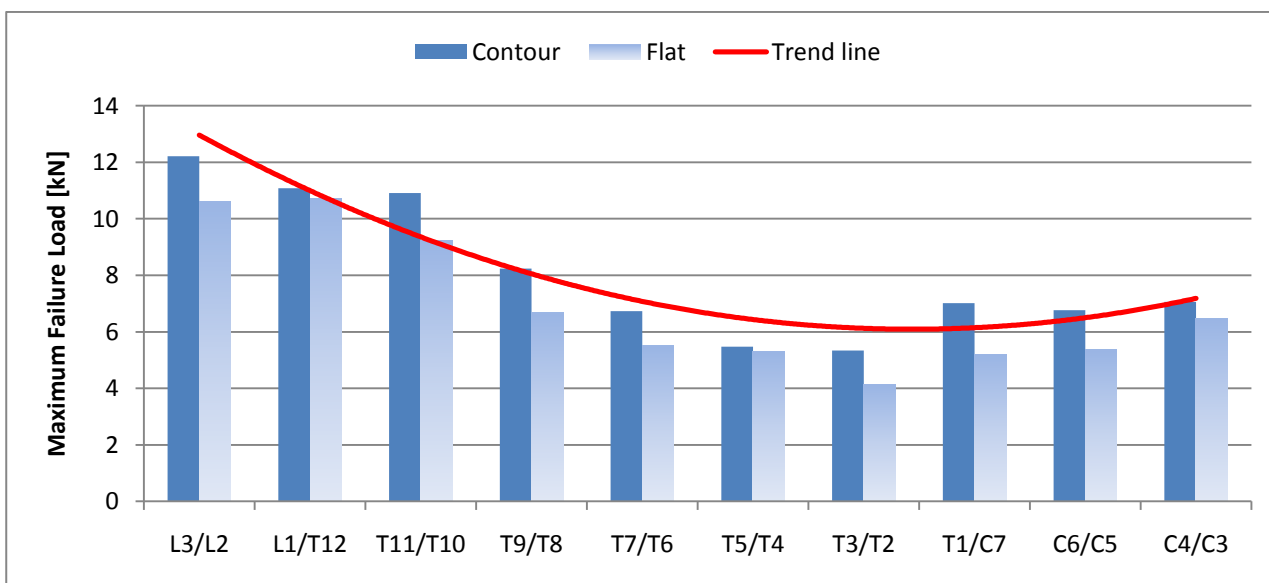


Figure 48 – Maximum failure loads for contour and flat implants per vertebra

Figure 49 is an example of a typical load-displacement response that was obtained during the failure tests, in this case using a contour implant on the T11 vertebra. The load-displacement graphs of the other vertebrae are included in Appendix C. Some points that are of importance to take note of:

- A: Lower load limit used during the derivation of the stiffness for the vertebra considered. There is usually some settling that takes place prior to reaching point A.
- B: The upper boundary load used for deriving stiffness. A linear regression line is fit to the graph between points A and B to derive sample stiffness.
- C: This is a point where vertebral failure starts to appear. Since the vertebrae are a heterogeneous combination of cortical and cancellous bone along with other internal soft tissue, it is to be expected that failure will be non-linear and progressive as is observed between points C and D.
- D: This is the point where maximum load is achieved and final yielding takes place. As the pressure continues to be applied between points D and E, the graph may exhibit a decline as the depressed implant reaches the softer cancellous bone after breaking through the cortical shell. Alternatively it may show a secondary incline as bone material becomes compressed, providing denser resistance.
- E: At this point, the test was terminated and a slow ramp down at 0.1mm/s was performed. The graph shows a corresponding drop in load, exhibiting a common hysteresis cycle and the amount of plastic deformation that has occurred.

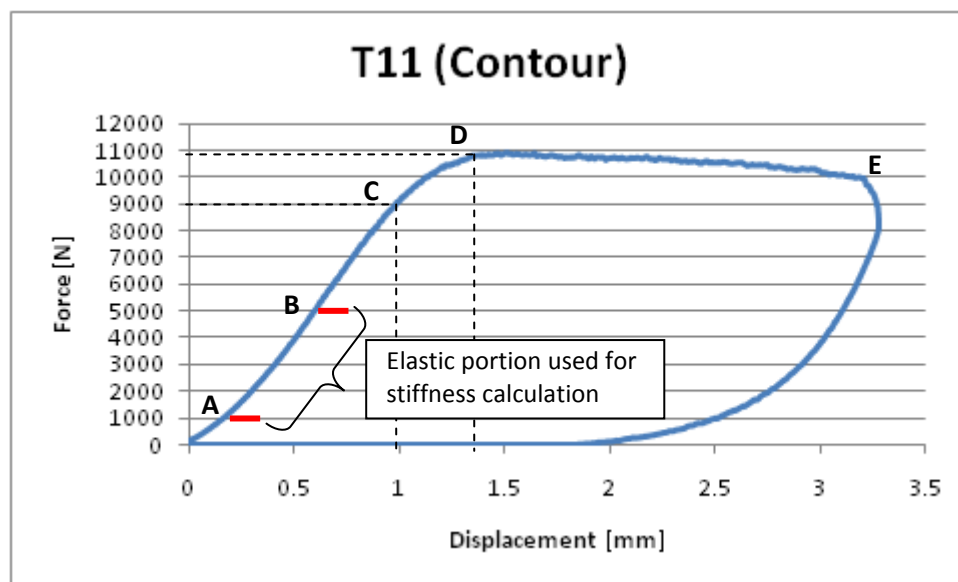


Figure 49 – Typical load-displacement response from failure testing of vertebrae

Figure 50 shows the stiffness values that were derived from the linear regression calculations on each vertebra's load-displacement curve. The contour implants are represented by dark blue bars while the flat implants are light blue. Stiffness is higher for contour implants in each case and the difference becomes

more pronounced from the mid-thoracic to the cervical vertebrae. The growing difference is due mostly to a decrease in stiffness of vertebrae using flat implant designs. Apart from the high stiffness observed for L3, the vertebrae using contour implants exhibited stiffness values that ranged between 8 and 10kN/mm.

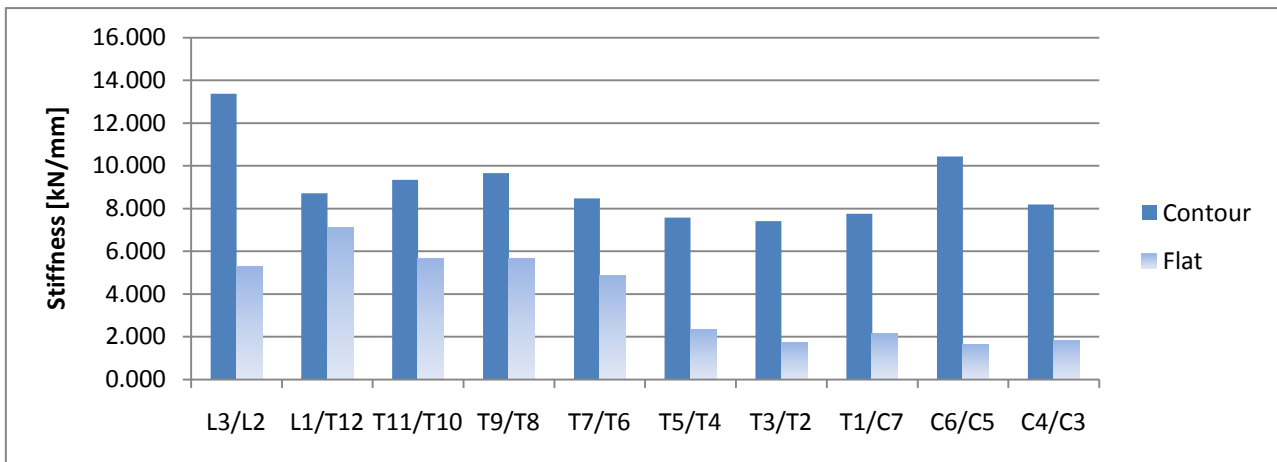


Figure 50 – Stiffness values per vertebra during failure testing

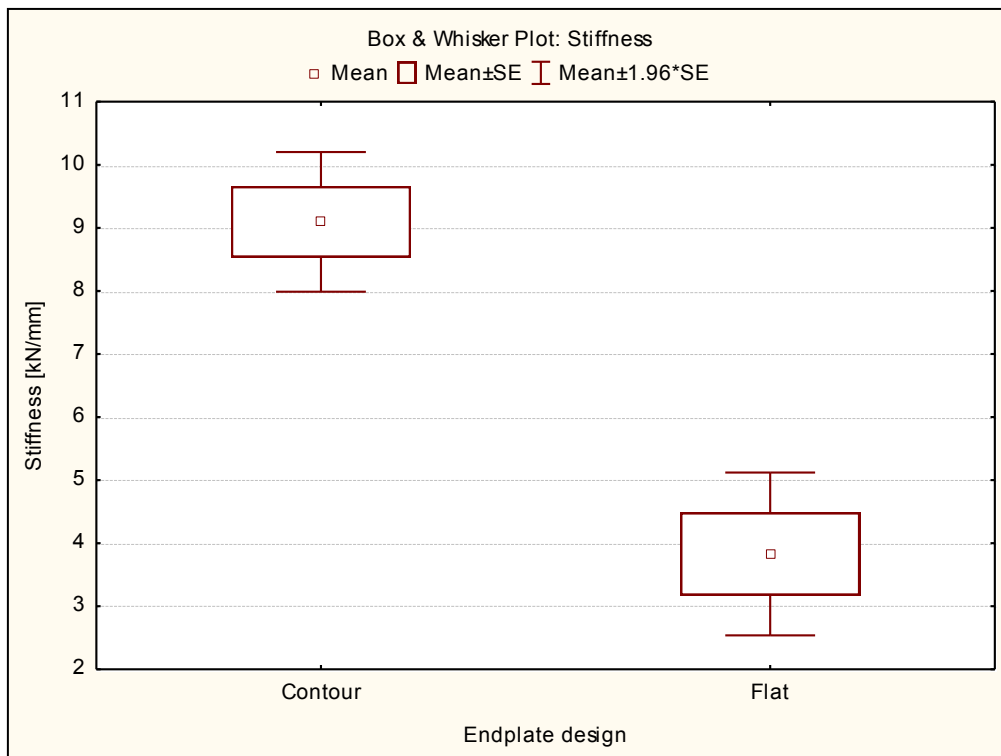


Figure 51 – Box & Whisker plot for stiffness during destructive failure tests

In general, the nature of the failures observed was more ductile than brittle as may be expected. This observation is supported by the non-linear and gradual failures that occurred as shown in the load-displacement graphs.

The vertebrae were inspected visually after destructive testing and photos taken are shown along with the load-displacement graphs in Appendix C. Also included with these photos, are comparative 3D CAD CT images showing the outlines of the implant footprint profiles.

The lumbar vertebrae show mostly a depression of the bone along the implant’s profile lines in the anterior region of the superior endplates. From T12, failure is noted to occur more circumferentially along the implant profile and includes subsidence into the posterior of the vertebral endplate. Hairline cracks were also noted on the outer posterior cortical rim of some of the endplates. T4 and T2 show similar cracks also appearing on the anterior cortical rim. This is again noted in the cervical bone of C5, where the Flat implant was supported by the concave geometry of the anterior part of the endplate, where failure seems to have occurred. The severe damage that was observed for C7 can be attributed to an extended application of the load after initial failure, as is confirmed by its load-displacement curve.

A hypothesis test was performed to investigate whether the difference in stiffness sample means for contour and flat implants are statistically significant. From the Box & Whisker plot above and the normal probability plot in Figure 52 below, the populations were assumed to have a normal distribution with equal but unknown variances.

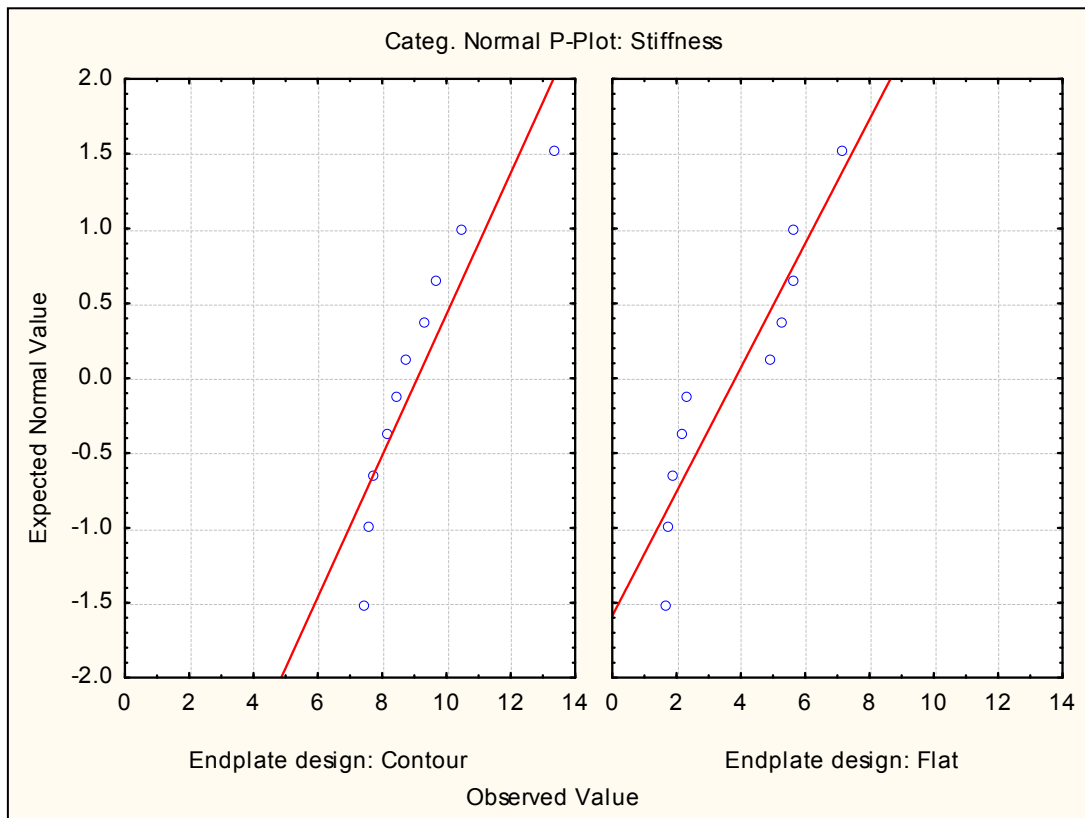


Figure 52 – Normal probability plot of stiffness for different implant designs during destructive tests

Letting X_1 and X_2 be random variables that refer to the stiffness of the contour and flat implants respectively, the pooled t-test is stated as follows:

Null hypothesis: $H_0: \mu_1 = \mu_2$

Alternative hypothesis: $H_1: \mu_1 \neq \mu_2$

Test statistic:

$$T_0 = \frac{\bar{X}_1 - \bar{X}_2 - \Delta_0}{S_p \sqrt{\frac{1}{n_1} + \frac{1}{n_2}}}$$

Where \bar{X}_1 and \bar{X}_2 are the sample means of the two random variables, and Δ_0 is some chosen value. In this case $\Delta_0 = 0$. The variable S_p is the pooled standard deviation and is calculated according to Equation 4.

The rejection criteria for the null hypothesis are as follows:

$$\text{Reject } H_0 \text{ in favour of } H_1 \text{ if: } t_{\alpha/2, n_1+n_2-2} < t_0 < -t_{\alpha/2, n_1+n_2-2}$$

Using the stiffness values found in Table 11 and Table 12, it follows that $s_1 = 1.79$ kN/mm and $s_2 = 2.08$ kN/mm, while $n_1 = n_2 = 10$. Therefore

$$s_p^2 = \frac{(9)(1.79)^2 + (9)(2.08)^2}{10 + 10 - 2} = 3.763 \quad \text{and} \quad s_p = \sqrt{3.763} = 1.9399$$

Using $\alpha = 0.05$, we would reject $H_0: \mu_1 = \mu_2$ if $t_0 > t_{0.025, 18} = 2.101$ or if $t_0 < -t_{0.025, 18} = -2.101$.

Therefore

$$t_0 = \frac{\bar{x}_1 - \bar{x}_2 - \Delta_0}{1.9399 \sqrt{\frac{1}{n_1} + \frac{1}{n_2}}} = \frac{9.09 - 3.83 - 0}{1.9399 \sqrt{\frac{1}{10} + \frac{1}{10}}} = 6.069$$

It is therefore concluded that the null hypothesis must be rejected because $t_0 = 6.069 > t_{0.025, 18} = 2.101$. The difference observed in the stiffness when using contour implants compared to flat implants is therefore statistically significant with a p-value < 0.0001 .



Conclusions & Recommendations

5 Conclusions and Recommendations

This study has proposed a new process chain for the design and manufacture of customized intervertebral disc implants with the use of medical scanning, simulation and CAD software as well as Rapid Manufacturing technologies. Customization specifically focused on matching the interfaces of the implant to the geometry of the vertebral endplates, while other implant features are customised based on anatomical landmarks identified by qualified surgeons.

The important factors to consider during each step of the process chain were highlighted, while emphasizing the benefits that can be obtained through customization. Certain areas of the process chain have already been conducted successfully, and are described in more detail, while others are still part of ongoing research. These mainly include the role of biomechanical simulation during the design stage and regulatory approval issues.

One of the main expected benefits from customizing the endplate geometry of disc implants is the reduced risk and potential for subsidence into the vertebral bone endplate. A sub-study was undertaken to identify if the expected benefit would be substantial and statistically significant. The study involved cadaver vertebrae that were subjected to pressure tests (non-destructive and failure testing) using two different endplate designs. One design, namely contour implants, matched the endplate geometry of the vertebrae, while the other design had a flat endplate surface profile. The non-destructive experimental results compared percentage contact area between contour and flat shaped implants and showed that the contour implants significantly outperformed the flat implants on average by more than three times. Contoured implants showed on average, a 137% increase in stiffness over flat implants during destructive tests. Although the subsidence of implants into the vertebral endplate is a complex phenomenon, literature has indicated that subsidence depends, in part, on the stiffness and strength of the implant-end plate interface and that an increased stiffness will result in reduced subsidence (Auerbach, Ballester, Hammond, Carine, Balderston, & Elliott, 2010), (Hasegawa, Abe, Washio, & Hara, 2001), (Lowe, et al., 2004), (Tan, Bailey, Dvorak, Fisher, & Oxland, 2005).

The corresponding maximum loads during failure also followed the same pattern with contour implants performing slightly (16.72%) better than the flat implants. As expected in both cases, the lumbar and low-thoracic vertebrae withstood higher loads, but showed a decline and then a slight incline again for the cervical vertebrae. This slight increase in cervical loads is attributed to the higher percentage cortical bone content in cervical vertebrae.

The results of this study show that there are indeed significant potential benefits that can be achieved through the use of customization during the design and manufacture of intervertebral disc implants. With

the process chain that has been proposed, these and other potential benefits can and should be exploited for the improvement of existing disc implant designs.

Research is however always an ongoing endeavour – and as such, the following recommendations for further work are suggested:

- The establishment of biomechanical simulation models during the design phase of the process chain needs to be incorporated. Specific motion capturing techniques and the automation thereof need to be defined and the link between the data captured and the simulation model must be established. Work in this field has already begun and literature has shown a trend towards the use of open-source software (OpenSim, <https://simtk.org/home/opensim>) for the design and dissemination of simulation models that can be shared between research groups. An added advantage in using open-source software, apart from the obvious cost savings, is the fact that shared research is done on a common platform by which results can be readily compared. Other simulation models that have been described in literature often make use of expensive and different software packages, which makes it difficult to repeat and compare their results. It is therefore recommended to pursue the continued use of open-source software such as OpenSim towards the development of simulation models for the spine.
- Regulatory issues were discussed as one of the key steps in the process chain, and yet it still remains a significant area that will need to be addressed to achieve a longer term solution than the current patient/surgeon consent process. A comprehensive study of the FDA approval system and how customization can be accommodated better needs to be undertaken. A strong emphasis on simulation as a tool for testing and design verification needs to be considered.
- Design of surgical tools for implantation of a customized intervertebral disc implant was not addressed comprehensively during this study since it was deemed to be an iterative design improvement problem. The importance of implantation and the role that customization can play in creation of custom jigs and fixtures is however still a significant topic for further study and should be investigated further. Especially since placement and orientation of the implant has been identified as such a crucial factor.
- Along with surgical tools, fixation of the disc to the vertebral endplate was also considered to be a design improvement problem. Existing disc designs incorporate a keel or a number of spikes to improve fixture and osteo-integration of the implant device. If endplates are customized and still make use of the keel mechanism, any incorrect keel alignment will result in a mismatching of the endplate surfaces and defeat the original purpose of customization. Several possible alternatives to the standard keel design should therefore be considered. The use of Rapid Manufacturing further enables the design of endplate features such as honeycomb structures (which can prove to be good for ingrowth and fixation) that can otherwise not be manufactured due to its complexity.

- Finally, this study investigated the use of customization during implant design for the spine and used the intervertebral disc implant as a demonstrator for this process chain. Other medical devices can however benefit from this same process chain, though slightly modified. Two obvious additional product applications that may be considered for further study, are the customization of the endplates of intervertebral cage devices as well as vertebral body replacement devices.



6 References

- Adams, M., & Roughley, P. (2006). What is intervertebral disc degeneration, and what causes it? *Spine*, Vol. 31 (18) , 2151-61.
- Alsema, R., Deutman, R., & Mulder, T. (1994). Stanmore Total Hip Replacement. A 15- to 16-year Clinical and Radiographic follow-up. *Journal of Bone & Joint Surgery (Brittish Volume)* 76 , pp. 240-244.
- Anderson, P., Sasso, R., Rouleau, J., Carlson, C., & Goffin, J. (2004). The Bryan Cervical Disc: wear properties and early clinical results. *The Spine Journal*, Vol. 4 (6) , S303-S309.
- Anonymous. (1973). *South African Department of Health, Hazardous Substances Act No. 15 of 1973*. Retrieved April 2008, from <http://www.doh.gov.za/docs/index.html>
- Anonymous. (1991). *Schedule of listed electronic products for Hazardous Substances Act No. 15 of 1973, Regulation no. 1302, 14 June 1991*. Retrieved April 2008, from <http://www.doh.gov.za/docs/regulations/index.html>
- Anonymous. (2003a). *Council Directive 93/42/EEC of 14 June 1993 concerning medical devices*. Retrieved April 2008, from <http://ec.europa.eu/enterprise/newapproach/standardization/harmstds/reflist.html>
- Anonymous. (2003b). *Council Directive of 20 June 1990 on the approximation of the laws of Member States relating to active implantable medical devices (90/385/EEC)*. Retrieved April 2008, from <http://ec.europa.eu/enterprise/newapproach/standardization/harmstds/reflist.html>
- Anonymous. (2004). *Phidias Newsletters 1-8*. Retrieved September 2004, from <http://www.phidias.org>
- Anonymous. (2006a). *EC Medical Devices Directives – Guidance notes for manufacturers of custom made devices - Public communications report*. Retrieved April 2008, from <http://www.mhra.gov.uk>
- Anonymous. (2006b). *Code of Federal Regulations, Title 21 – Food and Drugs, Chapter I – Food and Drug Administration Department of Health and Human Services, Subchapter H – Medical Devices*. Retrieved April 2008, from <http://www.accessdata.fda.gov/scripts/cdrh/cfdocs/cfcfr/CFRSearch.cfm?FR=812.3>
- Anonymous. (2007). *Council Directive 2007/47/EC of the European Parliament and of the Council of 5 September 2007 amending Council Directive 90/385/EEC on the approximation of the laws of the Member States relating to active implantable medical devices*. Retrieved April 2004, from <http://ec.europa.eu/enterprise/newapproach/standardization/harmstds/reflist.html>
- Anonymous. (2008a). *RP4Baghdad*. Retrieved April 2008, from <http://www.rp4baghdad.org>

- Anonymous. (2010). *Back Pain*. Retrieved January 2010, from eMedicineHealth: http://www.emedicinehealth.com/back_pain/article_em.htm
- Anonymous. (2008b). *CustomIMD*. Retrieved 2010, from Custom Implantable Medical Devices: <http://www.customimd.eu/index.php>
- Auerbach, J., Ballester, C., Hammond, F., Carine, E., Balderston, R., & Elliott, D. (2010). The effect of implant size and device keel on vertebral compression properties in lumbar total disc replacement. *The Spine Journal, Vol. 10* , 333-340.
- Beaurain, J., Bernard, P., Dufour, T., Fuentes, J., Hovorka, I., Huppert, J., et al. (2009). Intermediate clinical and radiological results of cervical TDR (Mobi-C) with up to 2 years of follow-up. *European Spine Journal, Vol. 18 (6)* , 841-50.
- Berg, S., Tullberg, T., Branth, B., Olerud, C., & Tropp, H. (2009). Total disc replacement compared to lumbar fusion: a randomised controlled trial with 2-year follow-up. *European Spine Journal, Vol. 18 (10)* , 1512-9.
- Bertagnoli, R. (2005). Complications and Rescue Strategies in TDR Procedures. *20th Annual Meeting of the North American Spine Society (NASS)*. Philadelphia, USA.
- Bertagnoli, R., & Kumar, S. (2002). Indications for full prosthetic disc arthroplasty: a correlation of clinical outcome against a variety of indications. *European Spine Journal, 11 (Suppl. 2)* , pp. S131-S136.
- Blumenthal, S. (2002). Artificial Intervertebral Discs and Beyond - A North American Spine Society Annual Meeting Symposium. *The Spine Journal, Vol. 2* , pp. 460-63.
- Blumenthal, S., McAfee, P., Guyer, R., Hochschuler, S., Geisler, F., Holt, R., et al. (2005). A Prospective, Randomized, Multicenter Food and Drug Administration Investigational Device Exemptions Study of Lumbar Total Disc Replacement With the CHARITE(TM) Artificial Disc Versus Lumbar Fusion: Part I: Evaluation of Clinical Outcomes. *Spine, Vol. 30 (14)* , 1565-75.
- Bono, C., & Garfin, S. (2004). History and Evolution of Disc Replacement. *The Spine Journal, Vol. 4* , pp. S145-S150.
- Borenstein, D. (2000). Epidemiology, etiology, diagnostic evaluation, and treatment of low back pain. *Current Opinion in Orthopedics, Vol. 11(3)* , pp. 225-31.
- Cheh, G., Bridwell, K., Lenke, L., Buchowski, J., Daubs, M., Kim, Y., et al. (2007). Adjacent Segment Disease Following Lumbar/Thoracolumbar Fusion With Pedicle Screw Instrumentation - A Minimum 5-Year Follow-up. *Spine, Vol. 32 (20)* .

- Christelis, L. (2008). *Evaluating scanning and motion capturing techniques to capture vertebral kinematics*. Unpublished MSc Thesis Report, Stellenbosch University.
- Cinotti, G., David, T., & Postacchini, F. (1996). Results of Disc Prosthesis After a Minimum Follow-Up Period of 2 Years. *Spine, Vol. 21 (8)* , 995-1000.
- Cleveland, D. (1955). The use of Methylacrylic for Spinal Stabilization after Disc Operations. *Marquette Med Rev, Vol 20.* , pp. 62-64.
- David, T. (2007). Long-term Results of One-Level Lumbar Arthroplasty: Minimum 10-Year Follow-up of the CHARITE Artificial Disc in 106 Patients. *Spine, Vol. 32 (6)* , 661-6.
- De Beer, N., Dimitrov, D., & Van der Merwe, A. (2008). Manufacturing of Custom-Made Medical Implants for Cranio/Maxillofacial and Orthopaedic Surgery - An Overview of the Current State of the Industry. *Journal of New Generation Sciences, Vol. 6 (2)* .
- De Kleuver, M., Oner, F., & Jacobs, W. (2003). Total Disc Replacement for Chronic Low Back Pain: Background and a Systemic Review of the Literature. *European Spine Journal, Vol. 12* , pp. 108-16.
- Dooris, A., Goel, V., Grosland, N., Gilbertson, L., & Wilder, D. (2001). Load-sharing between anterior and posterior elements in a lumbar motion segment implanted with an artificial disc. *Spine, Vol. 26 (6)* , E122-9.
- Du Toit, L. (2007). Existing regulations for medical devices in South Africa. (N. de Beer, Interviewer)
- Eksteen, J. (2009, October 7). Discussion related to the use of a custom-made disc prosthesis during spine surgery. (N. d. Beer, Interviewer)
- Fernström, U. (1966). Arthroplasty with Intercorporal Endoprosthesis in Herniated Disc and in Painful Disc. *Acta Chir Scand, Vol. 357 (suppl)* , pp. 154-159.
- Galbusera, F., Bellini, C., Zweig, T., Ferguson, S., Raimondi, M., Lamartina, C., et al. (2008). Design concepts in lumbar total disc arthroplasty. *European Spine Journal, Vol. 17* , 1635-50.
- Gamradt, S., & Wang, J. (2005). Lumbar Disc Arthroplasty - Contemporary Concepts in Spine Care. *Spine Journal, Vol. 5* , pp. 95-103.
- Gilroy, A., MacPherson, B., & Ross, L. (2008). *Atlas of Anatomy*. New York, USA: Thieme Medical Publishers, Inc.
- Goel, V., Grauer, J., Patel, T., Biyani, A., Sairyo, K., Vishnubhotla, S., et al. (2005). Effects of charité artificial disc on the implanted and adjacent spinal segments mechanics using a hybrid testing protocol. *Spine, Vol. 30 (24)* , 2755-64.

- Gstoettner, M., D, H., Liebensteiner, M., & Bach, C. (2008). Footprint mismatch in lumbar total disc arthroplasty. *European Spine Journal*, Vol. 17 , 1470-75.
- Guyer, R., & Ohnmeiss, D. (2003). Intervertebral Disc Prostheses. *Spine*, Vol. 28 (15S) , pp. S15-S23.
- Guyer, R., McAfee, P., Banco, R., Bitan, F., Cappuccino, A., Geisler, F., et al. (2009). Prospective, randomized, multicenter Food and Drug Administration investigational device exemption study of lumbar total disc replacement with the CHARITÉ artificial disc versus lumbar fusion: Five-year follow-up. *The Spine Journal*, Vol. 9 (5) , 374-86.
- Harrop, J., Youssef, J., Maltenfort, M., Vorwald, P., Jabbour, P., Bono, C., et al. (2008). Lumbar Adjacent Segment Degeneration and Disease After Arthrodesis and Total Disc Arthroplasty. *Spine*, Vol 33 (15) .
- Harrysson, O., Cansizoglu, O., Marcellin-Little, D., Cormier, D., & West, H. (2008). Direct Metal Fabrication of Titanium Implants with Tailored Materials and Mechanical Properties Using Electron Beam Melting Technology. *Materials Science & Engineering C*, Vol. 28, Nr. 3 , 366-373.
- Harrysson, O., Hosni, Y., & Nayfeh, J. (2007). Custom-Designed Orthopedic Implants Evaluated Using Finite Element Analysis of Patient-Specific Computed Tomography Data: Femoral-Component Case Study. *BMC Musculoskeletal Disorders*, Vol 8 , 91.
- Hasegawa, K., Abe, M., Washio, T., & Hara, T. (2001). An Experimental Study on the Interface Strength Between Titanium Mesh Cage and Vertebra in Reference to Vertebral Bone Mineral Density. *Spine*, Vol. 26 (8) , 957-63.
- Heidecke, V., Burkert, W., Brucke, M., & Rainov, N. (2008). Intervertebral disc replacement for cervical degenerative disease – clinical results and functional outcome at two years in patients implanted with the Bryan cervical disc prosthesis. *Acta Neurochirurgica*, Vol. 150 (5) , 453-59.
- Heller, J., Sasso, R., Papadopoulos, S., Anderson, P., Fessler, R., Hacker, R., et al. (2009). Comparison of BRYAN Cervical Disc Arthroplasty With Anterior Cervical Decompression and Fusion: Clinical and Radiographic Results of a Randomized, Controlled, Clinical Trial. *Spine*, Vol. 34 (2) , 101-107.
- Higashino, K., Hamasaki, T., Kim, J., Okada, M., Yoon, S., Boden, S., et al. (2010). Do the Adjacent Level Intervertebral Discs Degenerate After a Lumbar Spinal Fusion? An Experimental Study Using a Rabbit Model. *Spine*, Vol 35 (22) .
- Huang, R., & Cammisa, F. (2004). The Prevalence of Contraindications to Total Disc Replacement in a Cohort of Lumbar Surgical Patients. *Spine*, Vol. 29 , pp. 2538-2541.

- Huang, R., Girardi, F., Cammisa, F., Tropiano, P., & Marnay, T. (2003). Long-Term Flexion-Extension Range of Motion of the Prodisc Total Disc Replacement. *Journal of Spinal Disorders*, Vol. 16 , pp. 435-40.
- Khan, S., & Stirling, A. (2007). Controversial topics in surgery: degenerative disc disease: disc replacement. Against. *Annals of The Royal College of Surgeons of England*, Vol. 89 (1) .
- Kishen, T., & Diwan, A. (2010). Fusion Versus Disk Replacement for Degenerative Conditions of the Lumbar and Cervical Spine: Quid Est Testimonium? *Orthopedic Clinics of America*, Vol 41 , 167-181.
- Kostuik, J. (1997). Intervertebral Disc Replacement. Experimental Study. *Clinical Orthopedics*, Vol. 337 , pp. 27-41.
- Labrom, R., Tan, J.-S., Reilly, C., Tredwell, S., Fisher, C., & Oxland, T. (2005). The Effect of Interbody Cage Positioning on Lumbosacral Vertebral Endplate Failure in Compression. *Spine*, Vol. 30 (19) , E556-E561.
- Leary, S., Regan, J., Lanman, T., & Wagner, W. (2007). Revision and Explantation Strategies Involving the CHARITE Lumbar Artificial Disc Replacement. *Spine*, Vol 32 (9) , 1001-11.
- Lemaire, J., Carrier, H., Sariali, e.-H., Skalli, W., & Lavaste, F. (2005). Clinical and radiological outcomes with the Charité artificial disc: a 10-year minimum follow-up. *Journal of Spinal Disorders & Techniques*, Vol. 18 (4) , 353-9.
- Lowe, T., Hashim, S., Wilson, L., O'Brien, M., Smith, D., Diekmann, M., et al. (2004). A Biomechanical Study of Regional Endplate Strength and Cage Morphology as It Relates to Structural Interbody Support. *Spine*, Vol. 29 (21) , 2389-94.
- Matsumoto, M., Okada, E., Ichihara, D., Watanabe, K., Chiba, K., Toyama, Y., et al. (2009). Anterior Cervical Decompression and Fusion Accelerates Adjacent Segment Degeneration - Comparison With Asymptomatic Volunteers in a Ten-Year Magnetic Resonance Imaging Follow-up Study. *Spine*, Vol. 35 (1) , 36-43.
- McAfee, P. (2005). Comments on the Van Ooij Article. *Journal of Spinal Disorders & Techniques*, Vol. 18, No. 1 , pp. 116-117.
- McAfee, P., Cunningham, B., Hayes, V., Sidiqi, F., Dabbah, M., Seftor, J., et al. (2006). Biomechanical analysis of rotational motions after disc arthroplasty: implications for patients with adult deformities. *Spine*, Vol 31 (19 Suppl) , S152-60.
- Miller, J., Schmatz, C., & Schultz, A. (1988). Lumbar disc degeneration: correlation with age, sex, and spine level in 600 autopsy specimens. *Spine*, Vol.13 (2) , 173-8.

- Montgomery, D., & Runger, G. (2007). *Applied Statistics and Probability for Engineers*. Hoboken, NJ: John Wiley & Sons, Inc.
- Moore, K. (1992). *Clinically Oriented Anatomy* (3rd Edition ed.). Baltimore, Maryland: Williams & Wilkins.
- Mummaneni, P., Burkus, J., Haid, R., Traynelis, V., & Zdeblick, T. (2007). Clinical and radiographic analysis of cervical disc arthroplasty compared with allograft fusion: a randomized controlled clinical trial. *Journal of Neurosurgery: Spine*, Vol. 6 (3) , 198-209.
- Murrey, D., Janssen, M., Delamarter, R., Goldstein, J., Zigler, J., Tay, B., et al. (2009). Results of the prospective, randomized, controlled multicenter Food and Drug Administration investigational device exemption study of the ProDisc-C total disc replacement versus anterior discectomy and fusion for the treatment of 1-level symptomatic cervi. *The Spine Journal*, Vol. 9 (4) , 275-86.
- Nabhan, A., Ahlhelm, F., Shariat, K., Pitzen, T., Steimer, O., Steudel, W.-I., et al. (2007). The ProDisc-C Prothesis: Clinical and Radiological Experience 1 Year After Surgery. *Spine*, Vol. 32 (18) , 1935-41.
- Nachemson, A. (1962). Some Mechanical Properties of the Lumbar Intervertebral Disc. *Bull Hosp Joint Dis (NY)*, Vol. 23 , pp. 130-132.
- Odendaal, A. (2010). *Die Ontwikkeling van 'n Pasklaar-Vervaardigde Kunsmatige Intervertebrale Skyf-Implantaat*. Unpublished MSc Thesis Report, Stellenbosch University.
- Oxland, T., Grant, J., Dvorak, M., & Fisher, C. (2003). Effects of Endplate Removal on the Structural Properties of the Lower Lumbar Vertebral Bodies. *Spine*, Vol 28 (8) , 771-77.
- Park, J., Roh, K., Cho, J., Ra, Y., Rhim, S., & Noh, S. (2008). Comparative Analysis of Cervical Arthroplasty Using Mobi-C and Anterior Cervical Discectomy and Fusion Using the Solis -Cage. *J Korean Neurosurg Soc*, Vol. 44 (4) , 217-21.
- Park, P., Garton, H., Gala, V., Hoff, J., & McGillicuddy, J. (2004). Adjacent Segment Disease after Lumbar or Lumbosacral Fusion: Review of the Literature. *Spine*, Vol. 29 (17) .
- Pereira, C., Ventura, F., Gaspar, M., Fontes, R., & Mateus, A. (2007). Customized implant development for maxillo-mandibular reconstruction. *Proceedings of the 3rd International Conference on Advanced Research in Virtual and Rapid Prototyping*. Leiria, Portugal.
- Pimenta, L., McAfee, P., Cappuccino, A., Cunningham, B., Diaz, R., & Coutinho, E. (2007). Superiority of Multilevel Cervical Arthroplasty Outcomes Versus Single-Level Outcomes: 229 Consecutive PCM Prostheses. *Spine*, Vol. 32 (12) , 1337-44.

- Poukens, J., Haex, J., & Riediger, D. (2003). The Use of Rapid Prototyping in the Preoperative Planning of Distraction Osteogenesis of the Cranio-Maxillofacial Skeleton. *Computer Aided Surgery, Vol. 8, Nr. 3* , 146-154.
- Reitz, H., & Joubert, M. (1964). Intractable Headache and Cervicobrachialgia Treated by Complete Replacement of Cervical Intervertebral Discs with a Metal Prosthesis. *South African Medical Journal, Vol. 38* , pp. 881-889.
- Sasso, R., Smucker, J., Hacker, R., & Heller, J. (2007). Clinical Outcomes of BRYAN Cervical Disc Arthroplasty: A Prospective, Randomized, Controlled, Multicenter Trial With 24-month Follow-up. *Journal of Spinal Disorders & Techniques, Vol. 20 (7)* , 481-91.
- Schindel, R., Lampert, C., & Gross, W. (2005). Case Report TALUS: Application of Selective Laser Sintering Technology in Orthopaedics . *European Cells and Materials Vol. 10. Suppl. 5*.
- Shim, C., Lee, S., Maeng, D., & Lee, S.-H. (2005). Vertical Split Fracture of the Vertebral Body Following Total Disc Replacement Using ProDisc: Report of Two Cases. *Journal of Spinal Disorders & Techniques* , 465-69.
- Staffa, G., Nataloni, A., Compagnone, C., & Servadei, F. (2007). Custom made cranioplasty prostheses in porous hydroxy-apatite using 3D design techniques: 7 years experience in 25 patients. *Acta Neurochirurgica, Vol. 149 (2)* .
- Steffen, T., Tsantrizos, A., & Aebi, M. (2000). Effect of Implant Design and Endplate Preparation on the Compressive Strength of Interbody Fusion Constructs. *Spine, Vol. 25 (9)* , 1077–84.
- Szpalski, M., Gunzburg, R., & Mayer, M. (2002). Spine arthroplasty: a historical review. *European Spine Journal, Vol. 11 (Supplement 2)* , S65-S84.
- Tan, J.-S., Bailey, C., Dvorak, M., Fisher, C., & Oxland, T. (2005). Interbody Device Shape and Size Are Important to Strengthen the Vertebra–Implant Interface. *Spine, Vol. 30 (6)* , 638-44.
- Traynelis, V., & Haid, R. (2004). Retrieved June 2007, from Spine Universe: <http://www.spineuniverse.com/displayarticle.php/article501.html>
- Tropiano, P., Huang, R., Girardi, F., Cammisa, F., & Marnay, T. (2005). Lumbar Total Disc Replacement: Seven to Eleven-Year Follow-Up. *The Journal of Bone and Joint Surgery (American), Vol. 87 (3)* , 490-6.
- Ullrich, P. (2009, 10 21). *Lumbar Laminectomy Surgery for Spinal Stenosis (Open Decompression)*. Retrieved December 2009, from Spine-Health: <http://www.spine-health.com/treatment/back-surgery/lumbar-laminectomy-open-decompression>

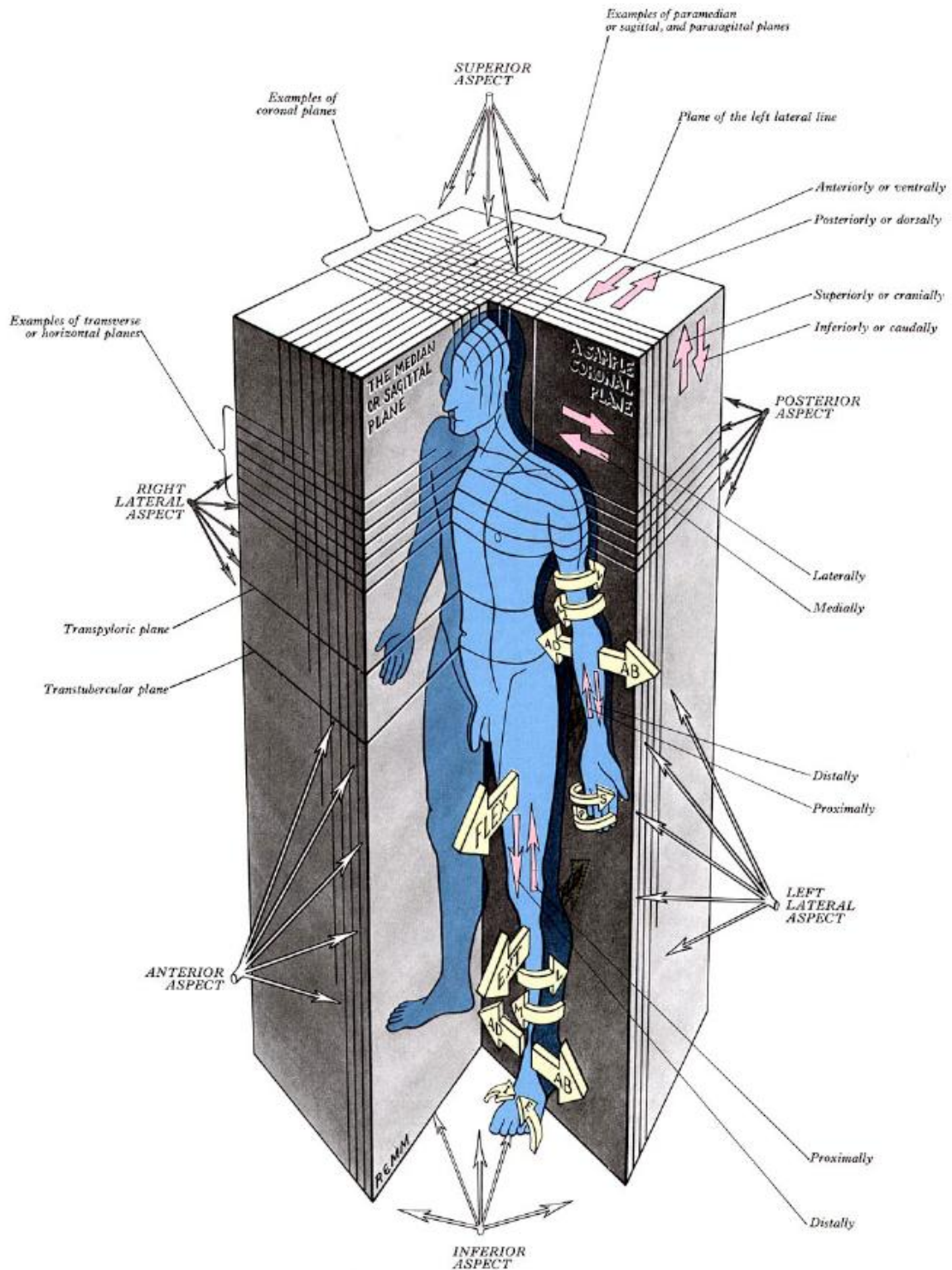
- Van der Houwen, E., Baron, P., Veldhuizen, A., Burgerhof, J., Van Ooijen, P., & Verkerke, G. (2010). Geometry of the Intervertebral Volume and Vertebral Endplates of the Human Spine. *Annals of Biomedical Engineering*, Vol. 38 (1) , 33-40.
- van Ooij, A., Kurtz, S., Stessels, F., Noten, H., & van Rhijn, L. (2007). Polyethylene wear debris and long-term clinical failure of the Charité disc prosthesis: a study of 4 patients. *Spine*, Vol. 32 (2) , 223-9.
- Van Ooij, A., Oner, F., & Verbout, A. (2003). Complications of Artificial Disc Replacement - A Report of 27 Patients with the SB Charité Disc. *Journal of Spinal Disorders & Techniques*, Vol. 16 (4) , 369-383.
- Van Ooij, A., Schurink, G., Oner, F., & Verbout, A. (2007). Findings in 67 patients with recurrent or persistent symptoms after implantation of a disc prosthesis for low back pain. *Nederlands Tijdschrift voor Geneeskunde*, Vol. 151 (28) , 1577-84.
- Van Zyl, A. (2010). *Developing a Graphical User Interface with MATLAB to Aid in the Design of a Custom Inter-Vertebral Disc*. Unpublished final-year project report, Stellenbosch University.
- Viscogliosi, A., Viscogliosi, J., & Viscogliosi, M. (2004). *Spine Industry Analysis Series - Beyond Total Disc, The Future of Spine Surgery*. Viscogliosi Bros, LLC.
- Voigt, C., Patel, M., & Howes, D. (2009). Sterilization of Medical Prototyped Models. *Proceedings from the 10th Annual RAPDASA conference*. East London.
- Wagner, W., Regan, J., Leary, S., Lanman, T., Johnson, J., Rao, R., et al. (2006). Access strategies for revision or explantation of the Charité lumbar artificial disc replacement. *Journal of Vascular Surgery*, Vol. 44 (6) , 1266-72.
- Wohlers, T. (2010). *Wohlers Report - Rapid Prototyping, Tooling & Manufacturing: State of the Industry Annual Worldwide Progress Report*. Fort Collins, USA: Wohlers Associates Inc.
- Wong, D. (2005). Incidence of Contraindications to TDA: A Retrospective Review of 100 Consecutive Fusion Patients with a Focused Analysis of Facet Arthrosis. *20th Annual Meeting of the North American Spine Society (NASS)*. Philadelphia, USA.
- Worland, R., Johnson, G., Alemparte, J., Jessup, D., Keenan, J., & Norambuena, N. (2002). Ten to Fourteen Year Survival and Functional Analysis of the AGC Total Knee Replacement System. *The Knee*, Vol. 9, Issue 2 , pp. 133-137.
- Wurm, G., Tomancok, B., Holl, K., & Trenkler, J. (2004). Prospective study on cranioplasty with individual carbon fiber reinforced polymere (CFRP) implants produced by means of stereolithography. *Surgical Neurology*, Vol. 62 (6) .

Zeegers, W., LMLJ, B., Laaper, M., & Verhaegen, M. (1999). Artificial disc replacement with the modular type SB Charité III: 2-year results in 50 prospectively studied patients. *European Spine Journal*, Vol. 8 (3) , 210-17.

Zigler, J., Delamarter, R., Spivak, J., Linovitz, R., Danielson, G., Haider, T., et al. (2007). Results of the Prospective, Randomized, Multicenter Food and Drug Administration Investigational Device Exemption Study of the ProDisc(R)-L Total Disc Replacement Versus Circumferential Fusion for the Treatment of 1-Level Degenerative Disc Disease. *Spine*, Vol. 32 (11) , 1155-62.

Appendix A: Medical and Anatomical Terminology

Anatomical Planes and Terms



Terms of Relationship

Various adjectives are used to describe the relationship of parts of the body in the anatomical positions. In the table below, are a selection of the terms used, and their related meaning.

Term	Meaning of the term	Example of its use
Superior (Cranial)	Nearer to the head	The heart is superior to the stomach
Inferior (Caudal)	Nearer to the feet	The stomach is inferior to the heart
Anterior (Ventral)	Nearer to the front	The sternum is anterior to the heart
Posterior (Dorsal)	Nearer to the back	The kidneys are posterior to the intestine
Medial	Nearer to the median plane	The 5 th digit (little finger) is on the medial side of the hand (palms in anterior position)
Lateral	Farther from the median plane	The 1 st digit (thumb) is on the lateral side of the hand (palms in anterior position)
Proximal	Nearer to the trunk or point of origin	The elbow is proximal to the wrist, and the proximal part of an artery is its beginning
Distal	Farther from the trunk or point of origin	The wrist is distal to the elbow and the distal part of the lower limb is the foot.
Superficial	Nearer to or on the surface	The muscles of the arm are superficial to its bone (humerus)
Deep	Farther from the surface	The humerus is deep to the arm muscles
External (Outer)	Toward or on the exterior	The auricle or pinna is external to the middle ear.
Internal (Inner)	Toward or in the interior	The spiral organ concerned with hearing is internal to the middle ear
Central	Nearer to or toward the centre	The spinal cord is part of the central nervous system
Peripheral	Farther or away from the centre	The spinal nerves leaving the spinal cord are part of the peripheral nervous system
Parietal	Pertaining to the external wall of a body cavity	The parietal pleura forms the external wall of the pleural cavity
Visceral	Pertaining to the covering of an organ	The visceral pleura covers the external surface of a lung

Terms of Movement

Anatomy is concerned with the living body. Therefore various terms are used to describe the different movements of the limbs and other parts of the body. Movements take place at joints where two or more bones meet or articulate with one another. The table below gives definitions to some of the basic movements of the body.

Term	Explanation of term and example of its use
Flexion	<i>Bending</i> or decreasing the angle between body parts, e.g. flexing the elbow joint.
Extension	Straightening or increasing the angle between body parts, e.g. extending the knee joint.
Abduction	Moving away from the median plane, e.g. abducting the upper limb.
Adduction	Moving toward the median plane, e.g. adducting the lower limb.
Rotation	Moving around the long axis, e.g. medial and lateral rotation of the lower limb.
Circumduction	Circular movement combining flexion, extension, abduction, and adduction, e.g. circumducting the upper limb.
Eversion	Moving the sole of the foot away from the median plane, e.g. when the lateral surface of the foot is raised.
Inversion	Moving the sole of the foot toward the median plane, e.g. when you examine the sole of your foot to remove a splinter.
Supination	Rotating the forearm and hand laterally so that the palm faces anteriorly, e.g. when a person extends a hand to beg.
Pronation	Rotating the forearm and hand medially so that the palm faces posteriorly, e.g. when a person pats a child on the head.
Protrusion	Moving anteriorly, e.g. sticking the chin out
Retrusion	Moving posteriorly e.g. tucking the chin in.

Appendix B: Comparison of published studies concerning TDR (Galbusera, et al., 2008)

Note:

The following appendix presents a list of studies that has been included in order to help future research on the topic of Total Disc Replacement. It was included because it contains most of the current and relevant literature relating to this field of study and will therefore enable students to find pertinent information quicker. All numbered references to literature in these tables are listed at the end of this appendix.

References	Model	Study type	Mechanical variables	Prosthesis	Compared to	Results
Auerbach et al. [1]	Human	Radiographic	Motion	ProDisc (semi-constrained)	Fusion	Preserved motion at implanted and adjacent levels, as compared to fusion
Bertagnoli and Kumar [2]	Human	Radiographic	Motion	ProDisc (semi-constrained)	-	Preserved average vertebral motion at the operated level
Bertagnoli et al. [4]	Human	Radiographic	Motion	ProDisc (semi-constrained)	-	3-7 degrees of motion in flexion-extension
Bertagnoli et al. [3]	Human	Radiographic	Motion	ProDisc (semi-constrained)	Smokers versus non-smokers	3-7 degrees of motion in flexion-extension
Cakir et al. [6]	Human	Radiographic	Segmental and total lordosis	ProDisc (semi-constrained)	-	Increased segmental lordosis, unchanged total lordosis
Cakir et al. [7]	Human	Radiographic	Method for measuring motion	-	-	Choice of different landmarks improves measure reliability
Chung et al. [9]	Human	Radiographic	Segmental and total lordosis	ProDisc (semi-constrained)	-	Increased segmental and total lordosis
Chung et al. [10]	Human	Radiographic	Motion	ProDisc (semi-constrained)	-	Increased average motion from 9.7 to 12.7 degrees
Cinotti et al. [11]	Human	Radiographic	Motion	Charité (unconstrained)	-	Average 9 degrees of motion at the implanted level, 16 degrees at the adjacent levels
Cunningham et al. [14]	Non-human primate	In vivo, ex vivo (histopathologic and histomorphometric)	Motion, trabecular ingrowth	Acroflex (unconstrained)	-	Reduced motion; no evidences of pathological changes; heterotopic ossification
Cunningham et al. [13]	Human	Ex vivo	Motion, IAR	Charité (unconstrained)	Fusion, instrumented fusion	Preserved motion and IAR
Cunningham et al. [12]	Non-human primate	In vivo, ex vivo	Motion, bone ingrowth	Charité, Acroflex (unconstrained)	Intact	Acroflex motion smaller than intact and Charité; excellent bone ingrowth
Cunningham [16]	Human, non-human primate	In vivo, ex vivo (histopathologic and histomorphometric)	Motion, IAR, bone ingrowth	Charité, Acroflex (unconstrained)	Intact, fusion	Preserved motion and IAR, excellent bone ingrowth
Cunningham et al. [15]	Human	Radiographic	Motion	Charité (unconstrained)	Fusion	Normal motion distribution along the lumbar spine
David [17]	Human	Radiographic	Motion	Charité(unconstrained)	-	Preserved motion
Delamarter et al. [19]	Human	Ex vivo	Motion	ProDisc (semi-constrained)	Fusion	1 operated level: preserved motion and coupling; 2 operated levels: not preserved motion and coupling in 50%

Table 13 – Published studies concerning lumbar kinematics after TDR (Galbusera, et al., 2008)

References	Model	Study type	Mechanical variables	Prosthesis	Compared to	Results
Denozière and Ku [20]	Human	Computational	Motion, stability, ligament tensions, facet pressure	Ball and socket (semi-constrained)	Fusion	Greater risk of instability and further degeneration relative to fusion
Dooris et al. [21]	Human	Computational	Motion, facet loads, intradiscal pressure, shear stresses	Ball and socket (semi-constrained)	-	Modification of the spinal bending stiffness in the sagittal plane
Eijkelkamp et al. [23]	-	-	Kinematics, load sharing, stability	-	-	Design guidelines for disc prostheses
Enker et al. [24]	Human	Radiographic	Motion, bone ingrowth	Acroflex (unconstrained)	-	Preserved motion, good bone ingrowth
Goel et al. [28]	Human	Computational	Motion, facet loads, intradiscal pressure, shear stresses	Charité (unconstrained)	-	Increased motion at the L5-S1 level in flexion-extension; decreased facet loads; higher shear stresses at the TDA L5 endplate relative to those at S1 interface
Hedman et al. [29]	-	-	Kinematics, endurance, safety	Generic	-	Design guidelines for disc prostheses
Hitchon et al. [30]	Human	Ex vivo	Motion	Maverick (semi-constrained)	-	Preserved motion
Huang et al. [34]	-	-	Constraint	Semi-constrained, unconstrained	-	Unconstrained disc prostheses may have a kinematical advantage; semi-constrained disc prostheses may protect the posterior structure in shear
Huang et al. [35]	Human	Radiographic	Motion, sagittal alignment	ProDisc (semi-constrained)	-	Preserved motion; improved global and segmental alignment
Huang et al. [33]	Human	Radiographic	Motion	ProDisc (semi-constrained)	-	Radiographic follow-up was positively correlated with the clinical outcome
Huang et al. [36]	Human	Radiographic	Motion, adjacent level degeneration	ProDisc (semi-constrained)	-	Correlation between motion and adjacent level degeneration
Kadoya et al. [37]	Ovine	Ex vivo	Static, viscoelastic and fatigue properties; histological analysis	3D fabric disc (unconstrained)	-	Mechanical behavior similar to natural sheep disc; no debris detected
Kim et al. [39]	Human	Radiographic	Motion	ProDisc (semi-constrained)	-	Reduced motion at L5-S1 implanted level

Table 13 – Continued

References	Model	Study type	Mechanical variables	Prosthesis	Compared to	Results
Kosmopoulos et al. [40]	Human	Radiographic	Method for measuring motion	-	-	Patient should be parallel to the plate; the beam should be directed to the disc prosthesis
Kotani et al. [42]	Ovine	In vivo, ex vivo	Motion, histological analysis	3D fabric disc (unconstrained)	3D fabric disc with internal fixation	Biomechanical properties nearly equivalent to that of the natural disc; excellent fusion capacity
Kotani et al. [43]	Ovine	In vivo, ex vivo	Motion, histological analysis	3D fabric disc (unconstrained)	3D fabric disc with internal fixation	Reduced motion, excellent fusion
Kotani et al. [44]	Human	Ex vivo	Motion, IAR	3D fabric disc (unconstrained)	Intact, instrumented fusion	Motion and IAR equivalent to that of the intact spine
Le Huec et al. [50]	Human	Radiographic	Sagittal alignment	Maverick (semi-constrained)	-	Preserved global and segmental lordosis, decreased lordosis at the above level
Leivseth et al. [55]	Human	Radiographic	Motion	ProDisc (semi-constrained)	-	Not preserved normal segmental rotational motion in the sagittal plane
Lemaire et al. [56]	Human	Radiographic	Motion	Charité (unconstrained)	-	Preserved motion in flexion-extension and axial rotation
Lim et al. [58]	Human	Radiographic	Method for measuring motion	-	-	Using the keels instead of the endplates for measuring the Cobb angles is recommended
Lim et al. [59]	Human	Radiographic	Errors in motion measures	-	-	Intraobserver variability: ± 4.6 degrees; interobserver variability: ± 5.2 degrees
McAfee et al. [61]	Human	Radiographic	Motion	Charité (unconstrained)	-	High accuracy during surgery induces better motion
McAfee et al. [62]	Human	Radiographic	Motion	Charité (unconstrained)	-	93.4% patients had motion over 7 degrees
Neal et al. [67]	Human	MRI	Motion, motion at the adjacent levels	-	-	Despite artifacts, MRI is a valuable tool for evaluating disc degeneration at the adjacent levels
Noailly et al. [68]	Human	Computational	Motion, stiffness	Novel composite disc	-	Higher stiffness than the intact disc
O'Leary et al. [69]	Human	Ex vivo	Motion	Charité (unconstrained)	Fusion + Charité	Preserved motion, not preserved motion patterns

Table 13 – Continued

References	Model	Study type	Mechanical variables	Prosthesis	Compared to	Results
Panjabi et al. [72]	Human	Ex vivo	Motion	Charité (unconstrained)	Fusion	Preserved motion at implanted and adjacent levels (TDA); affected motion redistribution at adjacent levels (fusion)
Panjabi et al. [71]	Human	Ex vivo	Motion	ProDisc (semi-constrained)	Fusion	Preserved motion (TDA) as compared to fusion at all spinal levels
Putzier et al. [74]	Human	Radiographic	Motion	Charité (unconstrained)	-	Spontaneous ankylosis in 60% patients after 17 years
Rohlmann et al. [77]	Human	Computational	Motion	ProDisc (semi-constrained)	-	TDA height and position. ALL and AF removing affect the segment biomechanics
Rousseau et al. [78]	Human	Computational	Motion, IAR, facet forces	Charité (unconstrained) ProDisc (semi-constrained)	-	ProDisc: decreased facet forces, IAR variable; Charité: increased facet forces, IAR less variable
SariAli et al. [79]	Human	Computational	Motion	Charité (unconstrained)	Healthy volunteers	Single level TDA: preserved motion and coupling; double level TDA: not preserved motion and coupling in 50%
Sasso et al. [80]	Human	Radiographic	Motion	FlexiCore (constrained)	Fusion	Preserved motion in flexion-extension and lateral bending
Tortolani et al. [87]	Human	Radiographic	Heterotopic ossification	Charité (unconstrained)	-	Heterotopic ossification in 4.3% patients; all these patients had motion increase after surgery
Tournier et al. [88]	Human	Radiographic	Motion, disc height, sagittal balance	Charité (unconstrained) Maverick, ProDisc (semi-constrained)	-	Preserved motion and disc height, preserved sagittal balance, modification of the lumbar curvature
Vuono-Hawkins et al. [92]	Canine	In vivo, ex vivo	Motion, bone ingrowth	Elastomeric spacer	-	Increased motion, no significant bone ingrowth after 12 months
Zigler et al. [98]	Human	Radiographic	Motion	ProDisc (semi-constrained)	-	Preserved motion (average 7.7 degrees)

IAR instantaneous axis of rotation, TDA total disc arthroplasty, MRI magnetic resonance imaging, ALL anterior longitudinal ligament, AF annulus fibrosus

Table 13 – Continued

References	Model	Study type	Mechanical variables	Prosthesis	Compared to	Results
Cakir et al. [6]	Human	Radiographic	Sagittal balance	ProDisc (semi-constrained)	-	Increased segmental lordosis, overall lordosis preserved
Chung et al. [9]	Human	Radiographic	Sagittal balance	ProDisc (semi-constrained)	-	Increased segmental and overall lordosis
Denozière and Ku [20]	Human	Computational	Motion, stability, ligament tensions, facet pressure	Ball and socket (semi-constrained)	Fusion	Greater risk of instability and further degeneration relative fusion
Dooris et al. [21]	Human	Computational	Motion, facet loads, intradiscal pressure, shear stresses	Ball and socket (semi-constrained)	-	Modification of the spinal bending stiffness in the sagittal plane
Goel et al. [28]	Human	Computational	Motion, facet loads, intradiscal pressure, shear stresses	Charité(unconstrained)	-	Increased motion at the L5-S1 level in flexion/extension; decreased facet loads; higher shear stresses at the TDA L5 endplate relative to those at S1 interface
Huang et al. [34]	-	-	Constraint	Semi-constrained, unconstrained	-	Unconstrained disc prostheses may have a kinematical advantage; semi-constrained disc prostheses may protect the posterior structure in shear
Kadoya et al. [37]	Ovine	Experimental	Static, viscoelastic and fatigue properties; histological analysis	3D fabric disc (unconstrained)	-	Mechanical behavior similar to natural sheep disc; no debris detected
Ledet et al. [53]	Non-human primate	In vivo	In vivo interbody force	Instrumented interbody spacer	-	The baboon may be an appropriate animal model of the human lumbar spine
Le Huec et al. [52]	Human	Radiographic	Sagittal balance	Maverick (semi-constrained)	-	Preserved sagittal balance
Le Huec et al. [51]	Human	Radiographic	Sagittal balance, facet loads	Maverick (semi-constrained)	-	Facet loads may be not increased after implantation of a semi-constrained disc prosthesis
Lemaire et al. [56]	Human	Radiographic	Sagittal balance	Charité (unconstrained)	-	87% patients had a restoration of lumbar sagittal balance
Mathew et al. [60]	Human	-	-	ProDisc (semi-constrained)	-	Complication: bilateral pedicle fracture, probably related to the lordosis angle distribution of the prosthesis design
McAfee et al. [62]	Human	Ex vivo	Motion	Charité (unconstrained)	-	TDA accentuates scoliotic tendencies in the lumbar spine
Moumene and Geisler [66]	Human	Computational	Loading on the facet joints, stress on the polyethylene core	Unconstrained, semi-constrained	-	Unconstrained TDA unloads facet joints and presents decreased core stress as compared to fixed-core (semi-constrained) TDA
Rohlmann et al. [77]	Human	Computational	Alignment in standing position and flexion	ProDisc (semi-constrained)	-	Implant position strongly influences intersegmental rotation in standing and flexion

Table 14 – Published studies concerning loads, stresses and sagittal balance after TDR (Galbusera, et al., 2008)

References	Model	Study type	Mechanical variables	Prosthesis	Compared to	Results
Rousseau et al. [78]	Human	Experimental	Motion, facet forces	Charité (unconstrained) ProDisc (semi-constrained)	–	ProDisc: decreased facet forces, IAR variable; Charité: increased facet forces, IAR less variable
Shim et al. [84]	Human	–	–	ProDisc (semi-constrained)	–	Case report of two split fractures of the vertebral body due to the keel design
Tournier et al. [88]	Human	Radiographic	Motion, disc height, sagittal balance	Charité (unconstrained) Maverick, ProDisc (semi-constrained)	–	Preserved motion and disc height, preserved sagittal balance, modification of the lumbar curvature
Trouillier et al. [89]	Human	Radiographic	Facet joint integrity	Charité (unconstrained)	–	Implantation of the disc prosthesis was not associated to increased loading in the facet joints
Van Ootj et al. [91]	Human	Radiographic	Degeneration, stability	Charité (unconstrained)	–	Observed complications: degeneration of adjacent discs, facet joint arthrosis at the implanted and other levels, subsidence
Wenzel and Sheperd [94]	Human	Computational	Contact stresses on the articulating surfaces	Ball-and-socket	–	Stresses below the fatigue strength of the employed materials

TDA total disc arthroplasty, IAR instantaneous axis of rotation

Table 14 – Continued

References	Model	Study type	Observed variables	Prosthesis	Compared to	Results
Büttner-Janz et al. [5]	Human	Experimental	Static and dynamic strength	Charité (unconstrained)	-	Sufficient strength
Chang et al. [8]	Lepoine	In vivo	Response to wear debris	Titanium particles	-	Minimal biological response
Cunningham et al. [14]	Non-human primate	Experimental, in vivo (histopathologic and histomorphometric)	Motion, trabecular ingrowth	Acroflex (unconstrained)	-	Reduced motion; no evidences of pathological changes; heterotopic ossification
Cunningham et al. [12]	Non-human primate	In vivo, ex vivo	Motion, bone ingrowth	Charité, Acroflex (unconstrained)	Intact	Acroflex motion smaller than intact and Charité; good bone ingrowth
Cunningham [16]	Human, non-human primate	In vivo, ex vivo (histopathologic and histomorphometric)	Motion, IAR, bone ingrowth	Charité, Acroflex (unconstrained)	Intact, fusion	Preserved motion and IAR, excellent bone ingrowth
David [18]	Human	Retrieval study, 1 patient	Wear	Charité (unconstrained)	-	Fractured polyethylene core, no wear debris observed
Edelund [22]	-	-	-	Composite	-	Proposal for material and design of a new disc prosthesis
François et al. [25]	Human	Retrieval study, 1 patient	-	Maverick (semi-constrained)	-	Gross metallosis around the articulation of the prosthesis
Fraser et al. [26]	-	-	Shock absorption	Acroflex (unconstrained)	-	The design of the prosthesis is aimed to optimize the shock absorption capacity
Gloria et al. [27]	-	Experimental	Compressive stiffness, viscoelasticity	Composite polymer	-	Adequate static and dynamic mechanical properties
Hou et al. [32]	Non-human primate	In vivo, experimental	Biocompatibility, fatigue	Silicone	-	Good biomechanics, applicability and biocompatibility
Kadoya et al. [37]	Ovine	Experimental, in vivo	Static, viscoelastic and fatigue properties	3D fabric disc (unconstrained)	-	Mechanical behavior similar to natural sheep disc; no debris detected
Kostuik [41]	-	Experimental	Wear	Spring-based	-	Low wear if compared to hip prostheses
Kotani et al. [43]	Ovine	In vivo, ex vivo	Motion, histological analysis	3D fabric disc (unconstrained)	3D fabric disc with internal fixation	Reduced motion, excellent fusion
Kotani et al. [44]	Ovine	Experimental	Motion, histological analysis	3D fabric disc (unconstrained)	3D fabric disc with internal fixation	Biomechanical properties nearly equivalent to that of the natural disc; excellent fusion capacity
Kurtz et al. [45]	Human	Retrieval study, 1 patient	Wear, cracks	Charité (unconstrained)	-	Cracks in the polyethylene core, damage around the periphery of the core
Kurtz et al. [46]	Human	Retrieval study, 21 patients	Surface damage	Charité (unconstrained)	-	Observed surface damage
Langrana et al. [47]	-	Computational	-	Fiber-reinforced composite	-	Pioneering model of an artificial disc, including realistic material properties
Langrana et al. [48]	-	Experimental	Compression and torsion stiffness	Fiber-reinforced composite	-	Adequate stiffness can be achieved with the use of a composite material

Table 15 – Published studies of biomaterials, wear and osseointegration (Galbusera, et al., 2008)

References	Model	Study type	Observed variables	Prosthesis	Compared to	Results
Lee et al. [54]	-	Experimental	Mechanical properties of the disc	Fiber-reinforced composite	-	Manufacturing and testing of composite disc prostheses
Le Huec et al. [49]	-	Experimental	Shock absorption capacity	ProDisc (semi-constrained), Maverick (unconstrained)	-	The two devices have identical shock and vibration transmission properties
Mizuno et al. [64]	Murine	In vivo	Biochemical analysis	Tissue-engineered disc	-	Morphology and histology resembled those of the native intervertebral disc
Moore et al. [65]	Murine	In vivo	Response to wear debris	Polyolefin rubber	-	Rubber particles induce a localized tissue response consistent to a normal foreign body reaction
Revell et al. [75]	Porcine	In vivo	-	Tissue engineered disc	-	Engineered disc histology similar to a native intervertebral disc
Schmiedberg et al. [82]	-	Experimental	Wear	Spring-based	-	Analyses of wear debris with a new method
Shaheen and Sheperd [83]	-	Computational	Lubrication regimes	Generic ball-and-socket	-	Metal-metal and metal-polymer couplings are likely to generate wear debris; ceramic-ceramic coupling may reduce wear
Takahata et al. [86]	Ovine	In vivo	Bone ingrowth	3D fabric disc (unconstrained)	-	Excellent bone ingrowth
Van Ooij et al. [90]	Human	Retrieval study, 4 patients	Wear	Charité (unconstrained)	-	Wear present in all devices, with different extent and severity
Vuono-Hawkins et al. [92]	Canine	In vivo, ex vivo	Motion, bone ingrowth	Elastomeric spacer	-	Increased motion, no significant bone ingrowth after 12 months
Zeh et al. [97]	Human	Ion concentration analysis in serum	Co-Cr ion concentrations	Maverick (semi-constrained)	-	Co-Cr ion concentration significant, similar or exceeding typical concentrations after total hip arthroplasty

IAR Instantaneous Axis of Rotation

Table 15 – Continued

[Reference listing for Table 13, Table 14 and Table 15](#)

- [1.] Auerbach JD, Wills BP, McIntosh TC, Balderston RA (2007) Evaluation of spinal kinematics following lumbar total disc replacement and circumferential fusion using in vivo fluoroscopy. *Spine* 32(5):527–536. doi:10.1097/01.brs.0000256915.90236.17
- [2.] Bertagnoli R, Kumar S (2002) Indications for full prosthetic disc arthroplasty: a correlation of clinical outcome against a variety of indications. *Eur Spine J* 11(Suppl 2):S131–S136
- [3.] Bertagnoli R, Yue JJ, Kershaw T, Shah RV, Pfeiffer F, Fenk- Mayer A et al (2006) Lumbar total disc arthroplasty utilizing the ProDisc prosthesis in smokers versus nonsmokers: a prospective study with 2-year minimum follow-up. *Spine* 31(9):992–997. doi: 10.1097/01.brs.0000214970.07626.68
- [4.] Bertagnoli R, Yue JJ, Shah RV, Nanieva R, Pfeiffer F, Fenk- Mayer A et al (2005) The treatment of disabling single-level lumbar discogenic low back pain with total disc arthroplasty utilizing the Prodisc prosthesis: a prospective study with 2-year minimum follow-up. *Spine* 30(19):2230–2236. doi:10.1097/01.brs.0000182217.87660.40
- [5.] Büttner-Janck K, Schellnack K, Zippel H (1989) Biomechanics of the SB Charité lumbar intervertebral disc endoprosthesis. *Int Orthop* 13(3):173–176. doi:10.1007/BF00268042
- [6.] Cakir B, Richter M, Kafer W, Puhl W, Schmidt R (2005) The impact of total lumbar disc replacement on segmental and total lumbar lordosis. *Clin Biomech (Bristol, Avon)* 20(4):357–364. doi:10.1016/j.clinbiomech.2004.11.019
- [7.] Cakir B, Richter M, Puhl W, Schmidt R (2006) Reliability of motion measurements after total disc replacement: the spike and the fin method. *Eur Spine J* 15(2):165–173. doi:10.1007/s00586-005-0942-2
- [8.] Chang BS, Brown PR, Sieber A, Valdevit A, Tateno K, Kostuik JP (2004) Evaluation of the biological response of wear debris. *Spine J* 4(6(Suppl)):239S–244S. doi:10.1016/j.spinee.2004.07.014
- [9.] Chung SS, Lee CS, Kang CS, Kim SH (2006) The effect of lumbar total disc replacement on the spinopelvic alignment and range of motion of the lumbar spine. *J Spinal Disord Tech* 19(5):307–311. doi:10.1097/01.bsd.0000208255.14329.1e
- [10.] Chung SS, Lee CS, Kang CS (2006) Lumbar total disc replacement using ProDisc II: a prospective study with a 2-year minimum follow-up. *J Spinal Disord Tech* 19(6):411–415. doi: 10.1097/00024720-200608000-00007
- [11.] Cinotti G, David T, Postacchini F (1996) Results of disc prosthesis after a minimum follow-up period of 2 years. *Spine* 21(8):995–1000. doi:10.1097/00007632-199604150-00015
- [12.] Cunningham BW, Dmitriev AE, Hu N, McAfee PC (2003) General principles of total disc replacement arthroplasty: seventeen cases in a nonhuman primate model. *Spine* 28(20):S118–S124. doi:10.1097/00007632-200310151-00005
- [13.] Cunningham BW, Gordon JD, Dmitriev AE, Hu N, McAfee PC (2003) Biomechanical evaluation of total disc replacement arthroplasty: an in vitro human cadaveric model. *Spine* 28(20): S110–S117. doi:10.1097/01.BRS.0000092209.27573.90
- [14.] Cunningham BW, Lowery GL, Serhan HA, Dmitriev AE, Orbegoso CM, McAfee PC et al (2002) Total disc replacement arthroplasty using the AcroFlex lumbar disc: a non-human primate model. *Eur Spine J* 11(Suppl 2):S115–S123. doi:10.1007/s005860100323
- [15.] Cunningham BW, McAfee PC, Geisler FH, Holsapple G, Adams K, Blumenthal SL et al (2008) Distribution of in vivo and in vitro range of motion following 1-level arthroplasty with the CHARITE artificial disc compared with fusion. *J Neurosurg Spine* 8(1):7–12. doi:10.3171/SPI-08/01/007
- [16.] Cunningham BW (2004) Basic scientific considerations in total disc arthroplasty. *Spine* 4(6(Suppl)):219S–230S (Review). doi: 10.1016/j.spinee.2004.07.015
- [17.] David T (2007) Long-term results of one-level lumbar arthroplasty: minimum 10-year follow-up of the CHARITE artificial disc in 106 patients. *Spine* 32(6):661–666. doi:10.1097/01.brs.0000257554.67505.45
- [18.] David T (2005) Revision of a Charité' artificial disc 9.5 years in vivo to a new Charité' artificial disc: case report and explant analysis. *Eur Spine J* 14(5):507–511. doi:10.1007/s00586-004-0842-x
- [19.] Delamarter RB, Fribourg DM, Kanim LE, Bae H (2003) ProDisc artificial total lumbar disc replacement: introduction and early results from the United States clinical trial. *Spine* 28(20):S167–S175. doi:10.1097/01.BRS.0000092220.66650.2B
- [20.] Denoziere G, Ku DN (2006) Biomechanical comparison between fusion of two vertebrae and implantation of an artificial intervertebral disc. *J Biomech* 39(4):766–775. doi:10.1016/j.jbiomech.2004.07.039
- [21.] Dooris AP, Goel VK, Grosland NM, Gilbertson LG, Wilder DG (2001) Load-sharing between anterior and posterior elements in a lumbar motion segment implanted with an artificial disc. *Spine* 26(6):E122–E129. doi:10.1097/00007632-200103150-00004

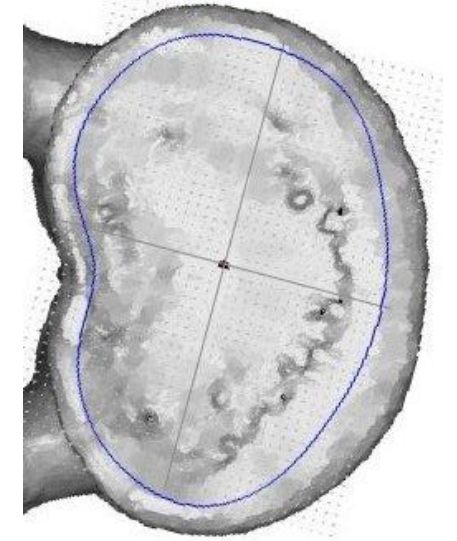
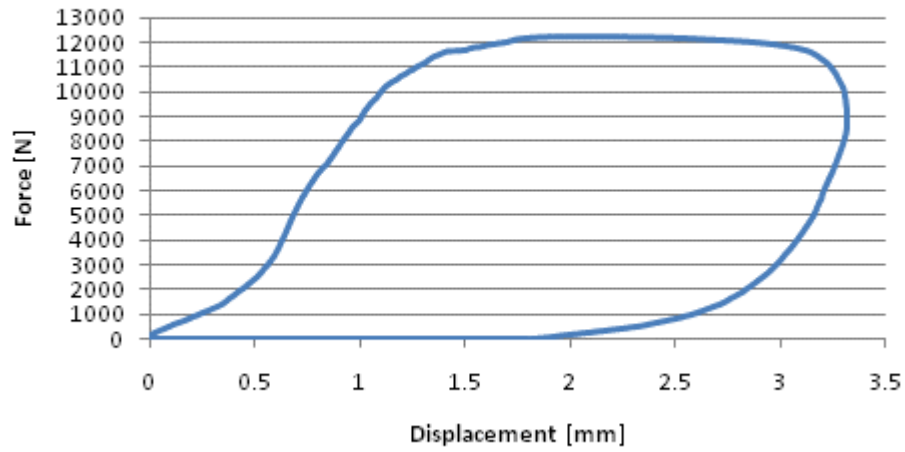
- [22.] Edeland HG (1981) Suggestions for a total elasto-dynamic intervertebral disc prosthesis. *Biomater Med Devices Artif Organs* 9(1):65–72
- [23.] Eijkelkamp MF, van Donkelaar CC, Veldhuizen AG, van Horn JR, Huyghe JM, Verkerke GJ (2001) Requirements for an artificial intervertebral disc. *Int J Artif Organs* 24(5):311–321
- [24.] Enker P, Steffee A, Mcmillin C, Keppler L, Biscup R, Miller S (1993) Artificial disc replacement. Preliminary report with a 3-year minimum follow-up. *Spine* 18(8):1061–1070. doi:10.1097/00007632-199308150-00017
- [25.] Francois J, Coessens R, Lauweryns P (2007) Early removal of a Maverick disc prosthesis: surgical findings and morphological changes. *Acta Orthop Belg* 73(1):122–127
- [26.] Fraser RD, Ross ER, Lowery GL, Freeman BJ, Dolan M (2004) *AcroFlex* design and results. *Spine* J 4(6)(Suppl):245S–251S (Review). doi:10.1016/j.spinee.2004.07.020
- [27.] Gloria A, Causa F, De Santis R, Netti PA, Ambrosio L (2007) Dynamic-mechanical properties of a novel composite intervertebral disc prosthesis. *J Mater Sci: Mater Med* 18(11):2159–2165. doi:10.1007/s10856-007-3003-z
- [28.] Goel VK, Grauer JN, Patel TC, Biyani A, Sairyo K, Vishnubhotla S et al (2005) Effects of Charite' artificial disc on the implanted and adjacent spinal segments mechanics using a hybrid testing protocol. *Spine* 30(24):2755–2764. doi:10.1097/01.brs.0000195897.17277.67
- [29.] Hedman TP, Kostuik JP, Fernie GR, Hellier WG (1991) Design of an intervertebral disc prosthesis. *Spine* 16(6(suppl)):S256–S260. doi:10.1097/00007632-199106001-00016
- [30.] Hitchon PW, Eichholz K, Barry C, Rubenbauer P, Ingahlalikar A, Nakamura S et al (2005) Biomechanical studies of an artificial disc implant in the human cadaveric spine. *J Neurosurg Spine* 2(3):339–343
- [32.] Hou TS, Tu KY, Xu YK, Li ZB, Cai AH, Wang HC (1991) Lumbar intervertebral disc prosthesis. An experimental study. *Chin Med J (Engl)* 104(5):381–386
- [33.] Huang RC, Girardi FP, Cammisa FP Jr, Lim MR, Tropiano P, Marnay T (2005) Correlation between range of motion and outcome after lumbar total disc replacement: 8.6-year follow-up. *Spine* 30(12):1407–1411. doi:10.1097/01.brs.0000166528.67425.0e
- [34.] Huang RC, Girardi FP, Cammisa FP Jr, Wright TM (2003) The implications of constraint in lumbar total disc replacement. *J Spinal Disord Tech* 16(4):412–417
- [35.] Huang RC, Girardi FP, Cammisa FP Jr, Tropiano P, Marnay T (2003) Long-term flexion-extension range of motion of the prodisc total disc replacement. *J Spinal Disord Tech* 16(5):435–440. doi:10.1097/00024720-200310000-00001
- [36.] Huang RC, Tropiano P, Marnay T, Girardi FP, Lim MR, Cammisa FP Jr (2006) Range of motion and adjacent level degeneration after lumbar total disc replacement. *Spine* J 6(3):242–247. doi:10.1016/j.spinee.2005.04.013
- [37.] Kadoya K, Kotani Y, Abumi K, Takada T, Shimamoto N, Shikunami Y et al (2001) Biomechanical and morphologic evaluation of a three-dimensional fabric sheep artificial intervertebral disc: in vitro and in vivo analysis. *Spine* 26(14):1562–1569. doi: 10.1097/00007632-200107150-00012
- [39.] Kim DH, Ryu KS, Kim MK, Park CK (2007) Factors influencing segmental range of motion after lumbar total disc replacement using the ProDisc II prosthesis. *J Neurosurg Spine* 7(2):131–138. doi:10.3171/SPI-07/08/131
- [40.] Kosmopoulos V, McManus J, Schizas C (2008) Consequences of patient position in the radiographic measurement of artificial disc replacement angles. *Eur Spine J* 17(1):30–35. doi:10.1007/s00586-007-0486-8
- [41.] Kostuik JP (1997) Intervertebral disc replacement. *Experimental study*. *Clin Orthop Relat Res* 337:27–41. doi:10.1097/00003086-199704000-00004
- [42.] Kotani Y, Abumi K, Shikunami Y, Takada T, Kadoya K, Shimamoto N et al (2002) Artificial intervertebral disc replacement using bioactive three-dimensional fabric: design, development, and preliminary animal study. *Spine* 27(9):929–935. doi: 10.1097/00007632-200205010-00008
- [43.] Kotani Y, Abumi K, Shikunami Y, Takahata M, Kadoya K, Kadosawa T, Minami A, Kaneda K (2004) Two-year observation of artificial intervertebral disc replacement: results after supplemental ultra-high strength bioresorbable spinal stabilization. *J Neurosurg* 100(4 Suppl Spine):337–342
- [44.] Kotani Y, Cunningham BW, Abumi K, Dmitriev AE, Hu N, Ito M et al (2006) Multidirectional flexibility analysis of anterior and posterior lumbar artificial disc reconstruction: in vitro human cadaveric spine model. *Eur Spine J* 15(10):1511–1520. doi: 10.1007/s00586-006-0086-z
- [45.] Kurtz SM, Pelozo J, Siskey R, Villarraga ML (2005) Analysis of a retrieved polyethylene total disc replacement component. *Spine* J 5(3):344–350. doi:10.1016/j.spinee.2004.11.011
- [46.] Kurtz SM, van Ooij A, Ross R, de Waal Malefijt J, Pelozo J, Ciccarelli L et al (2007) Polyethylene wear and rim fracture in total disc arthroplasty. *Spine* J 7(1):12–21. doi:10.1016/j.spinee.2006.05.012
- [47.] Langrana NA, Lee CK, Yang SW (1991) Finite-element modeling of the synthetic intervertebral disc. *Spine* 16(6(suppl)):S245–S252. doi:10.1097/00007632-199106001-00014
- [48.] Langrana NA, Parsons JR, Lee CK, Vuono-Hawkins M, Yang SW, Alexander H (1994) Materials and design concepts for an intervertebral disc spacer. I. fiber-reinforced composite design. *J Appl Biomater* 5(2):125–132. doi:10.1002/jab.770050205

- [49.] Le Huec JC, Kiaer T, Friesem T, Mathews H, Liu M, Eisermann L (2003) Shock absorption in lumbar disc prosthesis: a preliminary mechanical study. *J Spinal Disord Tech* 16(4):346–351
- [50.] Le Huec J, Basso Y, Mathews H, Mehbood A, Aunoble S, Friesem T et al (2005) The effect of single-level, total disc arthroplasty on sagittal balance parameters: a prospective study. *Eur Spine J* 14(5):480–486. doi:10.1007/s00586-004-0843-9
- [51.] Le Huec JC, Basso Y, Aunoble S, Friesem T, Bruno MB (2005) Influence of facet and posterior muscle degeneration on clinical results of lumbar total disc replacement: two-year follow-up. *J Spinal Disord Tech* 18(3):219–223
- [52.] Le Huec JC, Mathews H, Basso Y, Aunoble S, Hoste D, Bley B et al (2005) Clinical results of Maverick lumbar total disc replacement: two-year prospective follow-up. *Orthop Clin North Am* 36(3):315–322. doi:10.1016/j.ocl.2005.02.001
- [53.] Ledet EH, Tymeson MP, DiRiso DJ, Cohen B, Uhl RL (2005) Direct real-time measurement of in vivo forces in the lumbar spine. *Spine J* 5(1):85–94. doi:10.1016/j.spinee.2004.06.017
- [54.] Lee CK, Goel VK (2004) Artificial disc prosthesis: design concepts and criteria. *Spine J* 4(6)(Suppl):209S–218S (Review). doi:10.1016/j.spinee.2004.07.011
- [55.] Leivseth G, Braaten S, Frobin W, Brinckmann P (2006) Mobility of lumbar segments instrumented with a ProDisc II prosthesis: a two-year follow-up study. *Spine* 31(15):1726–1733. doi:10.1097/01.brs.0000224213.45330.68
- [56.] Lemaire JP, Carrier H, Sariali el H, Skalli W, Lavaste F (2005) Clinical and radiological outcomes with the Charite artificial disc: a 10-year minimum follow-up. *J Spinal Disord Tech* 18(4):353–359. doi:10.1097/01.bsd.0000172361.07479.6b
- [58.] Lim MR, Girardi FP, Zhang K, Huang RC, Peterson MG, Cammisa FP Jr (2005) Measurement of total disc replacement radiographic range of motion: a comparison of two techniques. *J Spinal Disord Tech* 18(3):252–256
- [59.] Lim MR, Loder RT, Huang RC, Lyman S, Zhang K, Sama A et al (2006) Measurement error of lumbar total disc replacement range of motion. *Spine* 31(10):E291–E297. doi:10.1097/01.brs.0000216452.54421.ea
- [60.] Mathew P, Blackman M, Redla S, Hussein AA (2005) Bilateral pedicle fractures following anterior dislocation of the polyethylene inlay of a ProDisc artificial disc replacement: a case report of an unusual complication. *Spine* 30(11):E311–E314. doi:10.1097/01.brs.0000164135.03844.b6
- [61.] McAfee PC, Cunningham B, Holsapple G, Adams K, Blumenthal S, Guyer RD et al (2005) A prospective, randomized, multicenter Food and Drug Administration investigational device exemption study of lumbar total disc replacement with the CHARITE artificial disc versus lumbar fusion: part II: evaluation of radiographic outcomes and correlation of surgical technique accuracy with clinical outcomes. *Spine* 30(14):1576–1583. doi:10.1097/01.brs.0000170561.25636.1c
- [62.] McAfee PC, Cunningham BW, Hayes V, Sidiqi F, Dabbah M, Seftor JC et al (2006) Biomechanical analysis of rotational motions after disc arthroplasty implications for patients with adult deformities. *Spine* 31(19(suppl)):S152–S160. doi:10.1097/01.brs.0000234782.89031.03
- [64.] Mizuno H, Roy AK, Vacanti CA, Kojima K, Ueda M, Bonassar LJ (2004) Tissue-engineered composites of annulus fibrosus and nucleus pulposus for intervertebral disc replacement. *Spine* 29(12):1290–1297. doi:10.1097/01.BRS.0000128264.46510.27 discussion 1297–8
- [65.] Moore RJ, Fraser RD, Vernon-Roberts B, Finnie JW, Blumbergs PC, Haynes DR et al (2002) The biologic response to particles from a lumbar disc prosthesis. *Spine* 27(19):2088–2094. doi:10.1097/00007632-200210010-00003
- [66.] Moumene M, Geisler FH (2007) Comparison of biomechanical function at ideal and varied surgical placement for two lumbar artificial disc implant designs: mobile-core versus fixed-core. *Spine* 32(17):1840–1851. doi:10.1097/BRS.0b013e31811ec29c
- [67.] Neal CJ, Rosner MK, Kuklo TR (2005) Magnetic resonance imaging evaluation of adjacent segments after disc arthroplasty. *J Neurosurg Spine* 3(5):342–347
- [68.] Noailly J, Lacroix D, Planell JA (2005) Finite element study of a novel intervertebral disc substitute. *Spine* 30(20):2257–2264. doi:10.1097/01.brs.0000182319.81795.72
- [69.] O’Leary P, Nicolakis M, Lorenz MA, Voronov LI, Zindrick MR, Ghanayem A et al (2005) Response of Charite total disc replacement under physiologic loads: prosthesis component motion patterns. *Spine J* 5(6):590–599. doi:10.1016/j.spinee.2005.06.015
- [71.] Panjabi M, Henderson G, Abjornson C, Yue J (2007) Multidirectional testing of one- and two-level ProDisc-L versus simulated fusions. *Spine* 32(12):1311–1319. doi:10.1097/BRS.0b013e318059af6f
- [72.] Panjabi M, Malcolmsen G, Teng E, Tominaga Y, Henderson G, Serhan H (2007) Hybrid testing of lumbar CHARITE discs versus fusions. *Spine* 32(9):959–966. doi:10.1097/01.brs.0000260792.13893.88
- [74.] Putzier M, Funk JF, Schneider SV, Gross C, Tohtz SW, Khodadadyan-Klostermann C et al (2006) Charite’ total disc replacement—clinical and radiographical results after an average follow-up of 17 years. *Eur Spine J* 15(2):183–195. doi:10.1007/s00586-005-1022-3

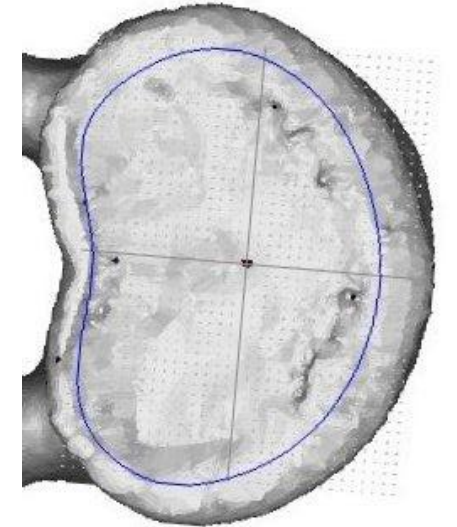
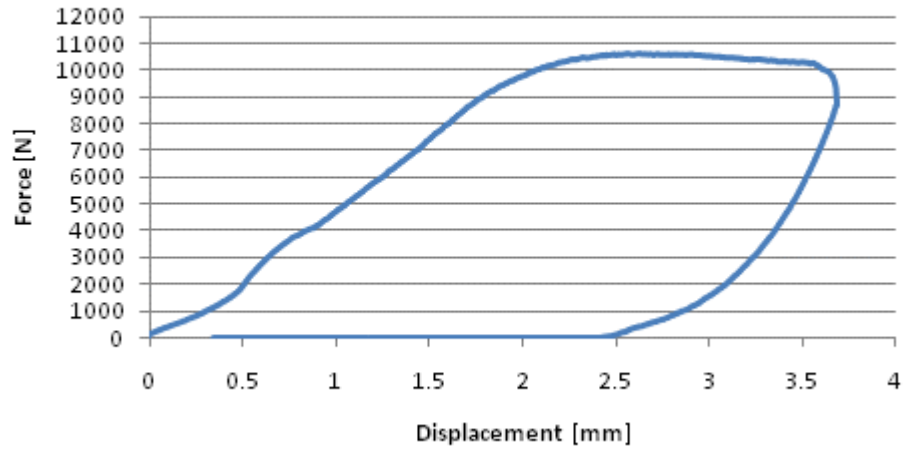
- [75.] Revell PA, Damien E, Di Silvio L, Gurav N, Longinotti C, Ambrosio L (2007) Tissue engineered intervertebral disc repair in the pig using injectable polymers. *J Mater Sci: Mater Med* 18(2):303–308. doi:10.1007/s10856-006-0693-6
- [77.] Rohlmann A, Zander T, Bergmann G (2005) Effect of total disc replacement with ProDisc on intersegmental rotation of the lumbar spine. *Spine* 30(7):738–743. doi:10.1097/01.brs.0000157413.72276.c4
- [78.] Rouseau MA, Bradford DS, Bertagnoli R, Hu SS, Lotz JC (2006) Disc arthroplasty design influences intervertebral kinematics and facet forces. *Spine J* 6(3):258–266. doi:10.1016/j.spinee.2005.07.004
- [79.] SariAli el H, Lemaire JP, Pascal-Mousseled H, Carrier H, Skalli W (2006) In vivo study of the kinematics in axial rotation of the lumbar spine after total intervertebral disc replacement: longterm results: a 10–14 years follow up evaluation. *Eur Spine J* 15(10):1501–1510
- [80.] Sasso RC, Foulk DM, Hahn M (2008) Prospective, randomized trial of metal-on-metal artificial lumbar disc replacement: initial results for treatment of discogenic pain. *Spine* 33(2):123–131
- [82.] Schmiedberg SK, Chang DH, Frondoza CG, Valdevit AD, Kostuik JP (1994) Isolation and characterization of metallic wear debris from a dynamic intervertebral disc prosthesis. *J Biomed Mater Res* 28(11):1277–1288. doi:10.1002/jbm.820281105
- [83.] Shaheen A, Shepherd DE (2007) Lubrication regimes in lumbar total disc arthroplasty. *Proc Inst Mech Eng [H]* 221(6):621–627. doi:10.1243/09544119JHEIM204
- [84.] Shim CS, Lee S, Maeng DH, Lee SH (2005) Vertical split fracture of the vertebral body following total disc replacement using ProDisc: report of two cases. *J Spinal Disord Tech* 18(5):465–469. doi:10.1097/01.bsd.0000159035.35365.df
- [86.] Takahata M, Kotani Y, Abumi K, Shikinami Y, Kadosawa T, Kaneda K et al (2003) Bone ingrowth fixation of artificial intervertebral disc consisting of bioceramic-coated three-dimensional fabric. *Spine* 28(7):637–644. doi:10.1097/00007632-200304010-00003 discussion 644
- [87.] Tortolani PJ, Cunningham BW, Eng M, McAfee PC, Holsapple GA, Adams KA (2007) Prevalence of heterotopic ossification following total disc replacement. A prospective, randomized study of two hundred and seventy-six patients. *J Bone Joint Surg Am* 89(1):82–88. doi:10.2106/JBJS.F.00432
- [88.] Tourmier C, Aunoble S, Le Huec JC, Lemaire JP, Tropicano P, Lafage V et al (2007) Total disc arthroplasty: consequences for sagittal balance and lumbar spine movement. *Eur Spine J* 16(3):411–421. doi:10.1007/s00586-006-0208-7
- [89.] Trouillier H, Kern P, Refior HJ, Muller-Gerbl M (2006) A prospective morphological study of facet joint integrity following intervertebral disc replacement with the CHARITE Artificial Disc. *Eur Spine J* 15(2):174–182. doi:10.1007/s00586-005-1010-7
- [90.] van Ooij A, Kurtz SM, Stessels F, Noten H, van Rhijn L (2007) Polyethylene wear debris and long-term clinical failure of the Charite disc prosthesis: a study of 4 patients. *Spine* 32(2):223–229. doi:10.1097/01.brs.0000251370.56327.c6 Erratum in: *Spine*.2007 32. 9:1052
- [91.] van Ooij A, Oner FC, Verbout AJ (2003) Complications of artificial disc replacement: a report of 27 patients with the SB Charite disc. *J Spinal Disord Tech* 16(4):369–383
- [92.] Vuono-Hawkins M, Zimmerman MC, Lee CK, Carter FM, Parsons JR, Langrana NA (1994) Mechanical evaluation of a canine intervertebral disc spacer: in situ and in vivo studies. *J Orthop Res* 12(1):119–127. doi:10.1002/jor.1100120115
- [94.] Wenzel SA, Shepherd DE (2007) Contact stresses in lumbar total disc arthroplasty. *Biomed Mater Eng* 17(3):169–173
- [97.] Zeh A, Planert M, Siebert G, Latke P, Held A, Hein W (2007) Release of cobalt and chromium ions into the serum following implantation of the metal-on-metal Maverick-type artificial lumbar disc (Medtronic Sofamor Danek). *Spine* 32(3):348–352. doi:10.1097/01.brs.0000253599.89694.c0
- [98.] Zigler J, Delamarter R, Spivak JM, Linovitz RJ, Danielson GO 3rd, Haider TT et al (2007) Results of the prospective, randomized, multicenter Food and Drug Administration investigational device exemption study of the ProDisc-L total disc replacement versus circumferential fusion for the treatment of 1-level degenerative disc disease. *Spine* 32(11):1155–1162. doi:10.1097/BRS.0b013e318054e377 discussion 1163

Appendix C: Load Displacement Curves and Failure Images for Destructive Tests

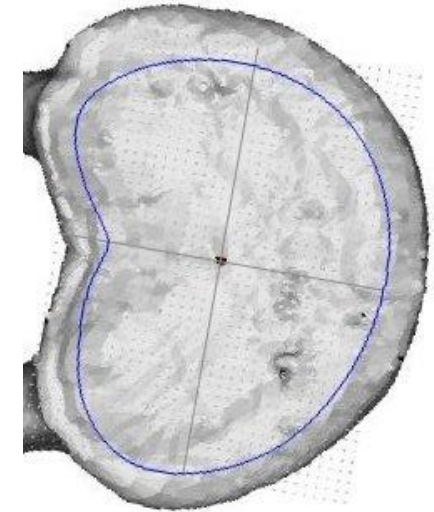
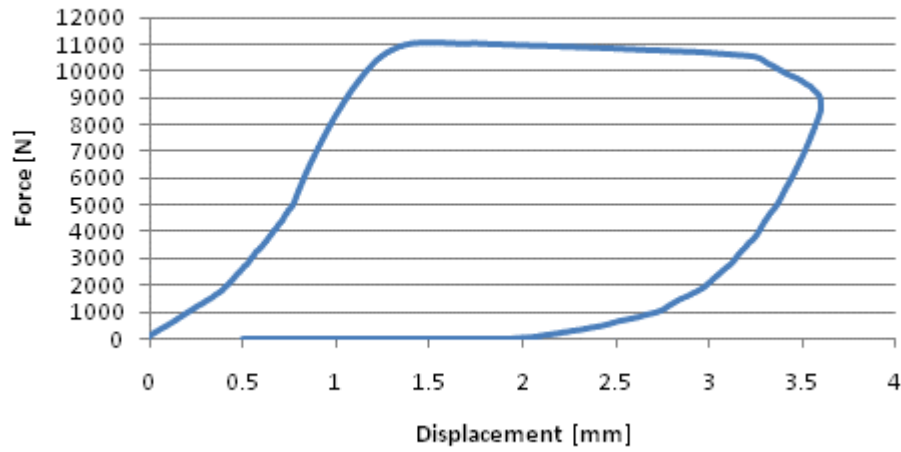
L3 (Contour)



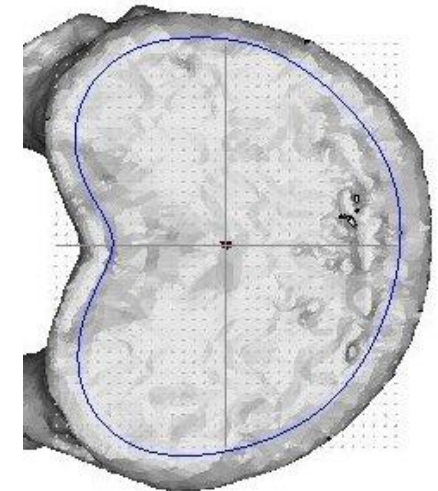
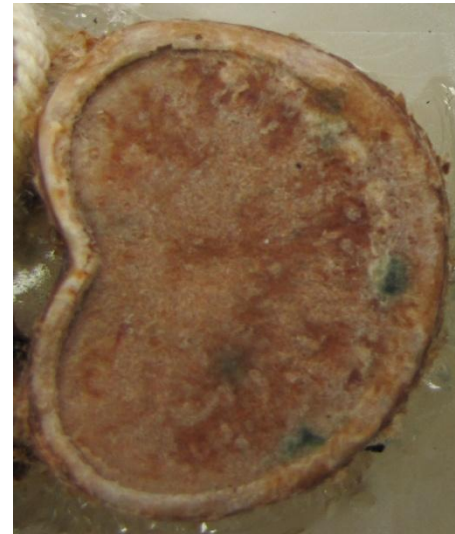
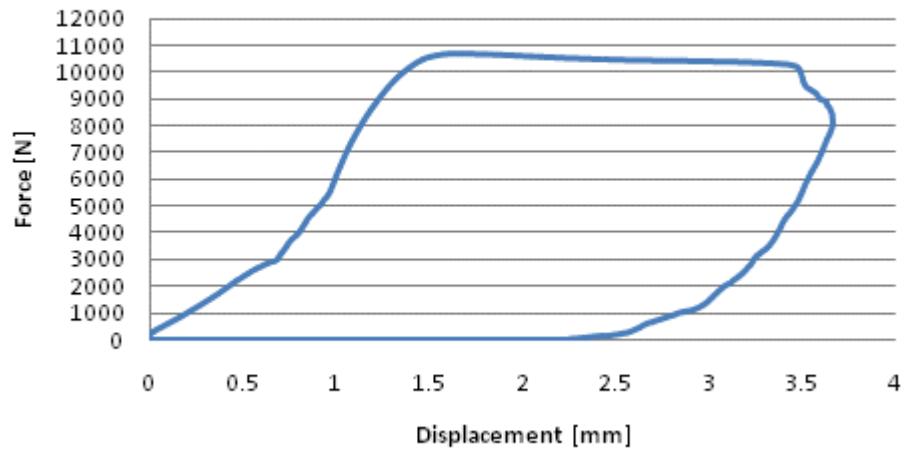
L2 (Flat)



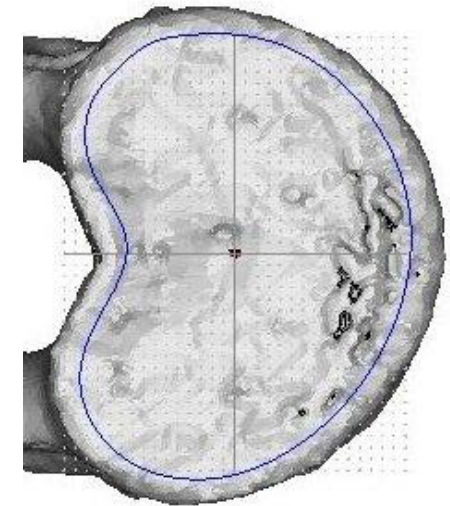
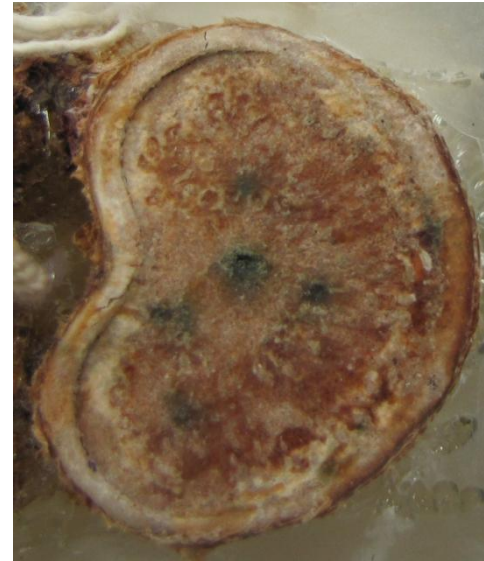
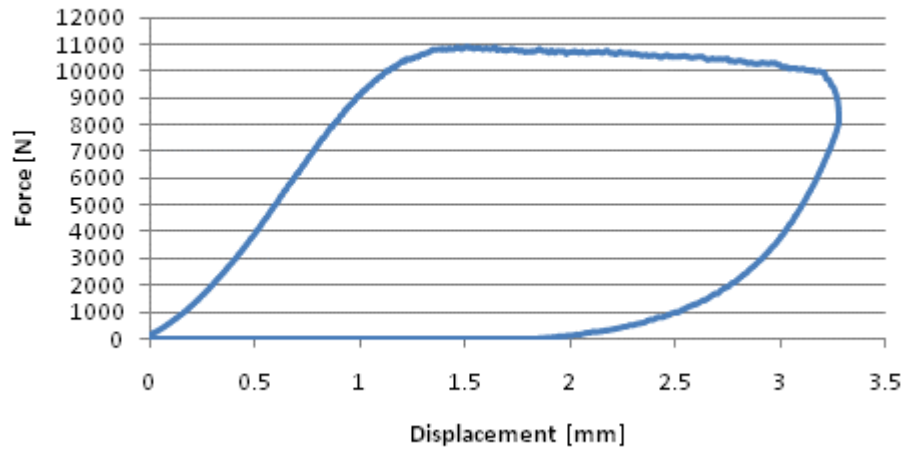
L1 (Contour)



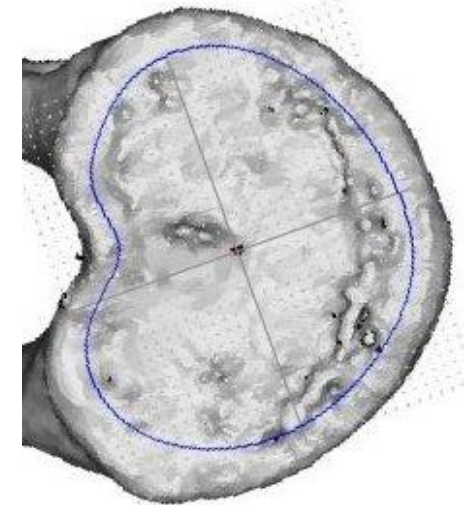
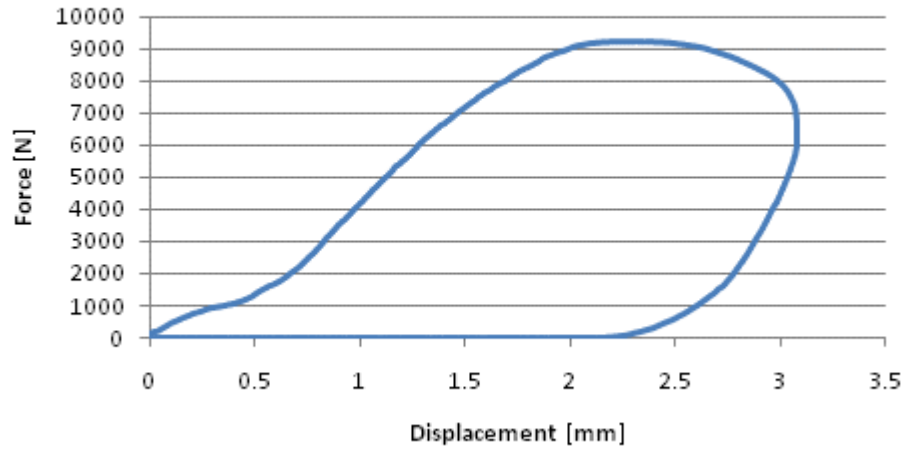
T12 (Flat)



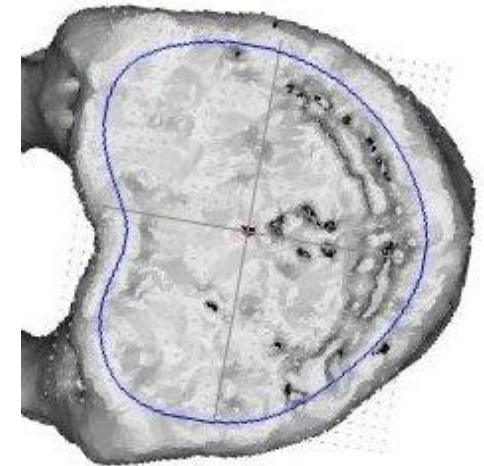
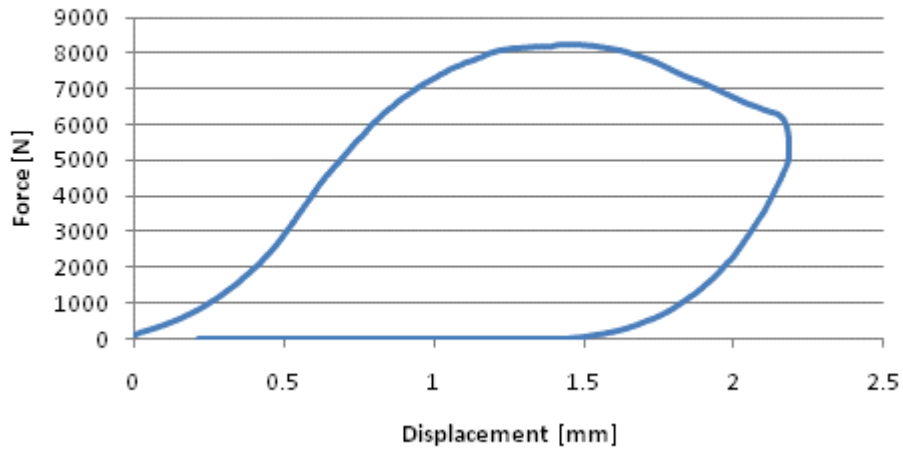
T11 (Contour)



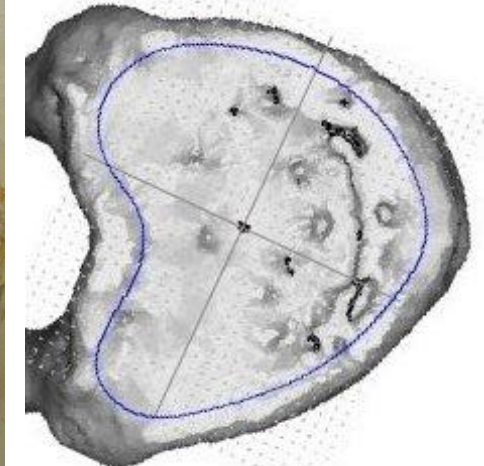
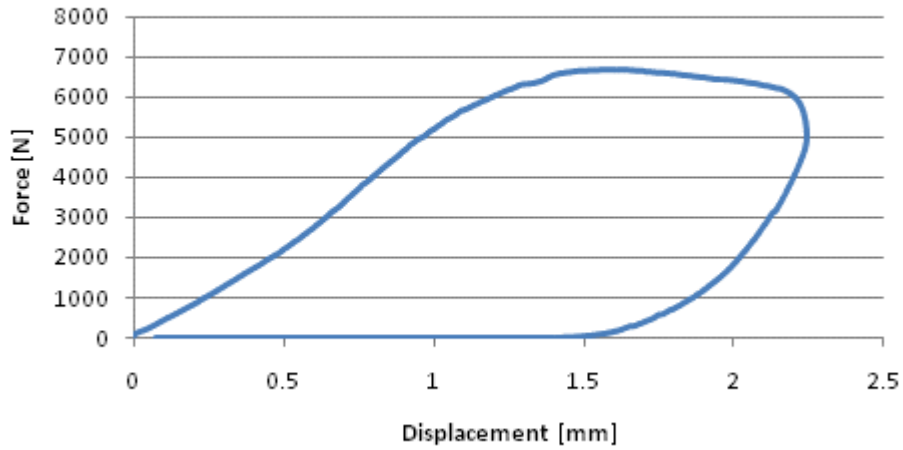
T10 (Flat)



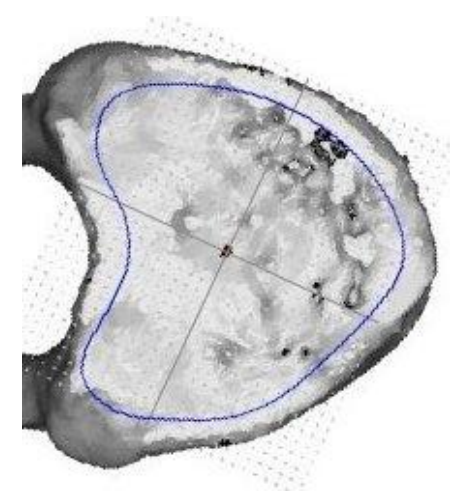
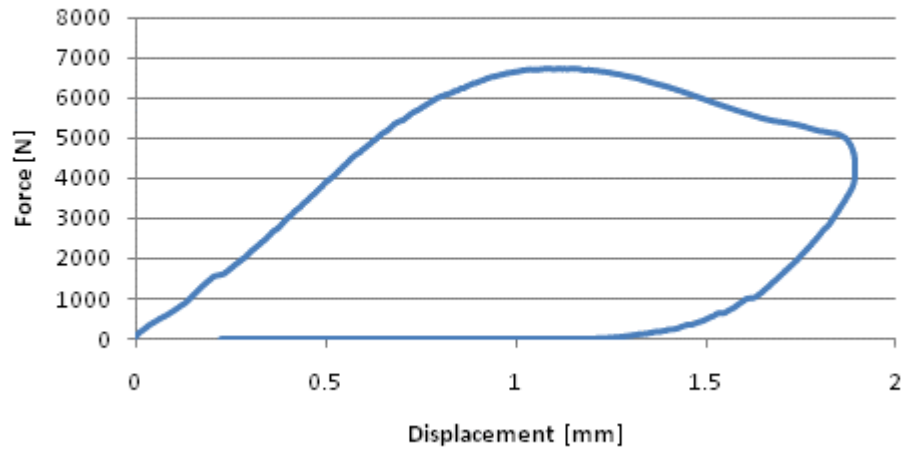
T9 (Contour)



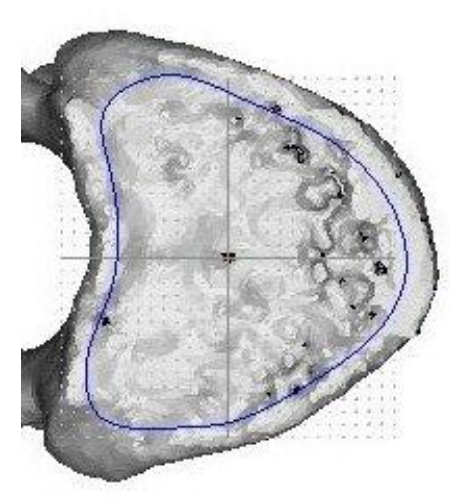
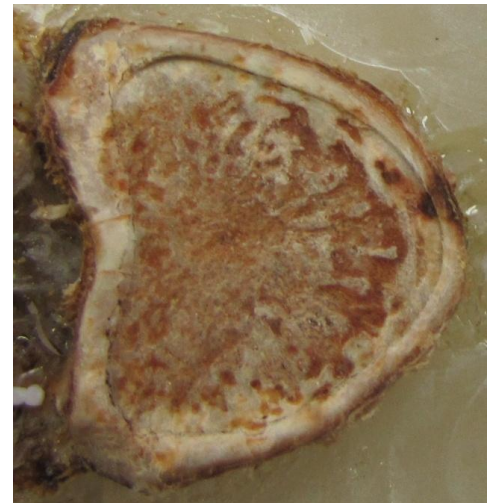
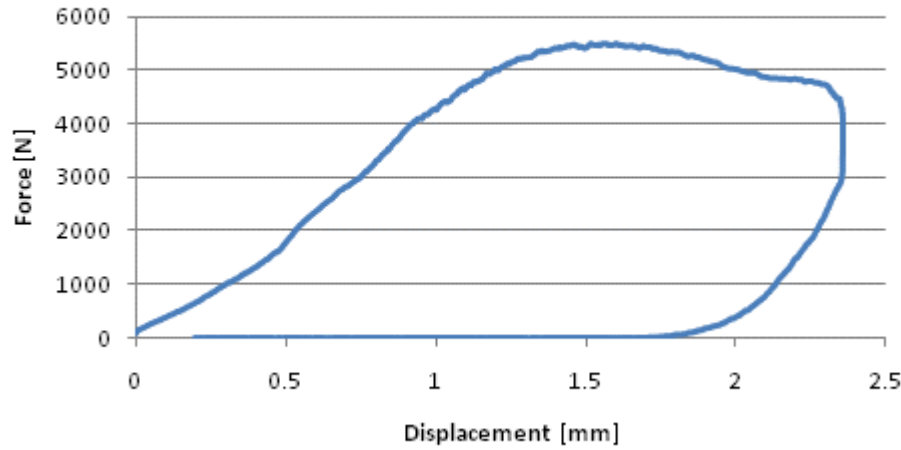
T8 (Flat)



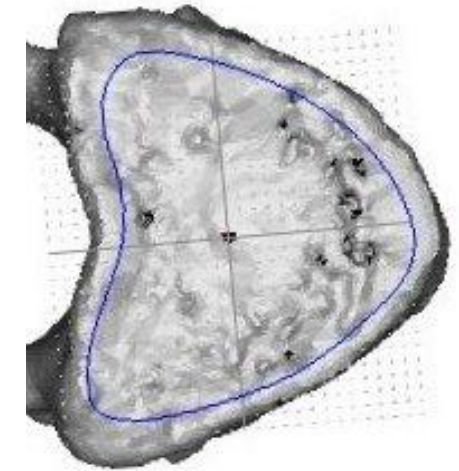
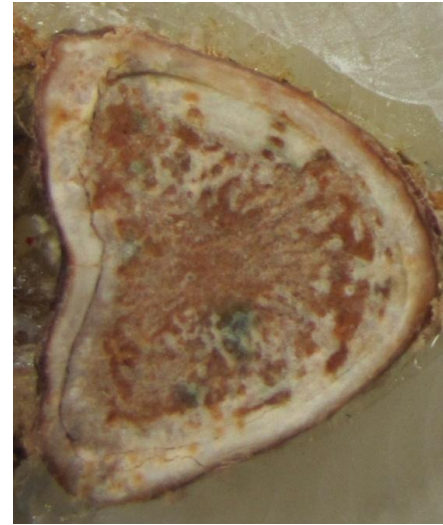
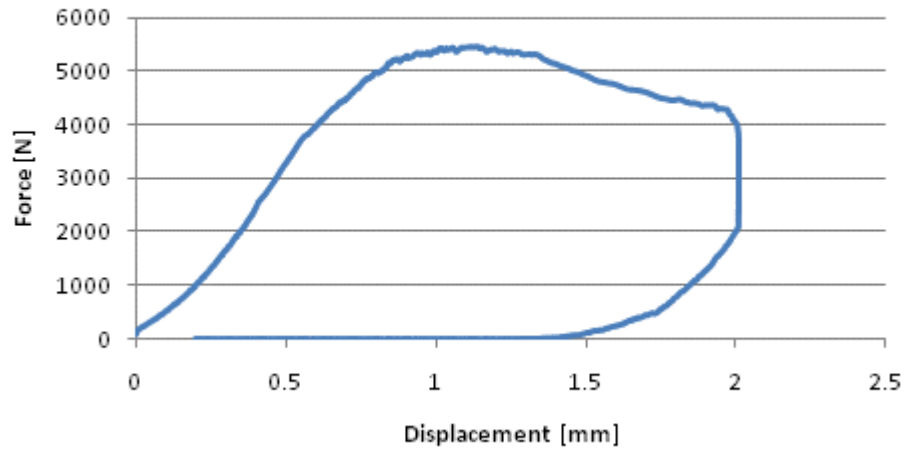
T7 (Contour)



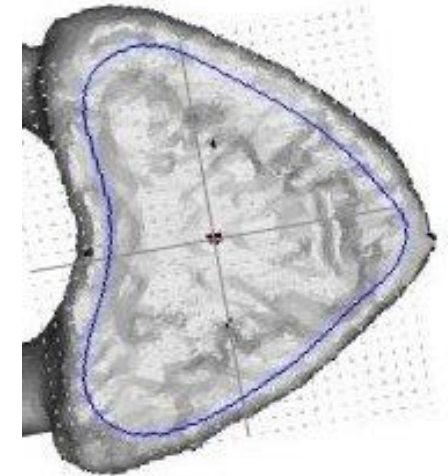
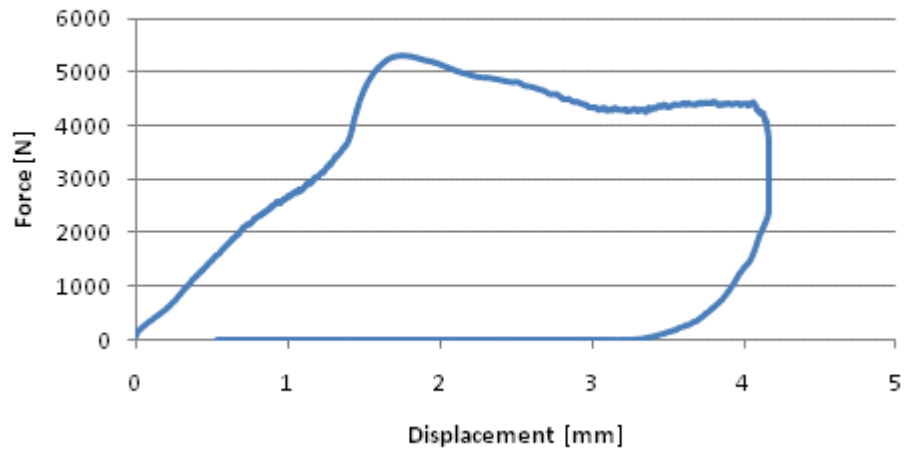
T6 (Flat)



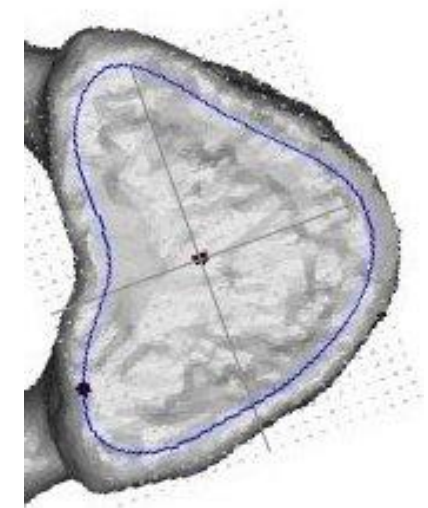
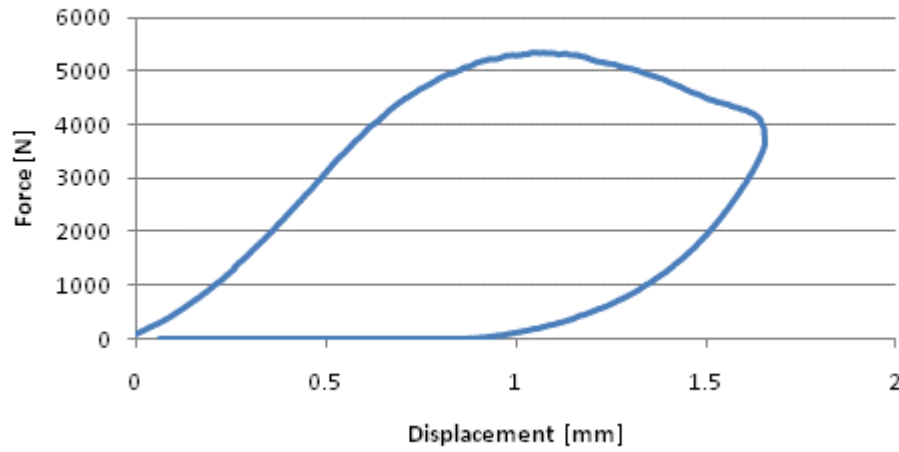
T5 (Contour)



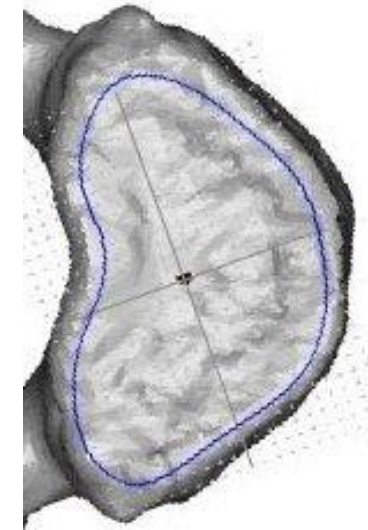
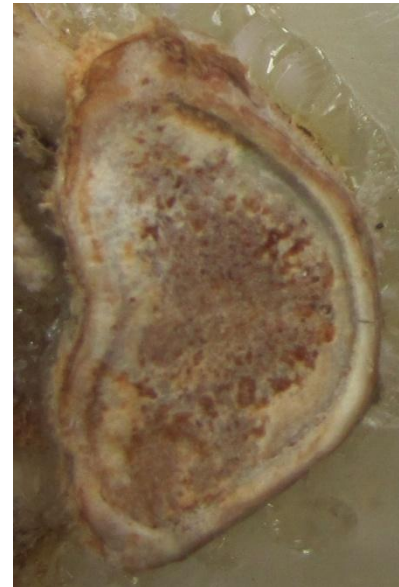
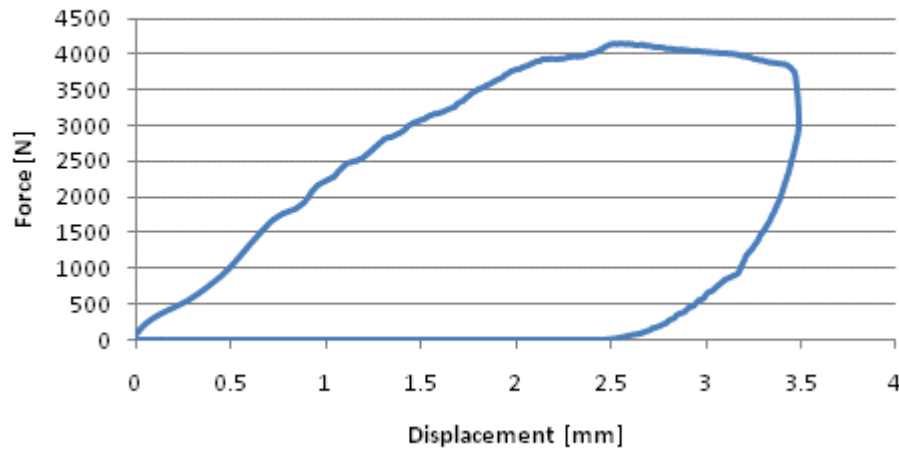
T4 (Flat)



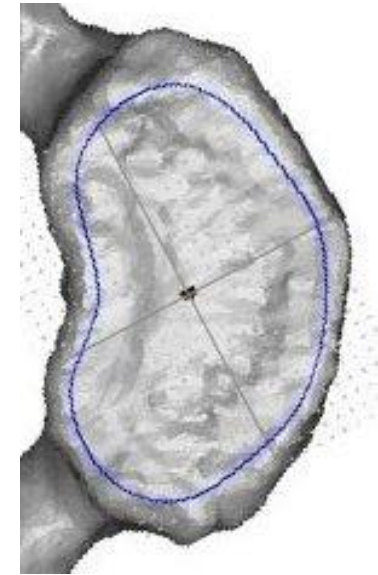
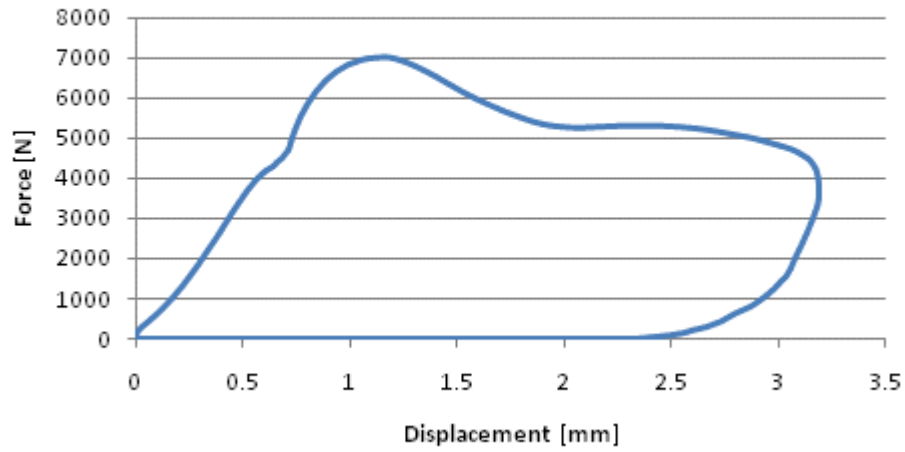
T3 (Contour)



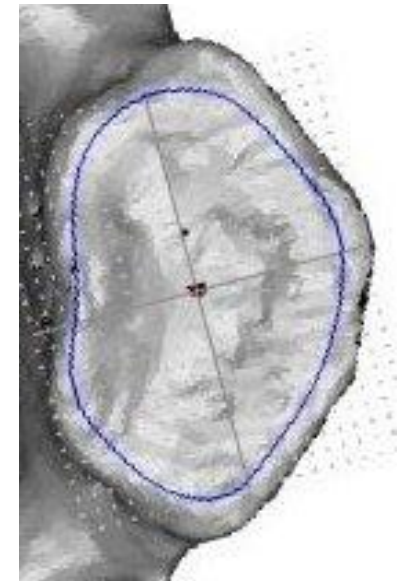
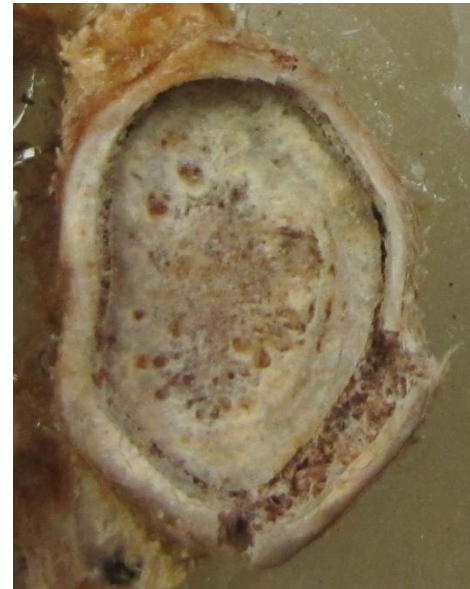
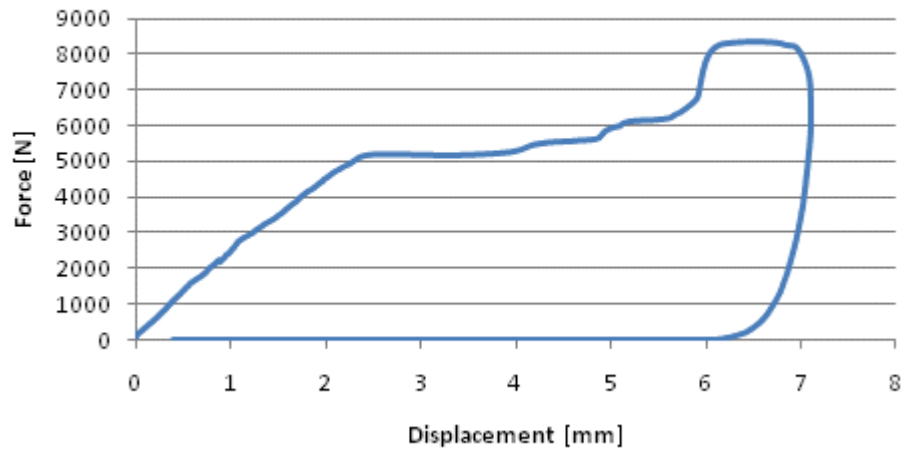
T2 (Flat)



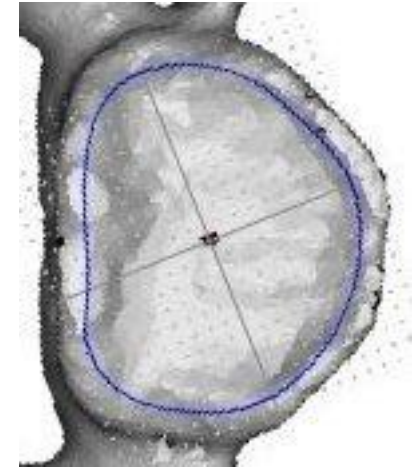
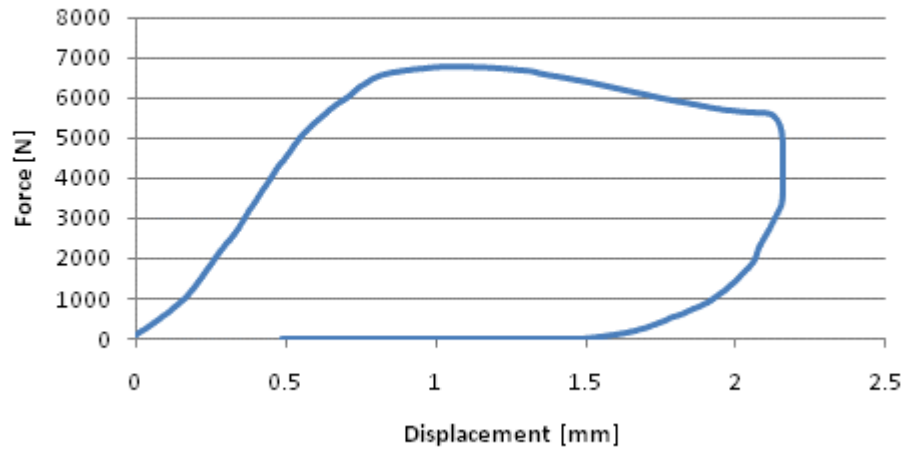
T1 (Contour)



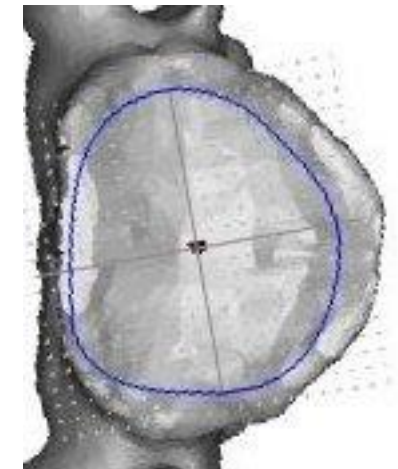
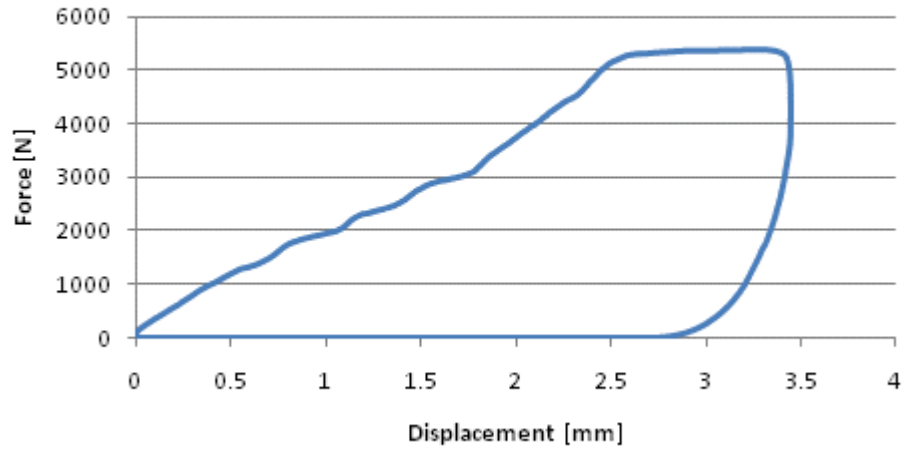
C7 (Flat)



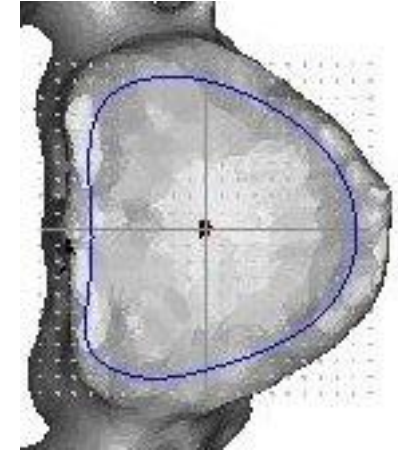
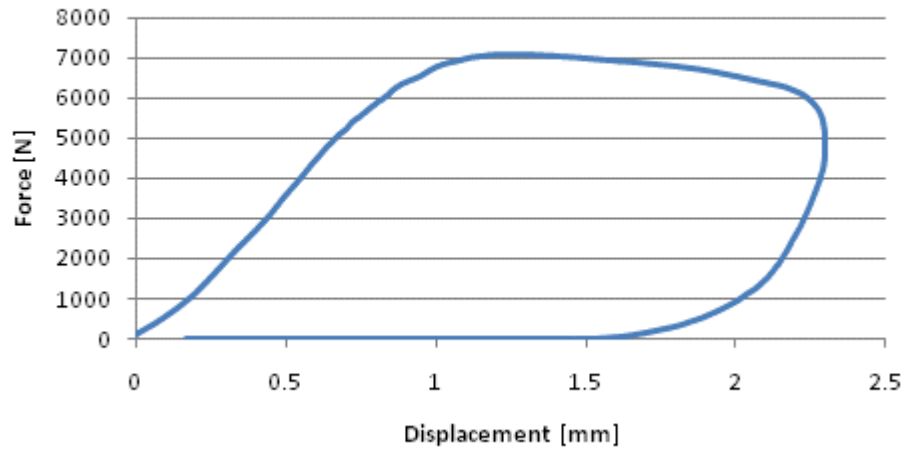
C6 (Contour)



C5 (Flat)



C4 (Contour)



C3 (Flat)

